ON THE SOLUTION OF EXTERNAL LAMINAR FREE CONVECTION TO POWER LAW FLUIDS

A Dissertation

Presented to

the Faculty of the Graduate School

University of Missouri-Columbia

In Partial Fulfillment

of the Requirements for the Degree

Doctor of Philosophy

---

by

Tommy Yih-Wen Chen

1971

John B. Miles Dissertation Supervisor

The undersigned, appointed by the Dean of the Graduate Faculty, have examined a thesis entitled

"On the Solution of External Laminar Free Convection to Power Law Fluids"

presented by Tommy Yih-Wen Chen

a candidate for the degree of Doctor of Philosophy

and hereby certify that in their opinion it is worthy of acceptance.

TABLE OF CONTENTS

LIST OF SYMBOLS

A, B, C = constants

$b(X)$, $c(X)$ = function of X, Equations (E.5) and (E.6), dimensionless

$C(N)$ = coefficient of heat transfer parameter, dimensionless

$C_d(x)$ = local drag coefficient, dimensionless

$C_f(N)$ = coefficient of flow parameter, dimensionless

C_p = specific heat at constant pressure, Btu/lbm-^oF

$d(x)$ = function of X, Equation (E.7), dimensionless

f_N = non-Newtonian factor, dimensionless

$f(\eta)$, $F(\eta)$ = velocity functions, dimensionless

g = gravitational acceleration, ft/sec^2

Gr = (plate) Grashof number, Table 5.1, dimensionless

Grx = local Grashof number, $(\frac{\rho}{\mu})^2 x^3 g\beta(t_w - t_\infty)$, or, $(\frac{\rho}{\mu})^2 x^4 \frac{g\beta q}{k}$, dimensionless

h = convective conductance, Btu/hr-ft^2-^oF

H = reduced temperature function, Newtonian, dimensionless

k = thermal conductivity, Btu/hr-ft-^oF

ℓ, l = constant, Equation (E.10)

L = characteristic length, ft

m = fluid consistency index, lbm/ft-sec^{2-N}

$M(N)$ = coefficient of heat transfer parameter, dimensionless

N = power law fluid index, dimensionless

Nux = local Nusselt number, hx/k or hL/k, dimensionless

F = velocity function, ft/sec

Pr = Prandtl number, $C_p \mu/k$, dimensionless

q = surface heat flux, Btu/hr-ft^2

r = constant, Equation (E.12)

Ra = Rayleigh number, Gr·Pr, dimensionless

s = constant, Equation (E.11)

S(X) = dimensionless function, Equation (3.29a)

t = temperature, ^oF

T = temperature variable, dimensionless

u = x-direction velocity component, ft/sec

U = velocity variable, dimensionless

v = y-direction velocity component, ft/sec

V = velocity variable, dimensionless

x = distance along the surface from the leading edge, ft

X = dimensionless distance variable, x/L

y = distance normal to the surface, ft

Y = distance variable, dimensionless

Greek Symbols

α = angle between the normal to the surface and the direction of the force of gravity, radian

β = coefficient of thermal expansion, $1/^oF$

η = similarity variable, dimensionless

ρ = density, lbm/ft^3

τ = shear stress, lbm/ft - sec^2

μ = absolute viscosity, lbm/ft - sec

ν = kinematic viscosity, ft^2/sec

θ = temperature function, dimensionless

ϕ = temperature function, dimensionless

ψ = stream function, dimensionless

ζ, ξ = perturbation variables, Appendix B, dimensionless

Subscripts

A = after Acrivos, generalized dimensionless group for uniform surface temperature case

a = apparent

C = generalized dimensionless group for uniform surface heat flux case

c = convective

T = after Tien, generalized dimensionless group

N = power law fluid, generalized dimensionless group

x = local, x local position

w = wall

∞ = undisturbed fluid

1, 2, 3, and 4 = sequential numbers designated to define the coefficients of heat transfer parameter

Superscripts

$\overline{}$ = average

* = generalized dimensionless group, Newtonian

LIST OF FIGURES

LIST OF TABLES

CHAPTER I

INTRODUCTION

1.1 Power Law Fluids

Pseudoplastic fluids (power law fluid index N<1), dilatant fluids (N>1), and even Newtonian fluids (N=1) are commonly called power law fluids, because they show an empirical shear stress (τ)-strain rate ($\frac{\partial u}{\partial y}$) relationship known as the power law

$$\tau = m \left|\frac{\partial u}{\partial y}\right|^{N-1} \frac{\partial u}{\partial y} \tag{1.1}$$

where N and m are empirical constants characteristic of the fluid; m is called the fluid consistency index. Equation (1.1) is also called the power model of Ostwald-de Waele-Nutting (1)*, or simply the Ostwald power model. It applies only to one-dimensional, incompressible flow in which $\frac{\partial u}{\partial y}$ is much larger than all the other elements in strain rate tensor. It should also be noted that all power law fluids have no yield stress and are time-independent; in other words, the time dependency of the properties is very small and thus may be neglected in most applications. Typical flow curves for power law fluids are plotted in Fig. 1.1.

If the apparent viscosity is defined to be

$$\mu_a \equiv \frac{\tau}{\frac{\partial u}{\partial y}} = m\left|\frac{\partial u}{\partial y}\right|^{N-1} \tag{1.2}$$

* Numbers in parenthesis refer to references.

the apparent viscosity of pseudoplastic fluids decreases as the strain rate increases, while the apparent viscosity of dilatant fluids increases with increasing the values of strain rates. Note that for Newtonian fluids (N=1) $\mu_a \equiv \mu$ with m replaced by μ.

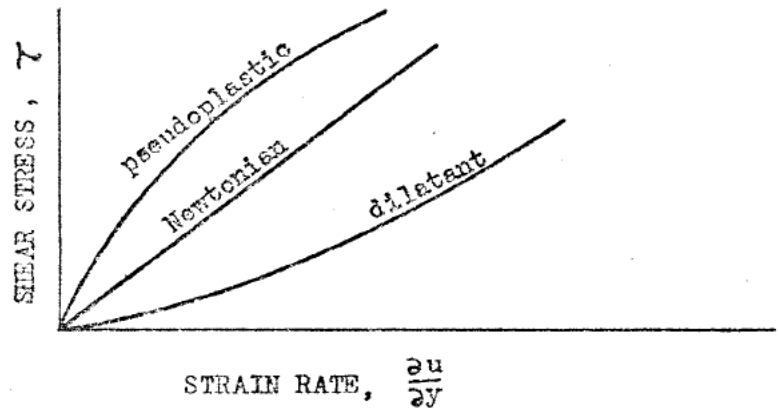

Fig. 1.1 Flow curves for various power law fluids.

Pseudoplastic fluids are probably the most common among industrial non-Newtonian fluids. They include rubber solutions, biological fluids, adhesives, polymer solutions or melts, starch suspensions, cellulose acetate, greases, mayonnaise, soap, detergent slurries, paper pulp, paints, napalm, solutions used in rayon manufacturing and dispersion media in certain pharmaceuticals. Dilatant fluids are those showing volumetric and rheological dilatancy, such as starch, potassium silicate, or gum arabic in water, quick-sand, wet beach sand, many defloculated pigment dispersions containing high concentrations of suspended solids and some corn flour or sugar solutions. (2,3)

1.2 External Laminar Free Convection

"Free" or "natural" convection is caused by the difference in density between a heated or cooled fluid and an undisturbed fluid. When free convection occurs about a body of interest in a fluid and the fluid flow is governed by laminar boundary layer theory, the process is called external laminar free convection. According to laminar boundary layer theory, the governing differential equations for laminar free convection of power law fluids can be obtained in the same manner as for the well-known laminar free convection of Newtonian fluids found in standard references (4, 5, 6). For a two-dimensional heated body which has a simple and symmetrical geometry and flow field such as a vertical plate, a horizontal cylinder, or a sphere in an incompressible power law fluid, the laminar free convection boundary layer equations can be simplified to become

$$\frac{\partial u}{\partial x} + \frac{\partial v}{\partial y} = 0 \tag{1.3}$$

$$u\frac{\partial u}{\partial x} + v\frac{\partial u}{\partial y} = g\beta(t-t_\infty)\sin\alpha + \frac{m}{\rho}\frac{\partial}{\partial y}\left(\left|\frac{\partial u}{\partial y}\right|^{N-1}\frac{\partial u}{\partial y}\right) \tag{1.4}$$

$$u\frac{\partial t}{\partial x} + v\frac{\partial t}{\partial y} = \frac{k}{\rho C_p}\frac{\partial^2 t}{\partial y^2} \tag{1.5}$$

where constant properties have been assumed, except for the density in the buoyancy term. The viscous dissipation is assumed negligible. The symbols used in these equations have the usual meaning and are shown in Fig. 1.2.

β is defined by the so-called "Taylor-made equation of state" (7) as

$$\rho = \rho_\infty - \rho_\infty \beta (t - t_\infty) \qquad (1.6)$$

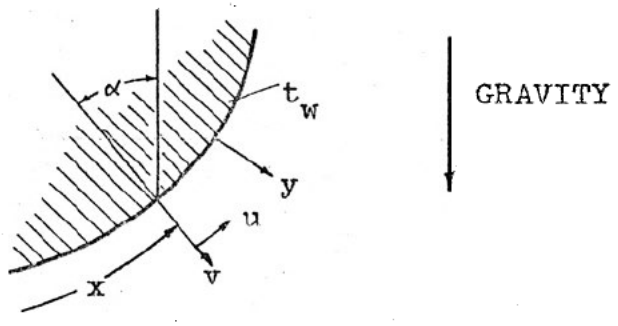

Fig. 1.2 The model of configuration for Equations (1.3-5).

1.3 Statement of the Problem

Since a realistic similarity solution of the coupled differential Equations (1.3-5) does not exist (8, 9, 11) (Note that the derivation and resulting conclusions of Reference 9 for laminar free convection are in error; see Appendix A1 for proof), this research seeks any possible realistic similarity solution of the external laminar free convection to power law fluids under prescribed boundary conditions, such as a body with a uniform surface temperature or uniform surface heat flux to which the experimental results are available. The motivation for seeking a realistic similarity solution is three-fold (10):

1. The general trends of the physical occurrences may be observed.

2. A standard of comparison can be provided and checked against experimental results and any other methods of solution such as integral approximate methods, finite difference techniques, etc. Once verified by this realistic similarity solution, the other method of solution may then be used for studying more complex flow situations where a realistic similarity solution does not exist.
3. The results may be directly usable in important technical applications.

Acrivos (11) appears to be the only one who attempted to obtain a realistic similarity solution for the laminar free convection of a power law fluid past an isothermal body. He used a similarity transformation to convert the partial differential equations into ordinary differential equations based on the assumption that most power law fluids have a high generalized Prandtl number and so the inertia terms in the momentum equation become negligible near the wall. He then obtained the similarity solution by applying the high Prandtl number theory developed for well-established Newtonian flow, first initiated by Morgan and Warner (12) and later illustrated by Stewartson and Jones (13). Acrivos postulated that for generalized Prandtl number higher than ten, the entire laminar flow field could be divided into two regions, an inner region in which the entire thermal boundary layer lies and an outer region where only a momentum boundary layer exists. Thus, the heat

transfer parameters could be calculated by simply obtaining the inner-region solution. He concluded that the average rates of heat transfer in laminar free convection could be adequately computed from the expression

$$\overline{Nu} = C\ Gr_A^{\frac{1}{2(N+1)}}\ Pr_A^{\frac{N}{3N+1}} \qquad (1.7)$$

where the constant C (approximately equal to 0.55) is only weakly dependent on the numerical value of N; Gr_A and Pr_A are the generalized Grashof number and generalized Prandtl number defined by Acrivos.

Unfortunately, the constant C is not conclusively verified by the experimental works of Reilly et al. (14) and Sharma and Adelman (15) for an isothermal vertical plate in a non-Newtonian fluid. Their experimental data indicates that the constant C depends somewhat on N.

In view of the differences of previous published results for laminar free convection of non-Newtonian power law fluids, the present analysis introduces a new concept of the so-called "generalized Prandtl number" so that the method of obtaining a similarity solution for high generalized Prandtl number non-Newtonian power law fluids can be justified. The similarity solutions for laminar free convection to a non-Newtonian power law fluid from a body with uniform surface temperature and uniform surface heat flux (which has not previously been solved) will be presented in terms of this new concept and method of solution. Previ-

ous analytical and experimental works will be compared with the present solution. Theoretical dimensionless temperature and velocity profiles will also be presented. The exact (similarity) solutions of the laminar free convection to Newtonian fluids from a vertical plate with a uniform surface temperature, obtained by Ostrach (16), and with a uniform surface heat flux, obtained by Sparrow and Gregg (17) will also be presented for comparison.

CHAPTER II

REVIEW OF RELATED LITERATURE

The literature covering free convection flow characteristics and heat transfer phenomena in non-Newtonian power law fluids is very limited. However, the experimental and analytical techniques learned from Newtonian flow theory form an excellent foundation for the non-Newtonian flow researchers to follow. The merit is clearly stated by Academician Gleb Maksimil'yanovich Krizhizhanovskii:

> "Try more to direct attention to the areas between already well-established sciences. These are usually the points of maximum growth of our knowledge."

Therefore, both reported Newtonian and non-Newtonian power law fluid flow studies will be reviewed. Because Newtonian flow studies in free convection are numerous and have been developed since early in the nineteenth century and their progress has been reported in most heat transfer text books (for example, (18, 19)), only those significant studies using similarity approaches and those related experimental works on vertical plates, horizontal cylinders and spheres will be mentioned.

2.1 Newtonian Fluids

2.1.1 Uniform surface temperature:

Possible similarity solutions for laminar free convection on a vertical plate in Newtonian fluids are summarized by Yang (20). It appears that Pohlhausen (21) was the first one to convert the governing partial differential equations for laminar free convection about an isothermal vertical plate into the ordinary differential equations by means of a similarity transformation. Later, Ostrach (16) used rigorous mathematical arguments and reduced the conservation differential equations to the ordinary differential equations obtained by (21). The governing partial differential equations are the same as Equations (1.3-5), if N=1, $\sin\alpha=1$, and m is replaced by μ. The ordinary differential equations and boundary conditions obtained after applying the similarity transformation are

$$F''' + 3FF'' - 2F'^2 + H=0 \qquad (2.1)$$

$$H'' + 3Pr\ FH' =0 \qquad (2.2)$$

B. C. $$F(0)=F'(0)=H(0)-1=F'(\infty)=H(\infty)=0 \qquad (2.3)$$

where the similarity variable η is

$$\eta = \left(\frac{Grx}{4}\right)^{\frac{1}{4}} \frac{y}{x} \qquad (2.4)$$

and the reduced functions are

$$H(\eta) = \frac{t - t_\infty}{t_w - t_\infty} \qquad (2.5)$$

$$F'(\eta) = \frac{ux}{\nu}\Big/(2Grx^{\frac{1}{2}}) \qquad (2.6)$$

with the local Grashof number Grx defined as

$$Grx = \left(\frac{\rho}{\mu}\right)^2 g\beta x^3 (t_w - t_\infty) \qquad (2.7)$$

Equations (2.1) and (2.2) with the boundary conditions (2.3) were solved by means of a series expansion for Pr=0.733 by Pohlhausen, and by means of numerical analysis for Pr=0.01 to 1000 by Ostrach (16). An improved method for the numerical solution of the differential equations was presented by Nachtsheim and Swigert (22) who demonstrated that the convergence rate becomes more rapid by establishing a least-squares convergence criterion.

Experimental results on an isothermal vertical plate are numerous. The most significant results are those of Schmidt and Beckmann (21); their experimental results verified the similarity solutions of Ostrach and Pohlhausen. Recently, Brodowicz (23) used a photographic dust tracing technique to obtain the velocity field and a Mach-Zehnder interferometer for the temperature field around an isothermal vertical plate and its leading edge. The Mach-Zehnder interferometer has been frequently used, such as (24), for temperature measurements of Newtonian free convection problems. Kierkus (25) presented experimental data on both vertical and inclined isothermal plates which were later supplemented with more information by Hassan and Mohamed (25).

A similarity solution for laminar free convection

around an arbitrary two-dimensional body was attempted by Merk and Prins (6) with less success; they concluded that a similarity solution exists only in the neighborhood of the lower stagnation point of a horizontal cylinder. So far, for the case of the isothermal horizontal cylinder or sphere, no similarity solution has been found. This is simply because the similarity solution for the governing differential equations, without further simplifying them, does not exist around the entire surface of the subject. Therefore most of the researchers (27, 28, 29) preferred to use a perturbation method or a series transformation to deal with this type of problem, obtaining a non-similarity solution, etc.

Experimental data on free convection from a horizontal cylinder in gases or liquids are plentiful (see, for example, (18)), while it is relatively sparce for a sphere. No experimental data on free convection to a single solid sphere in quiescent liquids has been found. So far, research experimentalists seem to concentrate on a fuel or liquid droplet during evaporation and then apply the analogy between heat and mass transfer (30, 31), or to concentrate on a rigid sphere of very small diameter in gases (32, 33).

2.1.2 Uniform surface heat flux:

Laminar free convection from a body with uniform heat flux has been studied extensively for vertical plates

in Newtonian fluids. Sparrow and Gregg (17) appear to be the first ones to have obtained a similarity solution for laminar free convection to a vertical plate with uniform surface heat flux. Later, they extended their work to become more generalized by specifying the wall temperature variation for both power law and exponential cases (34). Their work has been analysed and included in (20). A similar work of Sparrow and Gregg (34) has been presented by Gebhart (35) and later by Gebhart and Mollendorf (36) on the studies of laminar free convection to an isothermal or non-isothermal vertical plate with or without viscous dissipation. Similarity solutions and perturbation solutions respectively were obtained with a specified dissipation parameter.

Thus, according to Sparrow and Gregg (17) for a vertical plate with uniform heat flux and negligible viscous dissipation, the governing partial differential equations, which are the same as for the uniform surface temperature case, are transformed into ordinary differential equations to become

$$F''' - 3F'^2 + 4FF'' - H = 0 \qquad (2.8)$$

$$H'' + Pr\,(4H'F - HF') = 0 \qquad (2.9)$$

with boundary conditions

$$F(0)=F'(0)=H'(0)-1=F'(\infty)=H(\infty)=0 \qquad (2.10)$$

where the similarity variable η is

$$\eta = \frac{y}{x}\left(\frac{Grx^*}{5}\right)^{1/5} \tag{2.11}$$

and the reduced functions are

$$F'(\eta) = \frac{ux}{5\nu}\left(\frac{5}{Grx^*}\right)^{2/5} \tag{2.12}$$

$$H(\eta) = \frac{t_\infty - t}{\frac{qx}{k}}\left(\frac{Grx^*}{5}\right)^{1/5} \tag{2.13}$$

with the local modified Grashof number Grx^* defined as

$$Grx^* = \frac{g\beta q x^4}{k\nu^2} \tag{2.14}$$

Experimental results have been reported by Dotson (37) and Goldstein and Eckert (38). The comparison between measured heat transfer rates and those predicted by Sparrow and Gregg (17) is good. Unfortunately, no velocity measurements have been presented. Very recently, Vliet and Lieu (39) presented an experimental study of laminar and turbulent natural convection in water and found that the local Nusselt number can be correlated well with

$Nux = 0.60\ (Grx^* \cdot Pr)^{1/5}$ for laminar free convection

and

$Nux = 0.568(Grx^* \cdot Pr)^{0.22}$ for turbulent free convection

The correlation for laminar free convection compares favorably with Sparrow and Gregg's prediction. An experimental study of laminar free convection from a vertical

plate in a high Prandtl number Newtonian fluid (Pr = 6 to 10^6) is reported by Rajan and Picot (40). Unfortunately, all the experimental data reported in (40) were plotted and interpreted with the von Karman-Pohlhausen method (41, 42) which is suitable only for fluids having a Prandtl number near or equal to unity.

No information on free convection about a body with uniform surface heat flux other than those vertical plate cases has been found.

2.2 Non-Newtonian Power Law Fluids

In contrast to the numerous studies dealing with Newtonian fluids, less progress has been made analytically and experimentally on free convection to non-Newtonian power law fluids.

2.2.1 Uniform surface temperature:

Acrivos (11) is the first and only one to publish an analytical study on laminar free convection about an isothermal body in non-Newtonian fluids using similarity transformation under the assumption of a high generalized Prandtl number. He showed that the inner-region solution, namely, the solution near the wall, could be derived by transforming the governing partial differential Equations (1.3-5) into ordinary differential equations with the inertia terms of the momentum equation neglected to give

$$\frac{d}{d\eta}(f'')^N + \phi = 0 \qquad (2.15)$$

$$\phi'' + f\,\phi' = 0 \tag{2.16}$$

with the boundary conditions

$$f(0)=f'(0)=\phi(0)-1=f''(\infty)=\phi(\infty)=0,\quad f'(\infty)\neq 0 \tag{2.17}$$

where, according to Acrivos, the similarity variable is

$$\eta=\frac{y}{L}\,Gr_A^{\frac{1}{2(N+1)}}\,Pr_A^{\frac{N}{3N+1}}\,\frac{1}{\left[\frac{3N+1}{2N+1}\left(\frac{1}{\sin\alpha}\right)^{\frac{3N+1}{N(2N+1)}}\int_0^{x/L}(\sin\alpha)^{\frac{1}{2N+1}}\,d\left(\frac{x}{L}\right)\right]^{\frac{N}{3N+1}}} \tag{2.18}$$

and the reduced functions are

$$\phi(\eta)=\frac{t-t_\infty}{t_w-t_\infty}=\frac{t-t_\infty}{\Delta t} \tag{2.19}$$

$$f'(\eta)=\frac{u}{(Lg\beta\Delta t)^{\frac{1}{2}}}\,\frac{Pr_A^{\frac{N+1}{3N+1}}}{(\sin\alpha)^{1/N}}\,\frac{1}{\left[\frac{3N+1}{2N+1}\left(\frac{1}{\sin\alpha}\right)^{\frac{3N+1}{N(2N+1)}}\int_0^{x/L}(\sin\alpha)^{\frac{1}{2N+1}}\,d\left(\frac{x}{L}\right)\right]^{\frac{N}{3N+1}}} \tag{2.20}$$

The generalized Grashof number Gr_A and the generalized Prandtl number Pr_A are defined as

$$Gr_A=\left(\frac{\rho}{m}\right)^2 L^{N+2}\,(g\beta\Delta t)^{2-N} \tag{2.21}$$

$$Pr_A=\frac{\rho C_p}{k}\left(\frac{m}{\rho}\right)^{\frac{2}{1+N}} L^{\frac{1-N}{1+N}}\,(Lg\beta\Delta t)^{\frac{3(N-1)}{2(N+1)}} \tag{2.22}$$

Unfortunately, the heat transfer results from the inner-region solution predicted by Acrivos have not been experimentally verified, particularly for small values of power law fluid index N. ((14, 15), see also Section 1.3). No velocity profiles have been presented by these authors.

Tien (42) also attempted to solve the problem of laminar free convection from a vertical plate to power law fluids using an integral method with the same high generalized Prandtl number assumption for power law fluids as Acrivos (11). His results are difficult to justify because the assumption of a high generalized Prandtl number could contradict his assumption of approximately equal thermal and momentum boundary layer thickness. However, it will be shown later that the integral method gives fair results only for N>1 because of the special characteristics of the generalized Prandtl number.

A study related to the laminar free convection of non-Newtonian power law fluids was made by Kubair and Pei (43). They obtained a similarity solution of the combined laminar free and forced convection heat transfer to non-Newtonian power law fluids which merely verified the work of Na and Hansen (8) and Sparrow et al. (10). In fact, a realistic similarity solution (a non-realistic similarity solution may have a wall temperature varying inversely with distance along the plate from the leading edge) cannot be obtained for the coupled partial differential equations of the combined convection, because it can be demonstrated that the combined convection controlling parameter is a constant only when $t_w - t_\infty \equiv B\, x^{-1/3}$, and the generalized Prandtl number is a constant only when $u_\infty \equiv A\, x^{1/3}$. After a careful exami-

nation of the dimensionless groups, it was found that their derivation was invalid because using their dimensionless groups the continuity equation could not be satisfied. This is demonstrated in Appendix A2.

2.2.2 Uniform surface heat flux:

Very little progress has been made theoretically and experimentally on free convection to a non-isothermal body in non-Newtonian fluids. Tien (42) attempted to solve the laminar free convection about a vertical plate with uniform surface heat flux in a power law fluid by means of the integral method, using the same high generalized Prandtl number assumption as Acrivos (11) who obtained the "inner-region" solution with a similarity transformation for uniform surface temperature case. As in the case of uniform surface temperature, Tien's re-results are again difficult to justify because of the assumption of high Prandtl number.

An experimental investigation has been reported by Dale (44) on the behavior of non-Newtonian pseudoplastic power law fluids in the state of free convection from a vertical plate with uniform heat flux. He applied a finite difference computation technique to verify his experimental data with some success without using the condition of high generalized Prandtl number. In order to achieve convergence, he assigned experimentally and/or arbitrarily a critical value of strain rate to each spe-

cified power law fluid index and then matched the computation from non-Newtonian flow (where the strain rate is higher than the critical value) to Newtonian flow (where the strain rate is lower than the critical value). Therefore, as a result, the velocity and temperature fields far downstream from the wall are essentially Newtonian. He concluded his investigation with the following remark:

> "Acrivos' modified correlation, derived for the assumption that asymptotically the generalized Prandtl number approaches infinity, predicts the proper exponent for correlating the heat transfer data. However, the coefficient for the constant heat flux vertical flat plate correlation can not be predicted, limiting a complete solution by Acrivos' technique to the isothermal boundary condition."

Very recently, Emery et al. (45), in need of a theoretical analysis, applied Acrivos theoretical solution for an isothermal flat plate to their experimental data correlation on free convection through vertical plane layers with uniform surface heat flux. Fortunately, as with Newtonian flow (17), heat transfer parameters can be correlated in the same fashion for both uniform surface temperature and uniform surface heat flux cases; the only restriction is a proper definition of the Nusselt number.

CHAPTER III

LAMINAR FREE CONVECTION HEAT TRANSFER ABOUT A BODY WITH A UNIFORM SURFACE TEMPERATURE IN POWER LAW FLUIDS

3.1 Theoretical Analysis

For an arbitrary two-dimensional and isothermal body in an incompressible power law fluid, the laminar free convection boundary layer Equations (1.3-5) can be written in dimensionless forms as

$$\frac{\partial U}{\partial X} + \frac{\partial V}{\partial Y} = 0 \tag{3.1}$$

$$\frac{\partial}{\partial Y}\left(\left|\frac{\partial U}{\partial Y}\right|^{N-1}\frac{\partial U}{\partial Y}\right) + \theta \sin\alpha = \frac{1}{Pr_A^{2(N+1)/(3N+1)}}\left(U\frac{\partial U}{\partial X} + V\frac{\partial U}{\partial Y}\right) \tag{3.2}$$

$$\frac{\partial^2 \theta}{\partial Y^2} = U\frac{\partial \theta}{\partial X} + V\frac{\partial \theta}{\partial Y} \tag{3.3}$$

The dimensionless variables used in the above equations are

$$X = \frac{x}{L} \tag{3.4}$$

$$Y = \frac{y}{L} Gr_A^{\frac{1}{2(N+1)}} Pr_A^{\frac{N}{3N+1}} \tag{3.5}$$

$$\theta = \frac{t - t_\infty}{t_w - t_\infty} = \frac{t - t_\infty}{\Delta t} \tag{3.6}$$

$$U = \frac{u}{(Lg\beta\Delta t)^{\frac{1}{2}}} Pr_A^{\frac{N+1}{3N+1}} \tag{3.7}$$

$$V = \frac{v}{(Lg\beta\Delta t)^{\frac{1}{2}}} Gr_A^{\frac{1}{2(N+1)}} Pr_A^{\frac{2N+1}{3N+1}} \tag{3.8}$$

where L is the characteristic length in which the flow is laminar; Gr_A and Pr_A are respectively the generalized Grashof number and the generalized Prandtl number, defined by Acrivos (11). (See Equations (2.21) and (2.22)).

The boundary conditions for this uniform surface temperature case are: at y=0, u=v=0, $t=t_w$=constant; at $y=\infty$, u=0, $t=t_\infty$ =constant; and at x=0, u=0, $t=t_\infty$ =constant. Using the dimensionless variables, the boundary conditions may be written as

$$\begin{aligned} &\text{At} \quad Y=0,\ U=V=0,\ \theta=1 \\ &\text{At } Y=\infty \text{ and } X=0.\ U=\theta=0 \end{aligned} \tag{3.9}$$

Since a realistic similarity solution does not exist in the coupled differential Equations (3.1-3) and their boundary conditions (3.9), it is necessary to neglect the inertia terms of the momentum Equation (3.2) to make a realistic similarity solution possible. It is generally true that most non-Newtonian power law fluids have a relatively large generalized Prandtl number and, therefore, the right hand side of Equation (3.2) can be neglected. It becomes

$$\frac{\partial}{\partial Y}\left(\left|\frac{\partial U}{\partial Y}\right|^{N-1} \frac{\partial U}{\partial Y} \right) + \theta \sin\alpha = 0 \tag{3.2a}$$

Some authors (11, 12, 13, 46) argue that as the Prandtl number becomes very large, there are two distinct regions of flow, one is near the wall called the 'inner region' where the inertia terms become asymptotically unimportant; the other is far from the wall called the

'outer region' where both thermal and buoyancy forces, but not the inertia terms, vanish. Thus, the velocity and temperature distribution near the wall, which characterize most of the fluid flow phenomena, can be obtained just by looking into the inner region. They presumed that the boundary conditions in the inner region associated with the governing differential Equations (3.1), (3.2a) and (3.3) should be

$$\begin{aligned} &\text{At } Y=0,\ U=V=0,\ \theta=1 \\ &\text{At } X=0,\ U=\theta=0 \\ &\text{At } Y=\infty,\ \frac{\partial U}{\partial Y}=\theta=0,\quad U\neq 0 \end{aligned} \tag{3.10}$$

In fact, such an analysis is not necessary. Since the exact solution for Newtonian flow is well-known, (16), the difference between their inner-region solution which uses boundary conditions (3.10) and the present 'region-free' solution which uses boundary conditions (3.9) can be seen by comparing these two solutions with the exact solution. It will be shown later (see Table 3.1) that the region-free solution yields results which are equivalent or better than the inner-region solution for N=1. Furthermore, an examination of the generalized Prandtl number for this isothermal laminar free convection to power law fluids reveals a significant difference between the present analysis and that using a divided flow region. The generalized Prandtl number can be rearranged to give (see Equation (2.22))

Table 3.1

Comparison of the region-free and inner-region solutions with the exact solution for Newtonian flow (uniform surface temperature case)

Table 3.1a Comparison of F"(0) and H'(0)

Pr		Exact solution: Ostrech (16)	Exact solution: Present result*	Region-free solution**	Inner-region solution**
0.01	F"(0)	0.9862	0.98679	2.53091	2.60735
	H'(0)	-0.0812	-0.08101	-0.22051	-0.22483
0.1	F"(0)	———	0.85889	1.42323	1.46622
	H'(0)		-0.23015	-0.39212	-0.39982
1	F"(0)	0.6421	0.64209	0.80034	0.82452
	H'(0)	-0.5671	-0.56712	-0.69731	-0.71099
5	F"(0)	———	0.48099	0.53522	0.55139
	H'(0)		-0.95338	-1.04272	-1.06318
10	F"(0)	0.4192	0.41860	0.45007	0.46366
	H'(0)	-1.1694	-1.16851	-1.24001	-1.26434
100	F"(0)	0.2517	0.24973	0.25309	0.26073
	H'(0)	-2.1910	-2.18131	-2.20508	-2.24835
1000	F"(0)	0.1450	0.14319	0.14232	0.14662
	H'(0)	-3.9660	-3.93439	-3.92125	-3.99819

* Present results were calculated by the author using Nachtsheim and Swigert's method (22) which assures equal accuracy to each value by a specified maximum allowable error.

** $F''(0)=f''(0)/(3Pr)^{1/3}$; $H'(0)=\phi'(0)(3Pr)^{1/3}$

Table 3.1b Comparison of heat transfer parameters

Pr		Exact Solution Present result	Region-Free Solution Value	Region-Free Solution Deviation** %	Inner-Region Solution Value	Inner-Region Solution Deviation** %
0.01	LHTP*	0.08101	0.22051	-172.2	0.22483	-177.5
	AHTP*	0.03273	0.08910		0.09085	
0.1	LHTP	0.23015	0.39212	-70.4	0.39982	-73.7
	AHTP	0.09300	0.15844		0.16155	
1	LHTP	0.56712	0.69731	-23.0	0.71099	-25.4
	AHTP	0.22915	0.28175		0.28728	
5	LHTP	0.95338	1.04272	-9.4	1.06318	-11.5
	AHTP	0.38522	0.42132		0.42959	
10	LHTP	1.16851	1.24001	-6.1	1.26434	-8.2
	AHTP	0.47215	0.50104		0.51087	
100	LHTP	2.18131	2.20508	-1.1	2.24835	-3.1
	AHTP	0.88138	0.89099		0.90847	
1000	LHTP	3.93439	3.92125	0.3	3.99819	-1.6
	AHTP	1.58973	1.58442		1.61551	

* LHTP = $Nux / (\frac{Grx}{4})^{\frac{1}{4}}$

AHPT = $\overline{Nu} / Gr^{\frac{1}{4}}$

** Deviation = $(1 - \frac{\text{Present solution}}{\text{Exact solution}}) \times 100$

$$Pr_A = \frac{\frac{\mu}{\rho}}{\frac{k}{\rho C_p}} \frac{\rho}{\mu} \left(\frac{m}{\rho}\right)^{\frac{2}{1+N}} \frac{1}{L^{\frac{1-N}{2(1+N)}} (g\beta\Delta t)^{\frac{3(1-N)}{2(1+N)}}}$$

$$= Pr \frac{L^{\frac{3}{2}} (g\beta\Delta t)^{\frac{1}{2}}}{\frac{\mu}{\rho}} \frac{1}{\left(\frac{\rho}{m}\right)^{\frac{2}{1+N}} L^{\frac{2+N}{1+N}} (g\beta\Delta t)^{\frac{2-N}{1+N}}}$$

Hence,

$$Pr_A = Pr \cdot \frac{Gr^{\frac{1}{2}}}{Gr_A^{\frac{1}{1+N}}} \qquad (3.11)$$

Thus, there is a factor relating the generalized Prandtl number for power law fluids and the Prandtl number for Newtonian fluids. This 'non-Newtonian factor'

$$f_N = \frac{Gr^{\frac{1}{2}}}{Gr_A^{\frac{1}{1+N}}}$$

is a function of Gr, Gr_A and N. Note that f_N=1 for N=1. Whenever Pr_A becomes higher it does not necessarily mean a higher value of Pr, which usually indicates high momentum boundary layer to thermal boundary layer ratio. This is probably the reason why the inner-region solution (Acrivos' solution) does not agree with experiment well.

We will proceed to obtain both the region-free solution and the inner-region solution for comparison

purposes, although the latter has already been obtained by Acrivos (11) using a different numerical calculation scheme.

The solution of Equation (3.1) can be written in terms of a dimensionless stream function ψ

$$U=\frac{\partial\psi}{\partial Y} \quad , \quad V = -\frac{\partial\psi}{\partial X} \tag{3.12}$$

The partial differential Equations (3.2a) and (3.3) are again transformed, this time to ordinary differential equations with the following substitutions

$$\eta = Y\frac{(\sin\alpha)^{\frac{1}{2N+1}}}{\left[\frac{3N+1}{2N+1}\int_0^X (\sin\alpha)^{\frac{1}{2N+1}}dX\right]^{\frac{N}{3N+1}}} \tag{3.13}$$

$$\psi = \left[\frac{3N+1}{2N+1}\int_0^X (\sin\alpha)^{\frac{1}{2N+1}}\,dX\right]^{\frac{2N+1}{3N+1}} f(\eta) \tag{3.14}$$

$$\theta = \phi(\eta) \tag{3.15}$$

The expression for U can be obtained from Equations (3.12) and (3.14) as

$$U = (\sin\alpha)^{\frac{1}{2N+1}}\left[\frac{3N+1}{2N+1}\int_0^X (\sin\alpha)^{\frac{1}{2N+1}}dX\right]^{\frac{N+1}{3N+1}} f'(\eta) \tag{3.16}$$

Note that this equation differs from Equation (22) of (1) in which there appears to be a typographical error.

The governing differential equations become

$$\frac{d}{d\eta}(|f''|^{N-1} f'') + \phi = 0 \qquad (3.17)$$

$$\phi'' + f\phi' = 0 \qquad (3.18)$$

The absolute value sign for f" is very important because f" changes sign as the integration proceeds from the wall outward.

The boundary conditions are now

1). for the region-free solution:

$$f(0)=f'(0)=\phi(0)-1=f'(\infty)=\phi(\infty)=0 \qquad (3.19)$$

2). for the inner-region solution:

$$f(0)=f'(0)=\phi(0)-1=f''(\infty)=\phi(\infty)=0,\ f'(\infty)\neq 0 \qquad (3.20)$$

Equations (3.17) and (3.18) with boundary conditions (3.19) and (3.20) respectively were solved numerically by a shooting method, using a fourth order Runge-Kutta formula to integrate, and the technique described by Nachtsheim and Swigert (22) to correct the first choice of the missing initial values f"(0) and $\phi'(0)$ until a solution was found which gave $f'(\infty)=0$ and $\phi(\infty)=0$ for the region-free solution, and, $f''(\infty)=0$ and $\phi(\infty)=0$ for the inner-region solution. In order to have equal accuracy for all calculated results for the purpose of comparison, the missing initial values were set in an automatic iteration program with a specified value of error E, such that

1). for the region-free solution

$$E=[f'(\infty)]^2+[f''(\infty)]^2+[\phi(\infty)]^2+[\phi'(\infty)]^2 \qquad (3.21)$$

2). for the inner-region solution

$$E = [f''(\infty)]^2 + [\phi(\infty)]^2 + [\phi'(\infty)]^2 \qquad (3.21a)$$

All calculations were performed on an IBM 360/50 using double precision. The procedures of the numerical solution with a flow chart for the computer program are illustrated in Appendix B. The results, values of $f''(0)$ and $-\phi'(0)$ versus N, for both solutions are plotted in Figs. 3.1 and 3.2. It is surprising to find that the results are quite different between both solutions for $N<1$. Present solutions were also converted to $F''(0)$ and $H'(0)$ for comparing with the exact solution of Ostrach (16). The results were listed in Table 3.1a. Appendix C gives the numerical values of $f''(0)$ and $\phi'(0)$ for the region-free solution.

3.2 Heat Transfer Results

3.2.1 Velocity and temperature distributions:

The theoretical dimensionless temperature distributions for isothermal laminar free convection from an arbitrary two-dimensional body in power law fluids are shown in Fig. 3.3 for the region-free solution. Fig. 3.4 shows the dimensionless velocity distributions and compares them with the inner-region solution for values of N=0.1, 0.5, 1.0, and 1.5. Again the difference is significant for small values of N. In contrast to those of the region-free solution, the dimensionless temperature distributions for the inner-region solution all lie very close to the one corresponding to N=1. For this reason, they will not be shown.

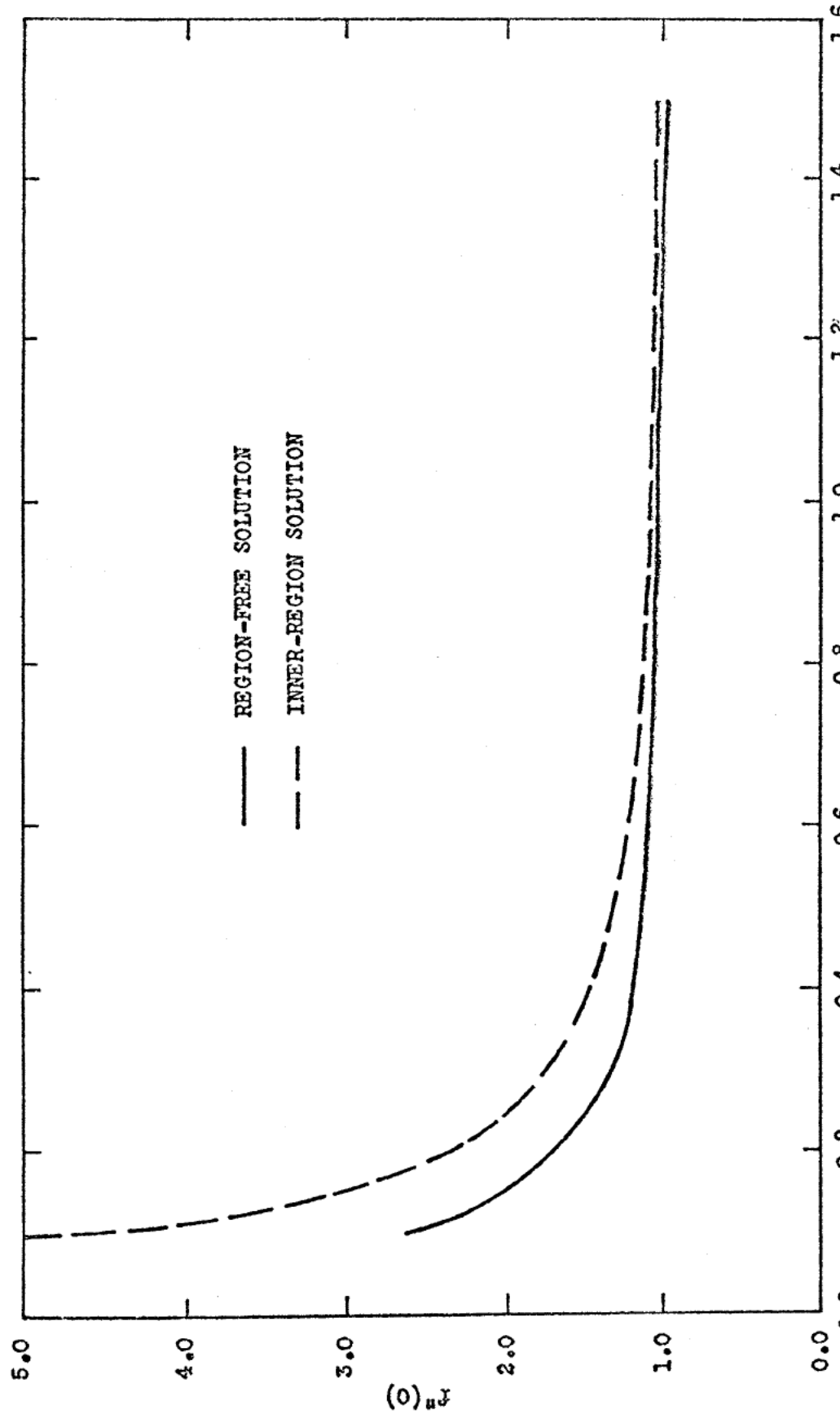

Fig. 3.1 Comparison of f"(0) versus N between the region-free and inner-region solutions.

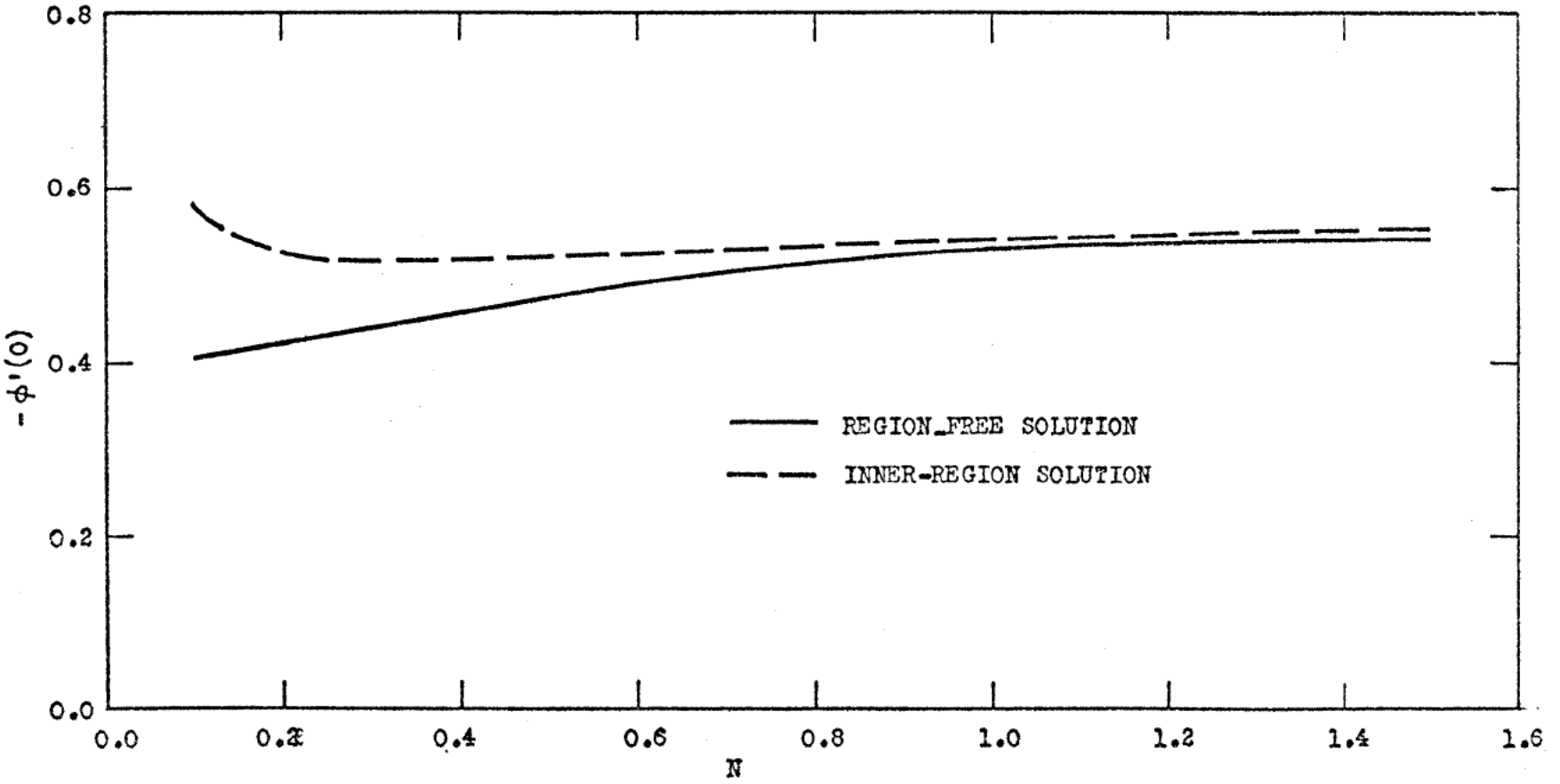

Fig. 3.2 Comparison of $-\phi'(0)$ versus N between the region-free and inner-region solutions.

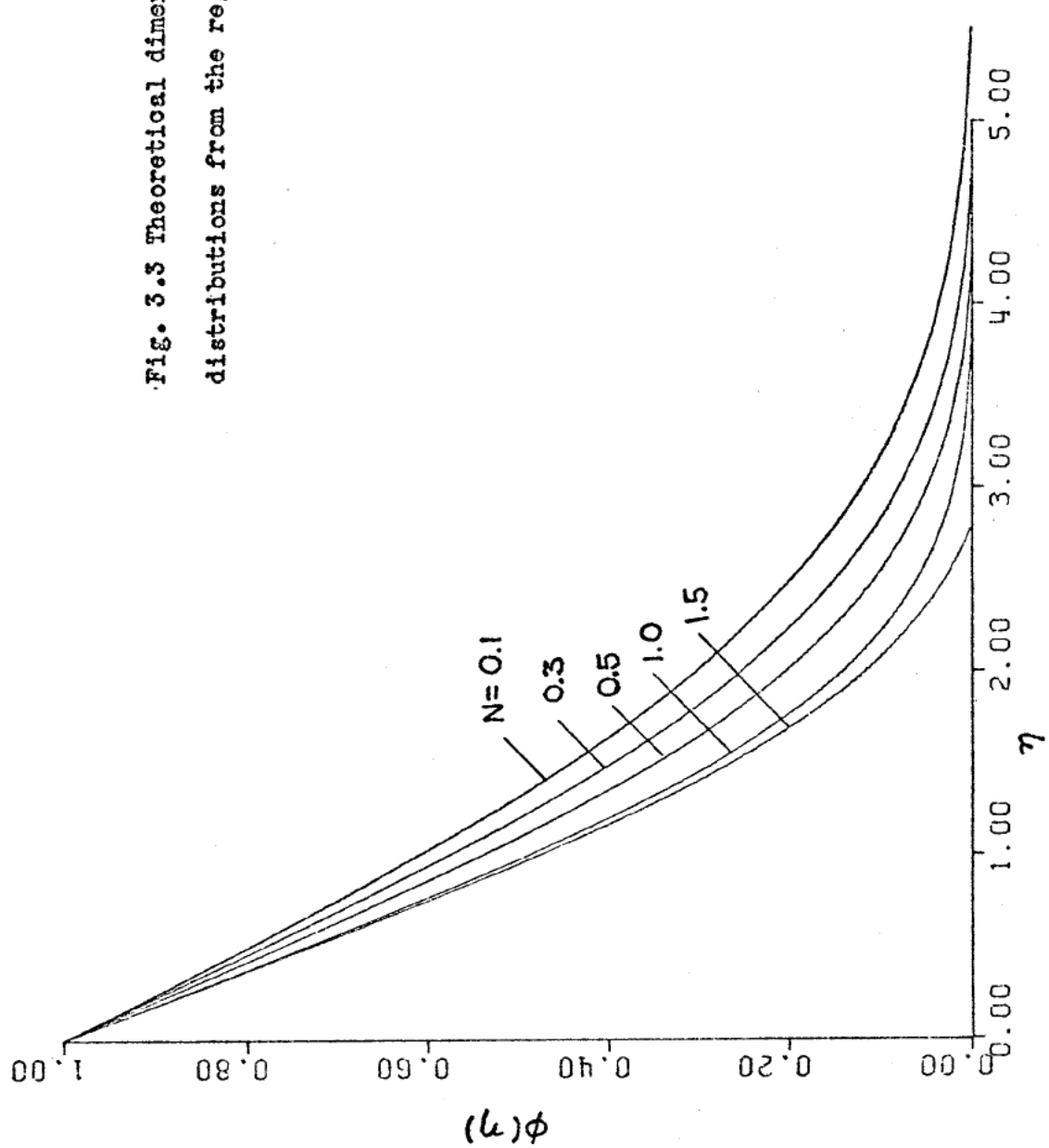

Fig. 3.3 Theoretical dimensionless temperature distributions from the region-free solution.

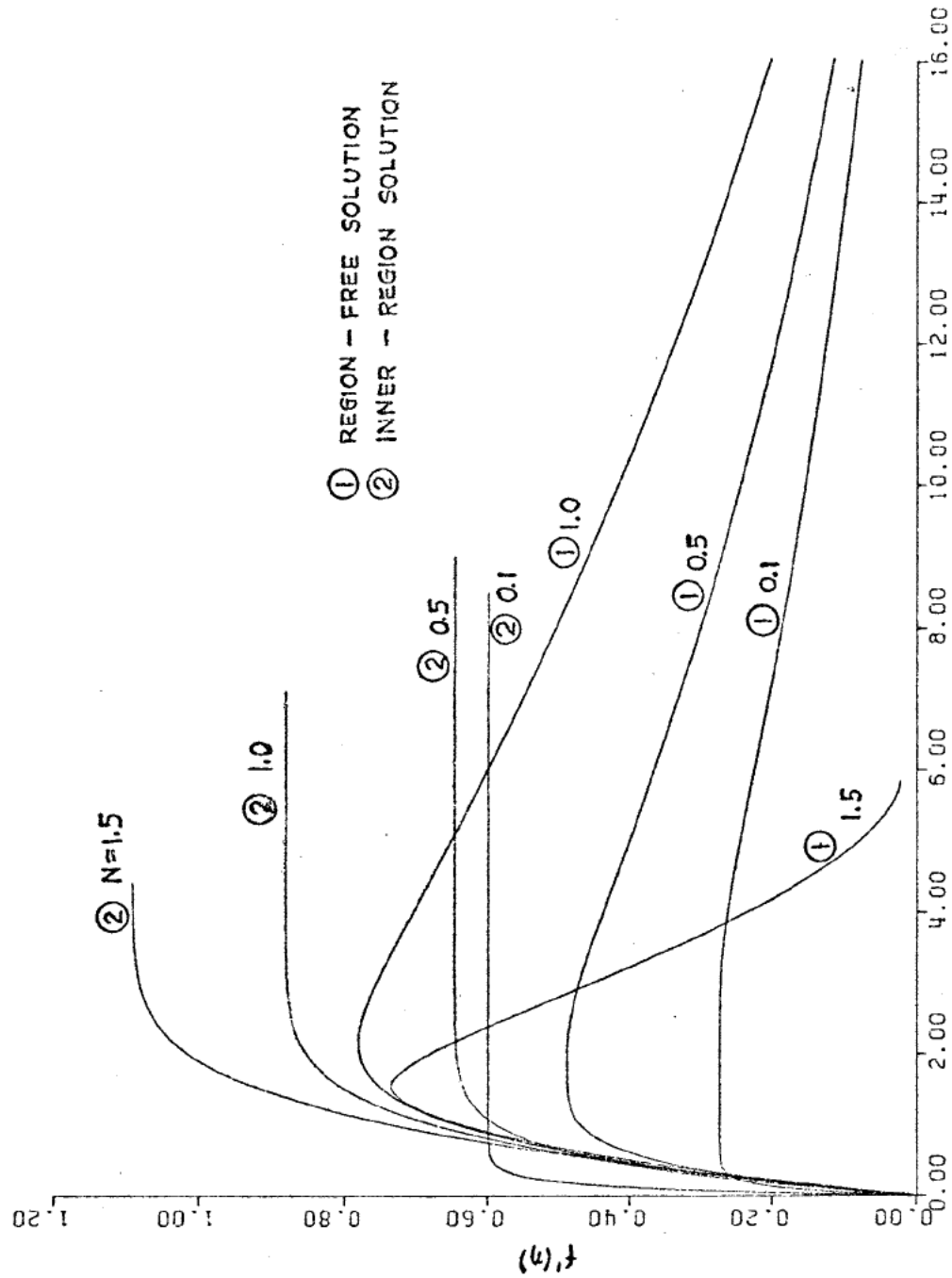

Fig. 3.4 Comparison of theoretical velocity distributions between the region-free and inner-region solutions.

For an isothermal vertical plate ($\sin\alpha=1$), it can be shown that

$$f'(\eta)=[(2N+1)\ Pr_A]^{\frac{N+1}{3N+1}}\frac{\left(\frac{u\ x^{\frac{2N(N+1)}{3N+1}}}{\frac{m}{\rho}}\right)\ L^{\frac{1-N^2}{2(3N+1)}}\ (g\beta\Delta t)^{\frac{1-N}{2}}}{(3N+1)^{\frac{N+1}{3N+1}}\ Grx_A^{\frac{1}{2}}} \tag{3.22}$$

and

$$\phi(\eta)=\frac{t-t_\infty}{t_w-t_\infty} \tag{3.23}$$

where

$$\eta=\frac{y}{L}\frac{Gr_A^{\frac{1}{2(N+1)}}\ Pr_A^{\frac{N}{3N+1}}}{\left(\frac{3N+1}{2N+1}\frac{x}{L}\right)^{\frac{N}{3N+1}}}$$

$$=\frac{y}{x}\left[\frac{Grx_A}{(3N+1)^{\frac{2N(N+1)}{3N+1}}}\right]^{\frac{1}{2(N+1)}}[(2N+1)\ Pr_A]^{\frac{N}{3N+1}} \tag{3.24}$$

and

$$Grx_A = Gr_A\left(\frac{x}{L}\right)^{\frac{2(2N+1)(N+1)}{3N+1}} \tag{3.25}$$

3.2.2 Flow parameter:

It is often desirable to define a flow parameter (16) from the shear stress at the wall

$$\tau_w = m\left(\frac{\partial u}{\partial y}\Big|_{y=0}\right)^N$$

By means of the various transformations made in the analysis, the flow parameter of laminar free convection to an isothermal two-dimensional body can be shown to have the following expression

$$\frac{\tau_w}{m\left(\frac{g\beta\Delta t}{L}\right)^{\frac{N}{2}} \frac{Gr_A^{\frac{N}{2(N+1)}}}{Pr_A^{\frac{N}{3N+1}}} (\sin\alpha)^{\frac{2N}{2N+1}} \left[\frac{3N+1}{2N+1}\int_0^{\frac{x}{L}} (\sin\alpha)^{\frac{1}{2N+1}} d\left(\frac{x}{L}\right)\right]^{\frac{N}{3N+1}}} = [f''(0)]^N \qquad (3.26)$$

For a vertical plate, Equation (3.26) becomes

$$\frac{\tau_w}{\left[(3N+1)^{\frac{2(2-N)(1+N)}{3N+1}} Grx_A^3\right]^{\frac{N}{2(2-N)(1+N)}} \frac{m\left(\frac{m}{\rho}\right)^{\frac{N}{2-N}}}{\left[(2N+1)Pr_A\right]^{\frac{N}{3N+1}} \left(\frac{x^{7N+1}}{L^{N-1}}\right)^{\frac{N}{(2-N)(3N+1)}}}} = [f''(0)]^N \qquad (3.27)$$

Note that Equation (3.27) is comparable with that from (16) when N=1. Fig. 3.5 shows the comparison between the region-free solution and the inner-region solution, calculated from Equation (3.26). The difference is again significant for small N.

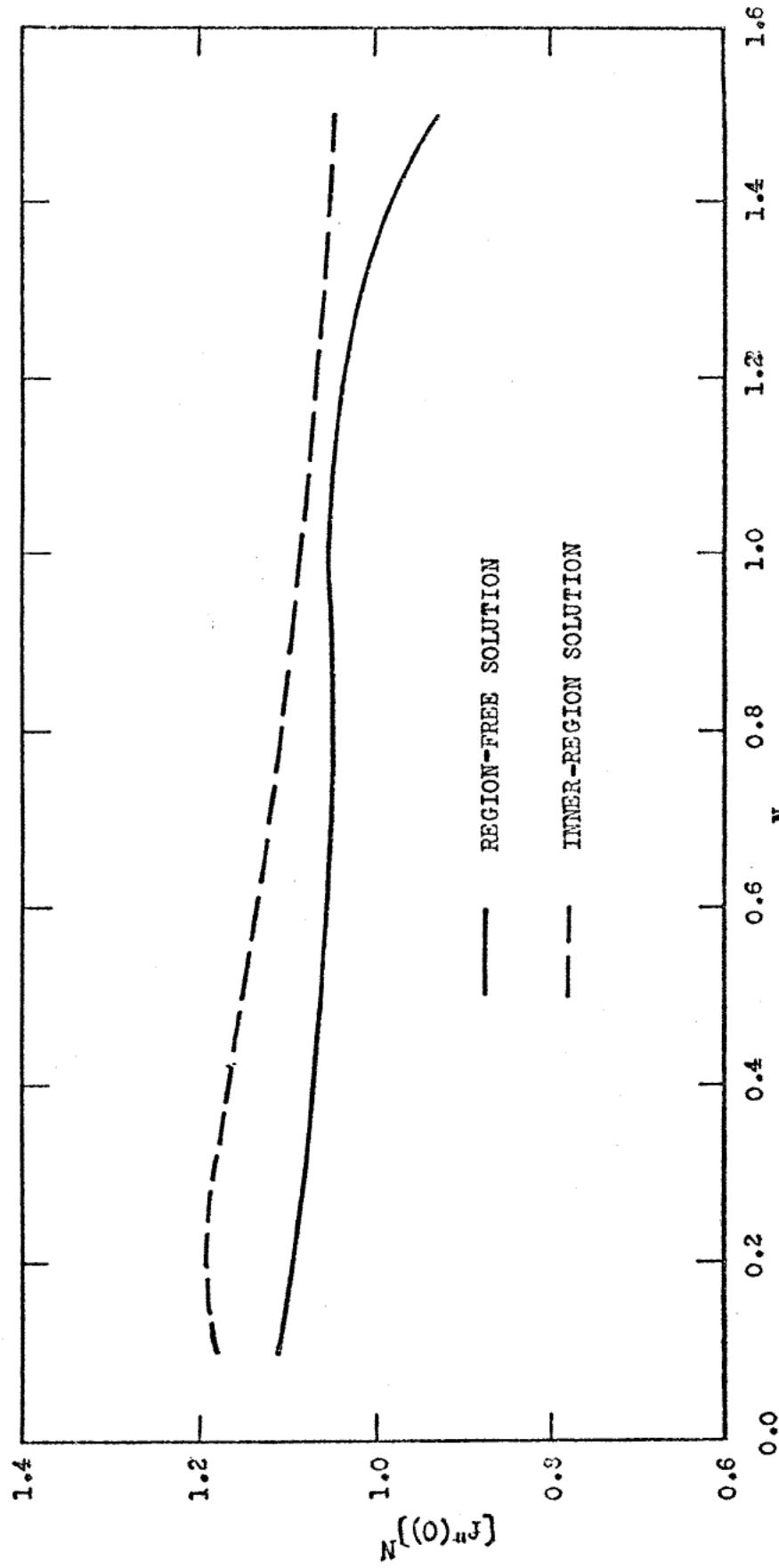

Fig. 3.5 Comparison of flow parameters between the region-free and inner-region solutions.

3.2.3 Heat transfer parameter:

Two different definitions of the local Nusselt number Nux have been used in the literature. Nux is defined by Ostrach (16) as

$$Nux = \frac{hx}{k} = - \frac{x}{t_w - t_\infty} \frac{\partial t}{\partial y}\Big|_{y=0} \qquad (3.28)$$

This can be written

$$Nux = -\phi'(0)\ Gr_A^{\frac{1}{2(N+1)}}\ Pr_A^{\frac{N}{3N+1}}\ \frac{x}{L}\ S(x) \qquad (3.29)$$

where

$$S(x) = \frac{(\sin\alpha)^{\frac{1}{2N+1}}}{\left[\frac{3N+1}{2N+1}\int_0^{\frac{x}{L}} (\sin\alpha)^{\frac{1}{2N+1}}\ d(\frac{x}{L})\right]^{\frac{N}{3N+1}}} \qquad (3.29a)$$

For a vertical plate, the local heat transfer parameter can be obtained from Equations (3.29) and (3.25) as

$$\frac{Nux}{\left[\dfrac{Grx_A}{(3N+1)^{\frac{2N(N+1)}{3N+1}}}\right]^{\frac{1}{2(N+1)}}} = -\phi'(0)\ [(2N+1)Pr_A]^{\frac{N}{3N+1}} \qquad (3.30)$$

or

$$Nux = -\phi'(0)\ (\frac{2N+1}{3N+1})^{\frac{N}{3N+1}}\ Pr_A^{\frac{N}{3N+1}}\ Gr_A^{\frac{1}{2(N+1)}}\ (\frac{x}{L})^{\frac{2N+1}{3N+1}} \qquad (3.30a)$$

The average heat trasnfer parameter can be obtained by defining the average Nusselt number $\overline{Nu}$ as

$$\overline{Nu} = \frac{1}{L}\int_0^L Nux\, dx \qquad (3.31)$$

to yield

$$\frac{\overline{Nu}}{Gr_A^{\frac{1}{2(N+1)}}} = -\phi'(0)\left[(2N+1)Pr_A\right]^{\frac{N}{3N+1}} \frac{(3N+1)^{\frac{2N+1}{3N+1}}}{5N+2} \qquad (3.32)$$

For N=1, Gr_A= Gr and Grx_A = Grx; the local and average heat transfer parameters, Equations (3.30) and (3.32), are summarized and compared with those of the exact solution in Table 3.2.

Table 3.2 Expressions for the local and average heat transfer parameters for N=1.

Heat transfer parameter	Exact solution	Present solution
$Nux/(\frac{Grx}{4})^{\frac{1}{4}}$	$-H'(0)$	$-\phi'(0)(3Pr)^{\frac{1}{4}}$
$\overline{Nu} \,/\, Gr^{\frac{1}{4}}$	$-H'(0)\,\frac{4}{7}^{\frac{3}{4}}$	$-\phi'(0)(3Pr)^{\frac{1}{4}}\,\frac{4}{7}^{\frac{3}{4}}$

Note that the average heat transfer parameter calculated by Ostrach (16) is $-H'(0)\, 4^{3/4}/3$ which could be obtained by substituting $Nux = \frac{hL}{k}$ into Equation (3.31). The results have been calculated and tabulated in Table 3.1b. Again the region-free solution is closer to the exact

solution than the inner-region solution.

Several authors (11, 14, 15, 42) define the local Nusselt number as

$$Nux = \frac{hL}{k} = - \frac{L}{t_w - t_\infty} \frac{\partial t}{\partial y}\bigg|_{y=0} \tag{3.33}$$

to yield

$$Nux = -\phi'(0)\ Gr_A^{\frac{1}{2(N+1)}}\ Pr_A^{\frac{N}{3N+1}}\ S(x) \tag{3.34}$$

where S(x) has already been defined in Equation (3.29a).

For an isothermal vertical plate, the local and average heat transfer parameters have the following forms

$$\frac{Nux}{Gr_A^{\frac{1}{2(N+1)}}\ Pr_A^{\frac{N}{3N+1}}\ (\frac{x}{L})^{\frac{-N}{3N+1}}} = -\phi'(0)\ (\frac{2N+1}{3N+1})^{\frac{N}{3N+1}} \tag{3.35}$$

$$\frac{\overline{Nu}}{Gr_A^{\frac{1}{2(N+1)}}\ Pr_A^{\frac{N}{3N+1}}} = -\phi'(0)\ (\frac{3N+1}{2N+1})^{\frac{2N+1}{3N+1}} \tag{3.36}$$

Equations (3.35) and (3.36) are plotted in Fig. 3.6 for the region-free and inner-region solutions. It is again found that the region-free solution separates from the others for N<1.

3.3 Experimental Verification

The only available experimental results were those of Reilly et al. (14) and Sharma and Adelman (15) on an isothermal vertical plate in a power law fluid. The former

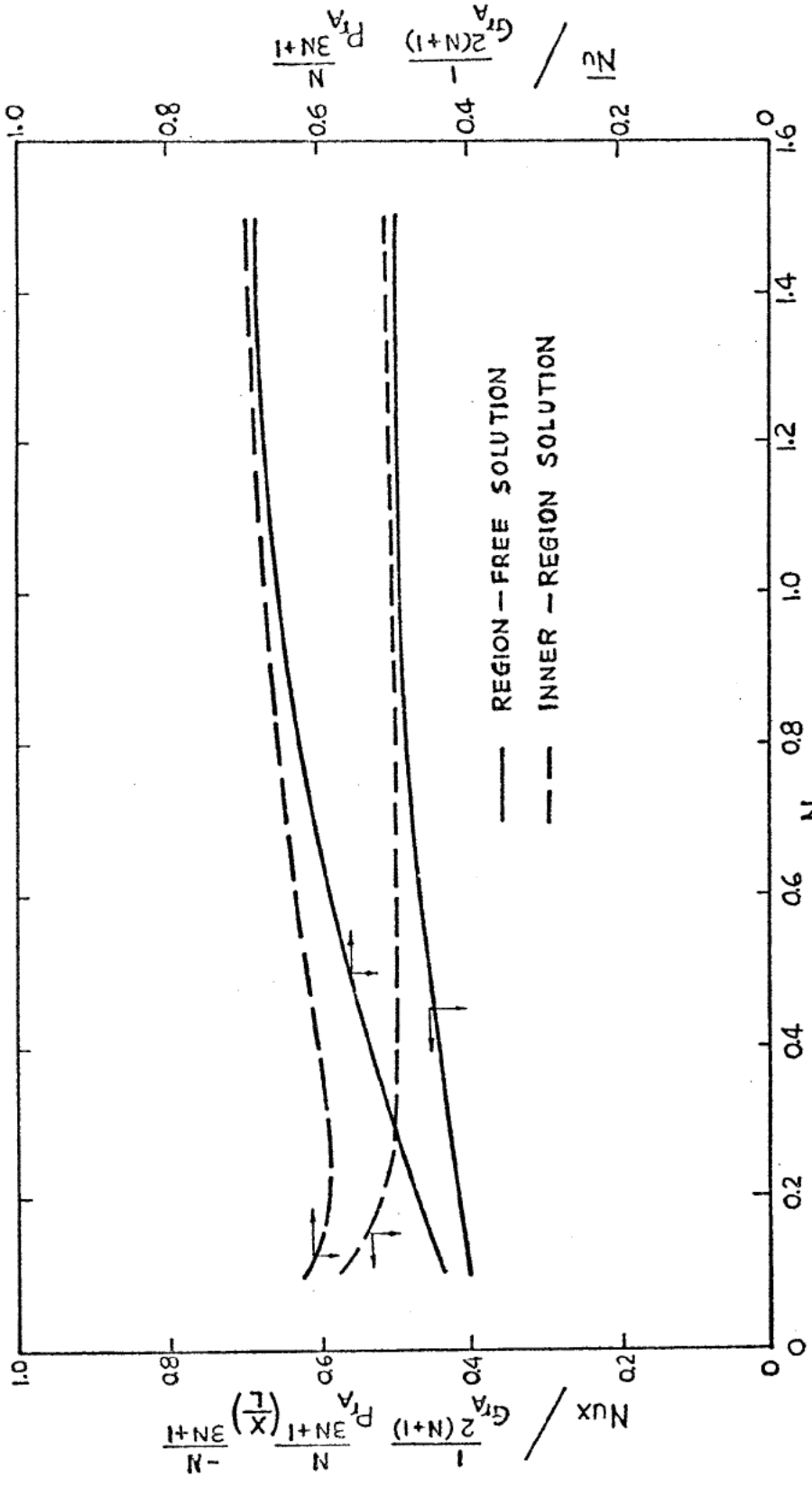

Fig. 5.6 Comparison of the local and average heat transfer parameters between the region-free and inner-region solutions for an isothermal vertical plate.

used 0.5% and 1% carbopol solutions to cover the range of power law fluid index N from 0.7 to 1.0, while the latter used 1.25%, 1.5% and 1.75% carbopol solutions to cover N from 0.2 to 0.7. Both investigations used the same equipment, namely, rectangular copper plates $3\frac{7"}{8}$ x $7\frac{7"}{8}$ high and $5\frac{7"}{8}$ x $11\frac{7"}{8}$ high in a stainless steel container 4' high x 2' wide x 3' long. The plate and fluid temperatures were measured with copper-constantan thermocouples. The fluid temperature was computed as the average value of the local temperatures of the fluid, measured by a movable thermocouple probe at different heights ranging from the bottom to the top edge of the plate. All dimensionless groups were evaluated using physical properties at the arithmetic mean of the plate and fluid temperatures. Unfortunately, no velocity measurements were presented.

Fig. 3.7 show a comparison of the predicted average heat transfer parameters with experimental results on an isothermal vertical plate. The work of Tien (42) using the integral method is plotted in the same figure. It shows that the region-free solution is in good agreement with the experimental results of (14). The experimental results were taken from Table 3 of (14) for N=0.891 and 0.72; while for $N<0.4$, they were calculated from the data on a small plate provided in Tables 3 and 5 of (15) where the values of N were determined from the average temperature. For reference purposes, the numerical values of the experimental results for $0.25<N<0.4$ are listed in Appendix D.

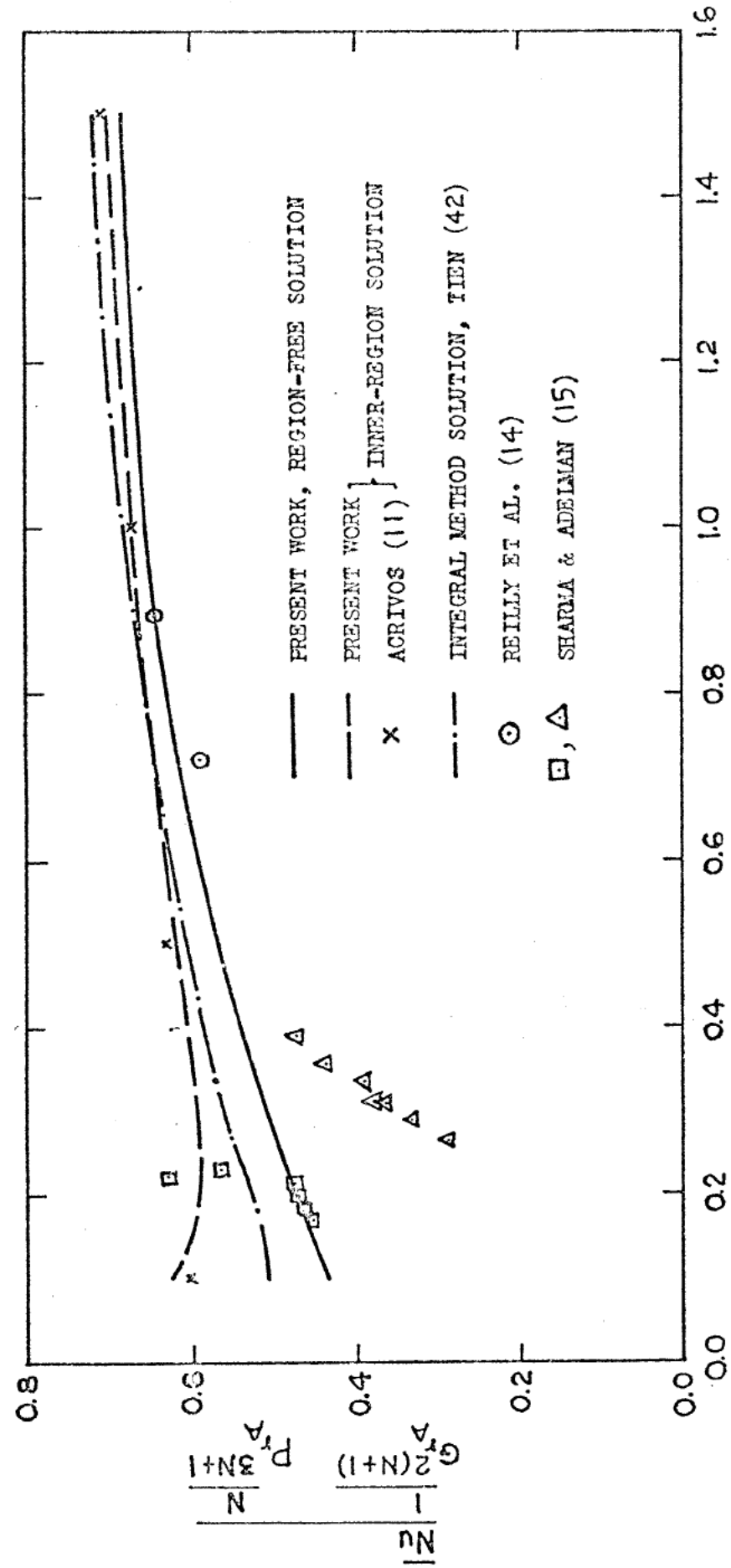

Fig. 3.7 Comparison of predicted average heat transfer parameters with experimental data for laminar free convection from an isothermal vertical plate.

CHAPTER IV

LAMINAR FREE CONVECTION HEAT TRANSFER ABOUT A BODY WITH A UNIFORM SURFACE HEAT FLUX IN POWER LAW FLUIDS

4.1 Theoretical Analysis

By defining the following dimensionless variables

$$X = \frac{x}{L} \tag{4.1}$$

$$Y = \frac{y}{L} Gr_C^{\frac{1}{N+4}} Pr_C^{\frac{N}{3N+4}} \tag{4.2}$$

$$U = u \left(\frac{k}{g\beta q L^2}\right)^{\frac{1}{2}} Gr_C^{\frac{1}{2(N+4)}} Pr_C^{\frac{N+2}{3N+2}} \tag{4.3}$$

$$V = v \left(\frac{k}{g\beta q L^2}\right)^{\frac{1}{2}} Gr_C^{\frac{3}{2(N+4)}} Pr_C^{\frac{2(N+1)}{3N+2}} \tag{4.4}$$

$$T = \frac{t - t_\infty}{\frac{qL}{k}} Gr_C^{\frac{1}{N+4}} Pr_C^{\frac{N}{3N+2}} \tag{4.5}$$

where Gr_C and Pr_C are the generalized Grashof number and generalized Prandtl number and are defined as (see also (44))

$$Gr_C = \left(\frac{\rho}{m}\right)^2 L^4 \left(\frac{g\beta q}{k}\right)^{2-N} \tag{4.6}$$

$$Pr_C = \frac{\rho C_p}{k} \left(\frac{m}{\rho}\right)^{\frac{5}{N+4}} L^{\frac{2(N-1)}{N+4}} \left(\frac{g\beta q}{k}\right)^{\frac{3(N-1)}{N+4}} \tag{4.7}$$

the governing differential Equations (1.3-5) for a two-dimensional body with uniform surface heat flux in an

incompressible power law fluid can be written in dimensionless form as

$$\frac{\partial U}{\partial X} + \frac{\partial U}{\partial Y} = 0 \tag{4.8}$$

$$\frac{\partial}{\partial Y}\left(\left|\frac{\partial U}{\partial Y}\right|^{N-1} \frac{\partial U}{\partial Y}\right) + T \sin\alpha = \frac{1}{Pr_C^{\frac{N+4}{3N+2}}} \left(U\frac{\partial U}{\partial X} + V\frac{\partial U}{\partial Y}\right) \tag{4.9}$$

$$U \frac{\partial T}{\partial X} + V \frac{\partial T}{\partial Y} = \frac{\partial^2 T}{\partial Y^2} \tag{4.10}$$

Using a high generalized Prandtl number for the same reason as explained in Chapter III for the isothermal case, the momentum Equation (4.9) is simplified to become

$$\frac{\partial}{\partial Y}\left(\left|\frac{\partial U}{\partial Y}\right|^{N-1} \frac{\partial U}{\partial Y}\right) + T \sin\alpha = 0 \tag{4.9a}$$

It is necessary to look at the effect of a high generalized Prandtl number on this uniform surface heat flux case. The generalized Prandtl number defined in Equation (4.7) can be rearranged to yield

$$Pr_C = \frac{\frac{\mu}{\rho}}{\frac{k}{\rho C_p}} \quad \frac{\frac{\rho}{\mu} L^2 \left(\frac{g\beta q}{k}\right)^{\frac{1}{2}}}{\left[\left(\frac{\rho}{m}\right)^2 L^4 \left(\frac{g\beta q}{k}\right)^{2-N}\right]^{\frac{5}{2(N+4)}}}$$

$$= Pr \cdot \frac{Gr^{\frac{1}{2}}}{Gr_C^{\frac{5}{2(N+4)}}} \tag{4.11}$$

Thus, the non-Newtonian factor becomes

$$f_N = \frac{Gr^{\frac{1}{2}}}{Gr_C^{\frac{5}{2(N+4)}}}$$

It can be shown that $Pr_C = Pr$ for N=1. Therefore, the analysis discussed in Section 3.1 for uniform surface temperature case should be applicable to the present uniform surface heat flux case. However, we will still proceed to obtain both the region-free and inner-region solutions for comparison purposes and also for strengthening the high generalized Prandtl number concept.

The boundary conditions for laminar free convection from a body having uniform heat flux are: at y=0, u=v=0, $q = -k \frac{\partial t}{\partial y}\Big|_{y=0}$ = constant; at x=0, u=0, $t=t_\infty$ = constant; and as $y \to \infty$, u=0, $t=t_\infty$ = constant. Utilizing the dimensionless variables (4.1-5), these boundary conditions become

1). for the region-free solution:

$$\begin{aligned} &\text{at } Y=0,\ U=V=0,\ \frac{\partial T}{\partial Y}\Big|_{Y=0} = -1 \\ &\text{at } Y=\infty,\ U=T=0 \\ &\text{at } X=0,\ U=T=0 \end{aligned} \qquad (4.12)$$

2). for the inner-region solution:

$$\begin{aligned} &\text{at } Y=0,\ U=V=0,\ \frac{\partial T}{\partial Y}\Big|_{Y=0} = -1 \\ &\text{at } Y=\infty,\ \frac{\partial U}{\partial Y} = T = 0,\ U \neq 0 \\ &\text{at } X=0,\ U=T=0 \end{aligned} \qquad (4.13)$$

Unfortunately, unlike the case of isothermal laminar free convection, a similarity solution exists only when $\sin\alpha = 1$, that is only for a vertical plate with uniform surface heat flux. (See Appendix E)

4.1.1 Laminar free convection about a vertical plate with uniform surface heat flux:

The solution of Equation (4.8) can be written in terms of a dimensionless stream function ψ

$$U = \frac{\partial \psi}{\partial Y} \quad , \quad V = -\frac{\partial \psi}{\partial X} \tag{4.14}$$

Then the partial differential Equations (4.9a) and (4.10) are transformed to ordinary differential equations by changing from the (X, Y) coordinate system to the (X, η) system with the following substitutions

$$\eta = \frac{Y}{[(3N+2)\,X]^{\frac{N}{3N+2}}} \tag{4.15}$$

$$\psi = [(3N+2)\,X]^{\frac{2(N+1)}{3N+2}} f(\eta)$$

$$T = [(3N+2)\,X]^{\frac{N}{3N+2}} \phi(\eta) \tag{4.17}$$

Expressions for the velocity components become

$$U = [(3N+2)\,X]^{\frac{N+2}{3N+2}} f'(\eta) \tag{4.18}$$

$$V = \frac{N}{[(3N+2)\,X]^{\frac{N}{3N+2}}} \left[\eta f'(\eta) - \frac{2(N+1)}{N} f(\eta)\right] \tag{4.19}$$

where the primes indicate differentiation with respect to η.

Substituting Equations (4.15-19) into Equations (4.9a) and (4.10), it was found that all terms containing X cancel out, leaving only functions which depend upon η. The result is

$$\phi + \frac{d}{d\eta}(\, |f''|^{N-1} \, f'') = 0 \qquad (4.20)$$

$$\phi'' + 2(N+1) f \phi' - N f' \phi = 0 \qquad (4.21)$$

The absolute value used in Equation (4.20) can be neglected only when the velocity gradient is positive.

When N=1, Equations (4.20) and (4.21) are the same as those derived for Newtonian fluids by Sparrow and Gregg (17) (See also Equations (2.8) and (2.9)), if the inertia terms of the momentum equation are neglected and the following transformations are substituted into Equation (2.8) and (2.9):

$$H = -\phi \, Pr^{-1/5}, \quad F = f \, Pr^{-4/5}, \quad \eta = \eta \, Pr^{-1/5}$$

The boundary conditions are

1). for the region-free solution:

$$f'(0) = f(0) = \phi'(0) + 1 = 0$$
$$f'(\infty) = \phi(\infty) = 0 \qquad (4.22)$$

2). for the inner-region solution

$$f'(0) = f(0) = \phi'(0) + 1 = 0$$
$$f''(\infty) = \phi(\infty) = 0, \quad f'(\infty) \neq 0 \qquad (4.23)$$

Equations (4.20) and (4.21) with boundary conditions (4.22) and (4.23) have been solved numerically by the method described in Chapter III (see also Appendix B). The results, the missing initial values f"(0) and $\phi(0)$ versus N, for both the region-free and inner-region solutions are plotted in Figs. 4.1 and 4.2. The solutions were also converted to F"(0) and H(0) for comparison with the exact solution of Sparrow and Gregg (17). The results are listed in Table 4.1a. Appendix F gives the numerical values of f"(0) and $\phi(0)$ for various values of N for the region-free solution.

4.2 Heat Transfer Results

4.2.1 Surface temperature variation: Substituting Equations (4.1) and (4.5) into Equation (4.17), one obtains the surface temperature variation for a specified constant heat flux rate

$$t_w(x) - t_\infty = \left[(3N+2)\frac{x}{L}\right]^{\frac{N}{3N+2}} \frac{qL}{k} \frac{\phi(0)}{Gr_C^{\frac{1}{N+4}} Pr_C^{\frac{N}{3N+2}}} \qquad (4.24)$$

Equation (4.24) can be rearranged in dimensionless form by introducing a generalized local Grashof number Grx_C

$$Grx_C = Gr_C \left(\frac{x}{L}\right)^{\frac{2(N+1)(N+4)}{3N+2}} \qquad (4.25)$$

to give

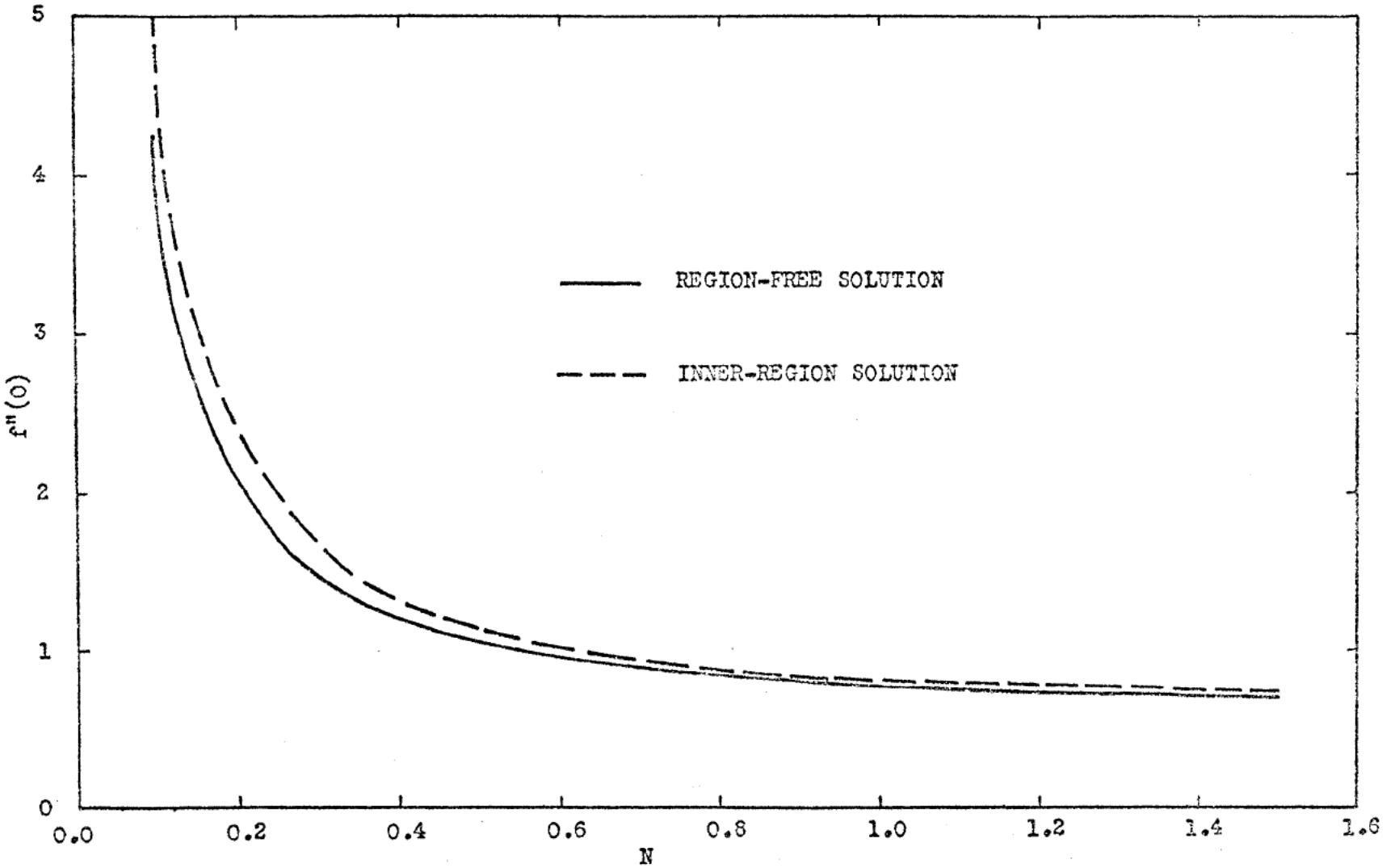

Fig. 4.1 Comparison of f"(0) versus N between the region-free and inner-region solutions of laminar free convection about a vertical plate.

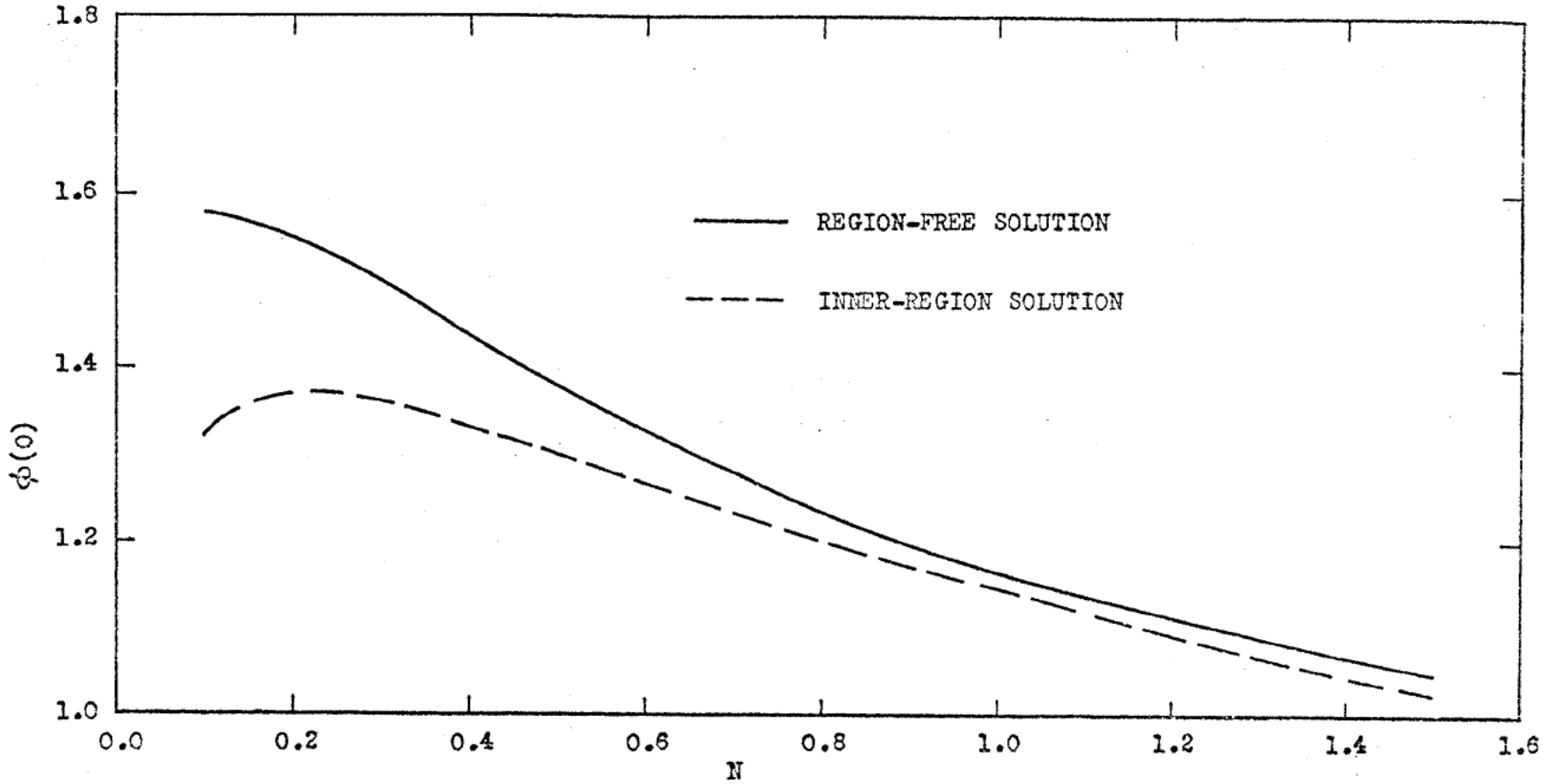

Fig. 4.2 Comparison of $\phi(0)$ versus N between the region-free and inner-region solution of laminar free convection about a vertical plate.

Table 4.1

Comparison of the region-free and inner-region solutions with the exact solution for Newtonian flow (uniform surface heat flux case)

Table 4.1a Comparison of F"(0) and H(0)

Pr		Exact solution: Sparrow & Gregg (17)	Exact solution: Present result	Region-free solution	Inner-region solution
0.1	F"(0)	1.6434	1.6435	2.00609	2.03926
	H(0)	-2.7507	-2.7509	-1.84550	-1.81857
1	F"(0)	0.72196	0.72196	0.79864	0.81185
	H(0)	-1.3574	-1.3574	-1.16444	-1.14744
5	F"(0)		0.39756	0.41953	0.42647
	H(0)		-0.90195	-0.84396	-0.83164
10	F"(0)	0.30639	0.30610	0.31794	0.32320
	H(0)	-0.76746	-0.76804	-0.73417	-0.72399
20	F"(0)		0.23491	0.24096	0.24494
	H(0)		-0.65815	-0.63960	-0.63027
40	F"(0)		0.17973	0.18261	0.18563
	H(0)		-0.56665	-0.55681	-0.54868
80	F"(0)		0.13653	0.13839	0.14068
	H(0)		-0.49124	-0.48473	-0.47765
100	F"(0)	0.12620	0.12610	0.12658	0.12867
	H(0)	-0.46566	-0.46597	-0.46357	-0.45680
200	F"(0)		0.09551	0.09593	0.09751
	H(0)		-0.40546	-0.40356	-0.39767
500	F"(0)		0.06634	0.06649	0.06759
	H(0)		-0.33678	-0.33599	-0.33108
1000	F"(0)		0.05042	0.05039	0.05122
	H(0)		-0.29244	-0.29249	-0.28822

Table 4.1b Comparison of average heat transfer parameters

Pr	N=1 for Equation	Exact Solution Present result	Region-Free Solution Value	Region-Free Solution Deviation %	Inner-Region Solution Value	Inner-Region Solution Deviation %
0.1	(5.5)	0.23710	0.39047	-64.68	0.39771	-67.74
	(5.6)	0.22450	0.36972		0.37658	
1	(5.5)	0.57326	0.69437	-21.12	0.70725	-23.37
	(5.6)	0.54279	0.65746		0.66966	
5	(5.5)	0.95556	1.03832	- 8.66	1.05758	-10.68
	(5.6)	0.90477	0.98313		1.00137	
10	(5.5)	1.16817	1.23478	- 5.70	1.25768	- 7.66
	(5.6)	1.10608	1.16915		1.19083	
20	(5.5)	1.41688	1.46841	- 3.64	1.49564	- 5.56
	(5.6)	1.34157	1.39036		1.41615	
40	(5.5)	1.70841	1.74624	- 2.21	1.77863	- 4.11
	(5.6)	1.61761	1.65343		1.68409	
80	(5.5)	2.04230	2.07664	- 1.68	2.11516	- 3.57
	(5.6)	1.93375	1.96627		2.00274	
100	(5.5)	2.18167	2.19579	- 0.65	2.23651	- 2.51
	(5.6)	2.06571	2.07908		2.11964	
200	(5.5)	2.59593	2.61124	- 0.59	2.65967	- 2.46
	(5.6)	2.45795	2.47245		2.51831	
500	(5.5)	3.27382	3.28347	- 0.29	3.34436	- 2.15
	(5.6)	3.09981	3.10894		3.16660	
1000	(5.5)	3.90561	3.90472	0.02	3.97714	- 1.83
	(5.6)	3.69802	3.69718		3.76575	

$$\frac{t_w - t_\infty}{\frac{qx}{k}} Grx_C^{\frac{1}{N+4}} Pr_C^{\frac{N}{3N+2}} = (3N+2)^{\frac{N}{3N+2}} \phi(0) \qquad (4.26)$$

Equation (4.26) is plotted versus N for both the region-free and inner-region solutions in Fig. 4.3. On any given location along the vertical plate, Equation (4.24) indicates $(t_w - t_\infty)$ is proportional to $x^{N/(3N+2)}$. The variation of the wall temperature with distance along the wall is obtained from Equation (4.25) in dimensionless form

$$\frac{t_w - t_\infty}{(t_w - t_\infty)_L} = \left(\frac{x}{L}\right)^{\frac{N}{3N+2}} \qquad (4.27)$$

where L is the length of surface for which the flow is laminar. Note that Equation (4.27) is exactly the same expression as that derived by Sparrow and Gregg (17) when N equals 1. Thus, this expression is also an exact solution for non-Newtonian power law fluids. Fig. 4.4 shows the variation of $t_w - t_\infty$ along the plate surface for various flow index N. The rate of increase of the wall temperature is greatest near x=0, and the variation increases as N decreases. Note that Equation (4.27) is only a function of the distance along the plate and the power law fluid index, and is free from the method of solution, such as the region-free or inner-region solution discussed here.

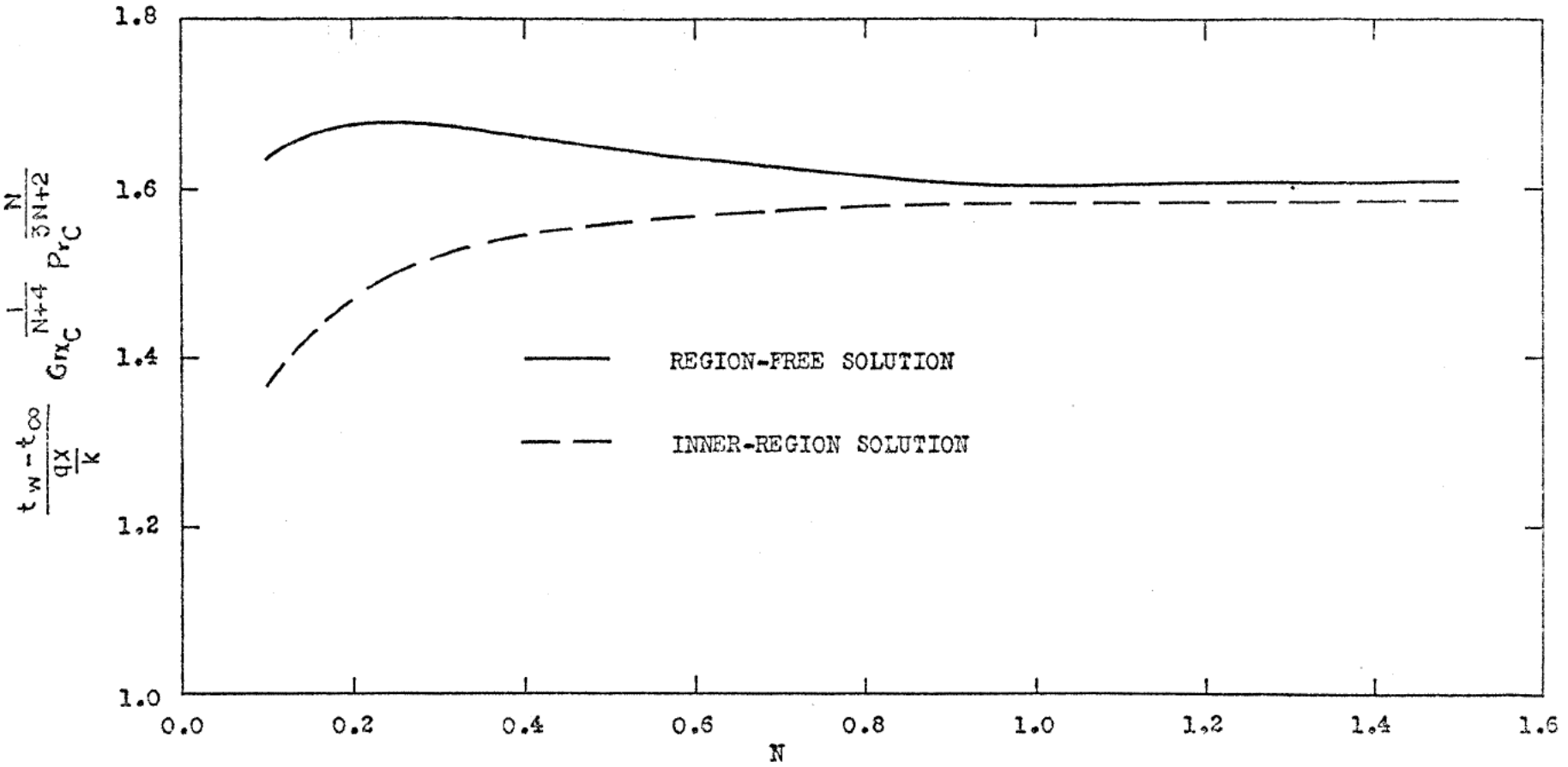

Fig. 4.3 Variation of $\frac{t_w - t_\infty}{\frac{q\,x}{k}} Grx_C^{\frac{1}{N+4}} Pr_C^{\frac{N}{3N+2}}$ versus power law fluid index N.

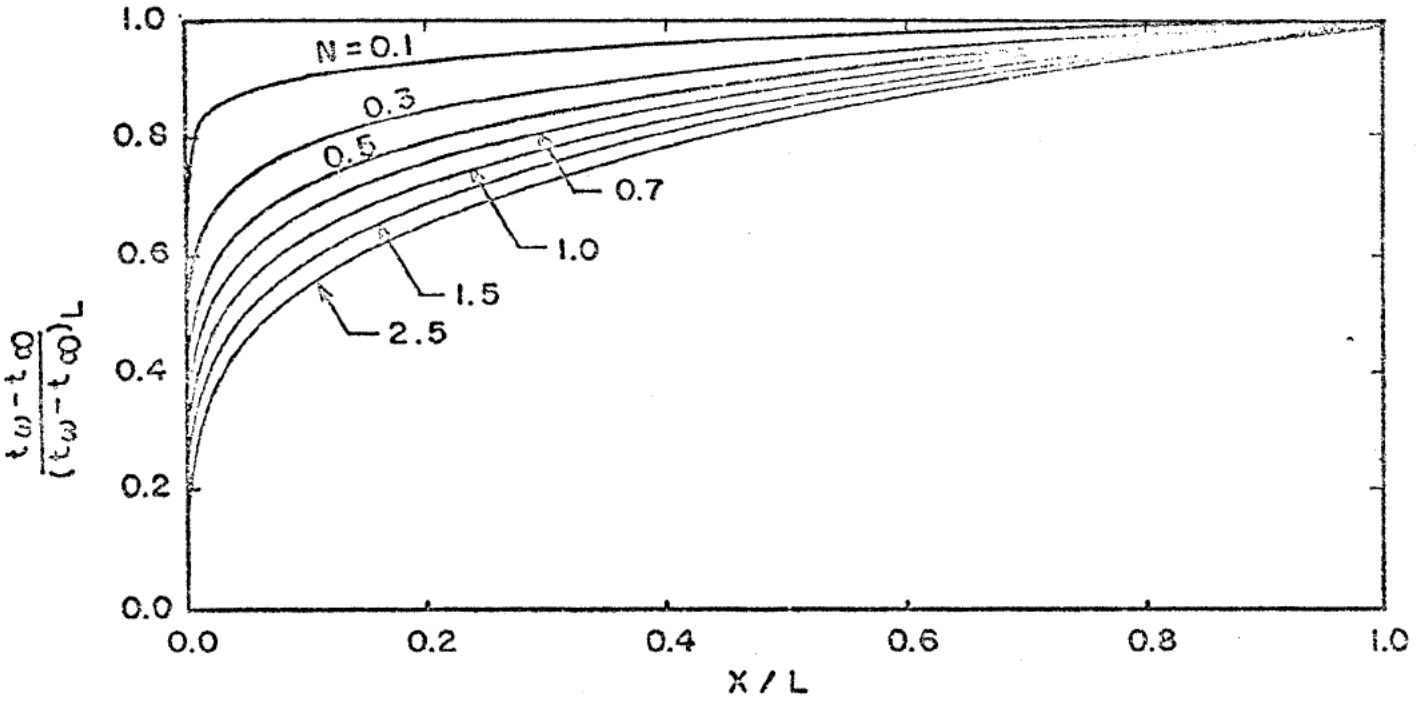

Fig. 4.4 Wall temperature variation $\frac{t_w - t_\infty}{(t_w - t_\infty)_L}$ along the plate x/L from the leading edge for various power law fluid index N.

4.2.2 Local Nusselt number: The local Nusselt number is conventionally defined as

$$Nux = \frac{hx}{k} = \frac{q}{t_w - t_\infty} \frac{x}{k} \tag{4.28}$$

Rearranging Equation (4.26) and substituting it into this equation, it follows that

$$Nux = C(N)\ Grx_C^{\frac{1}{N+4}}\ Pr_C^{\frac{N}{3N+2}} \tag{4.29}$$

or,

$$Nux = C(N)\ Gr_C^{\frac{1}{N+4}}\ Pr_C^{\frac{N}{3N+2}}\ (\frac{x}{L})^{\frac{2(N+1)}{3N+2}}$$

where

$$C(N) = \frac{1}{(3N+2)^{\frac{N}{3N+2}}\ \phi(0)}$$

Some authors (11, 42) prefer to define the local Nusselt number as $Nux = \frac{hL}{k}$. Using this definition,

$$Nux = C(N)\ Gr_C^{\frac{1}{N+4}}\ Pr_C^{\frac{N}{3N+2}}\ (\frac{x}{L})^{-\frac{N}{3N+2}} \tag{4.30}$$

It is possible to define a generalized local Rayleigh number Rax_C by rearranging Equation (4.29) to give

$$Nux = C(N)\ Rax_C^{\frac{1}{3N+2}} \tag{4.29a}$$

where

$$Rax_C = Grx_C^{\frac{3N+2}{N+4}}\ Pr_C^{N}$$

When N=1, the Grx_C =Grx, Pr_C =Pr, and Rax_C= Rax=Gr·Pr.

C(N) from Equations (4.29a) and (4.30) will be calculated and compared with experimental data.

4.2.3 Velocity and temperature distributions: Substituting Equation (4.3) into Equation (4.18) and rearranging the expression, one obtains the following expression for the dimensionless velocity distribution in the boundary layer

$$f'(\eta) = \left(\frac{Pr_C}{3N+2}\right)^{\frac{N+2}{3N+2}} \frac{\left[\frac{u\, x^{\frac{3N^2+4N-2}{(3N+2)(2-N)}}}{\left(\frac{m}{\rho}\right)^{1/(2-N)}}\right] L^{\frac{2(1-N)}{(2-N)(3N+2)}}}{Grx_C^{\frac{N+1}{(N+4)(2-N)}}} \qquad (4.31)$$

The dimensionless temperature distribution in the boundary layer is obtained by substituting Equations (4.1) and (4.5) into Equation (4.17) to give

$$\phi(\eta) = \frac{1}{\left[(3N+2)\frac{x}{L}\right]^{\frac{N}{3N+2}}} \frac{t-t_\infty}{\frac{qL}{k}} Gr_C^{\frac{1}{N+4}} Pr_C^{\frac{N}{3N+2}} \qquad (4.32)$$

or,

$$\frac{t-t_\infty}{t_w-t_\infty} = \frac{\phi(\eta)}{\phi(0)} \qquad (4.32a)$$

where η in Equations (4.31) and (4.32) can easily be verified by means of the various transformations made in the analysis to yield

$$\eta = \frac{y}{x} \frac{1}{(3N+2)^{\frac{N}{3N+2}}} Grx_C^{\frac{1}{N+4}} Pr_C^{\frac{N}{3N+2}} \qquad (4.33)$$

The temperature profiles are plotted in Figs. 4.5 and 4.6 respectively for various values of N for the region-free solution. Comparison of dimensionless velocity distributions from the exact solution (N=1, Pr=1000), the region-free solution, and the inner-region solution is shown in Fig. 4.7 for N=1.5, 1.0, 0.5, and 0.1. Because the temperature distributions from the inner-region solution are all very close together, no further comparison is made. It is found that the observations made here for uniform surface heat flux are very similar to those of Chapter III for uniform wall temperature.

4.2.4 Average Nusselt number: Several definitions of the average Nusselt number $\overline{Nu}$ have been reported in the literature.

a). $\overline{Nu}$ based on integration over the entire characteristic length L:

1. $$\overline{Nu} = \frac{1}{L}\int_0^L Nux\, dx = \frac{1}{L}\int_0^L \frac{hx}{k}\, dx \qquad (4.34)$$

Using Equation (4.29), this expression becomes

$$\overline{Nu} = C_1(N)\, Gr_C^{\frac{1}{N+4}} Pr_C^{\frac{N}{3N+2}} \qquad (4.35)$$

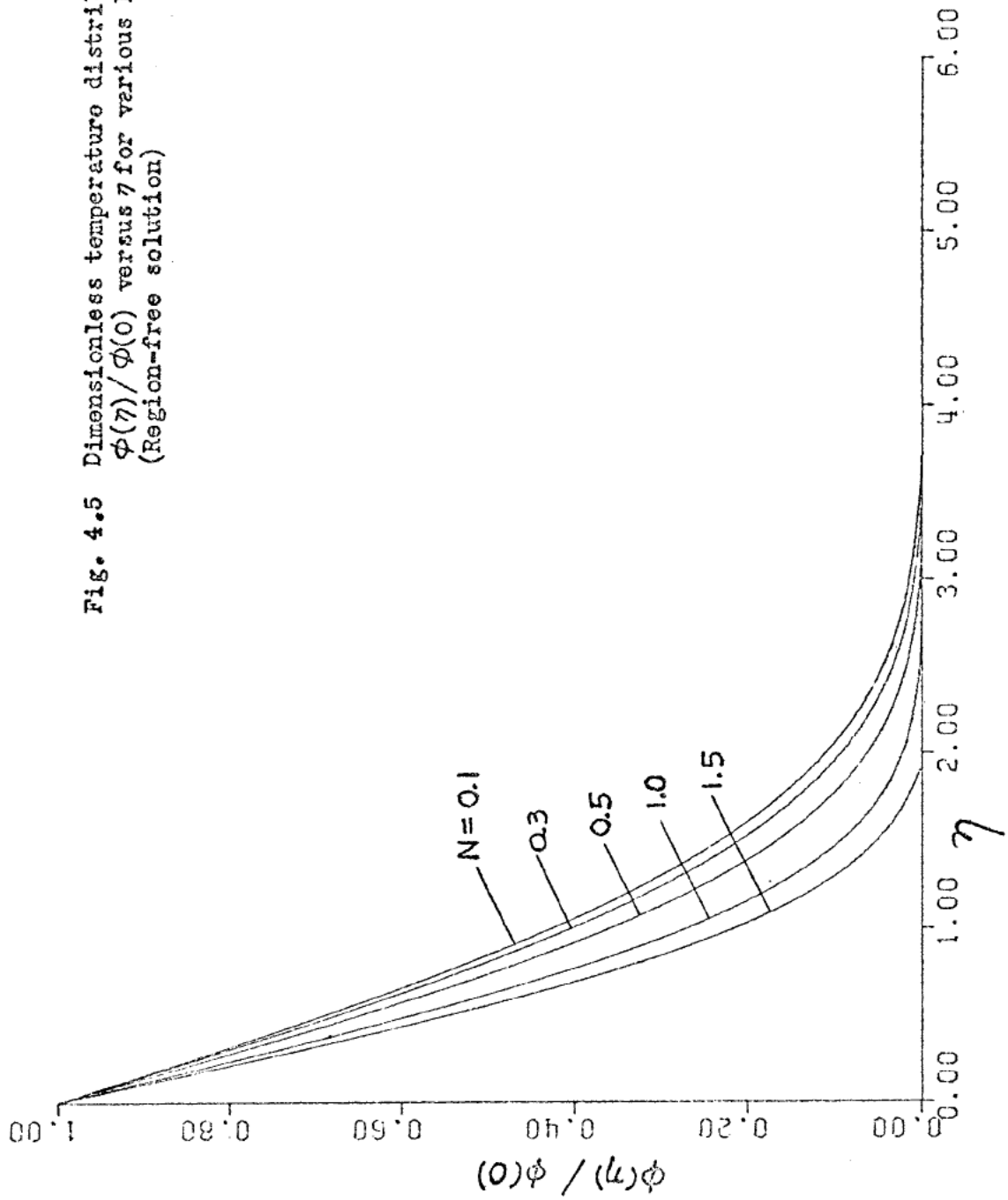

Fig. 4.5 Dimensionless temperature distributions $\phi(\eta)/\phi(0)$ versus η for various N. (Region-free solution)

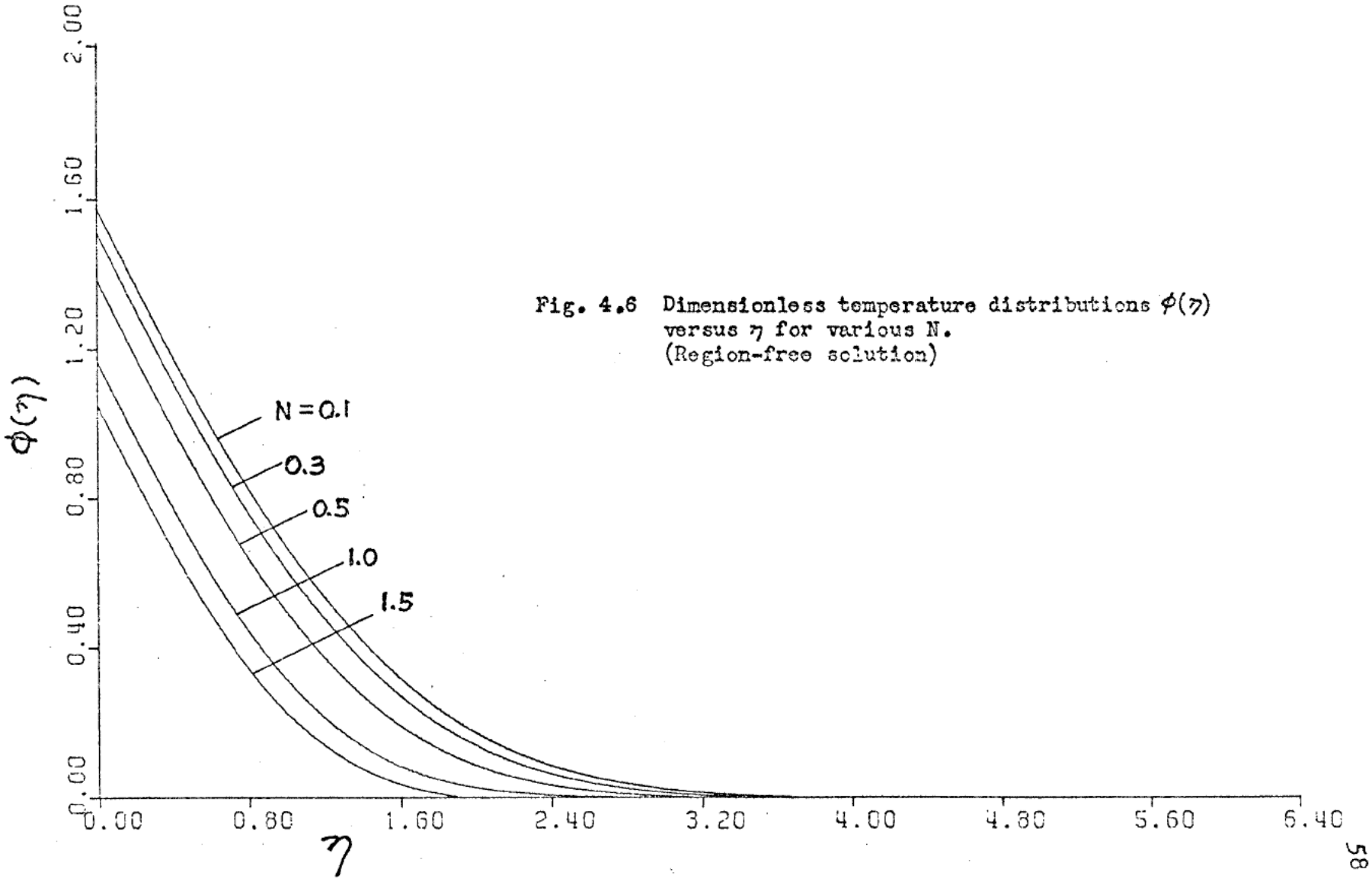

Fig. 4.6 Dimensionless temperature distributions $\phi(\eta)$ versus η for various N.
(Region-free solution)

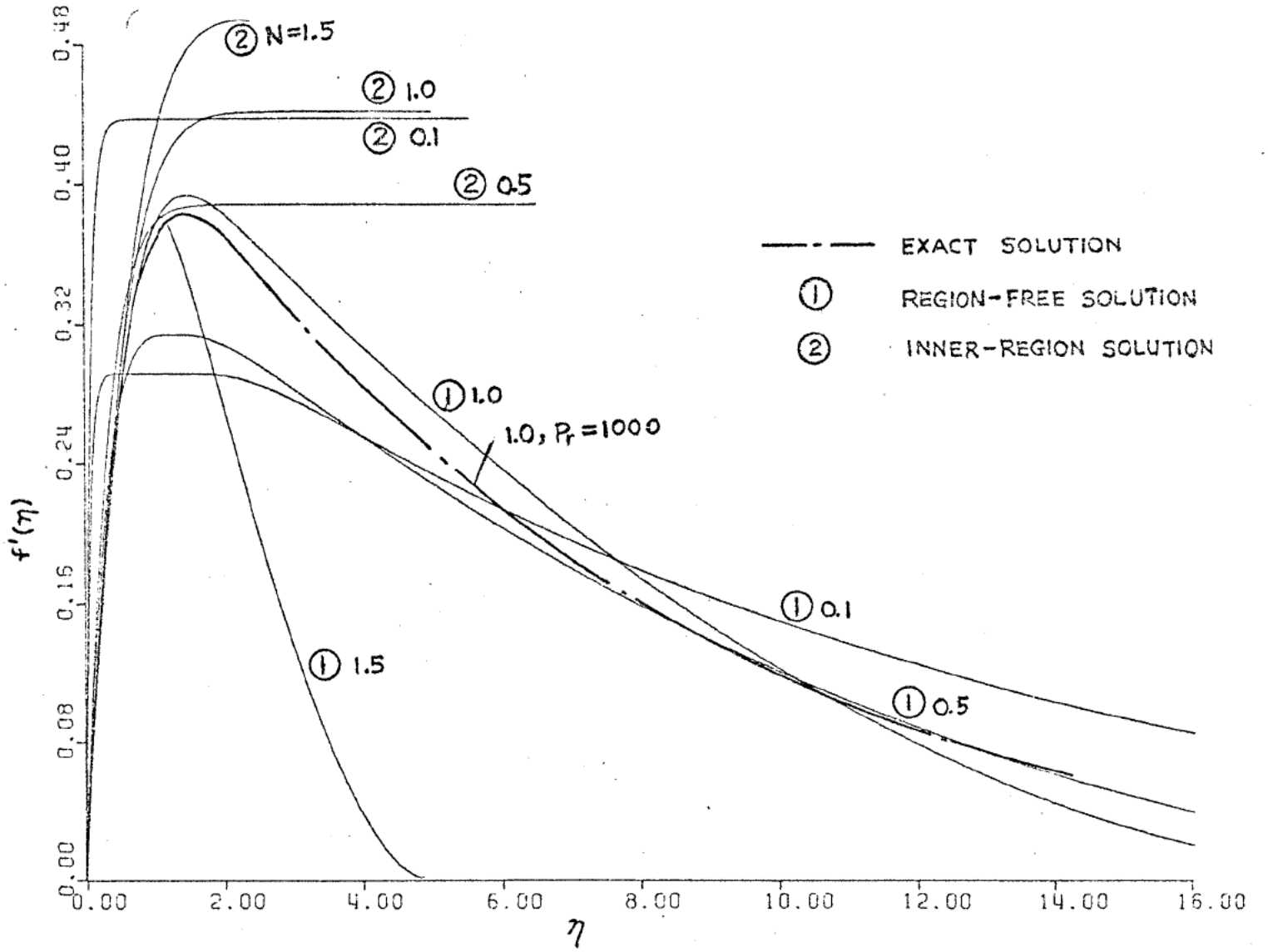

Fig. 4.7 Comparison of velocity distributions for the exact solution with the region-free and inner-region solutions.

where

$$C_1(N) = \frac{(3N+2)^{\frac{2(N+1)}{3N+2}}}{(5N+4)\ \phi(0)}$$

2. $\overline{Nu} = \frac{1}{L}\int_0^L \frac{hL}{k}\,dx$ (4.36)

then

$$\overline{Nu} = C_2(N)\ Gr_C^{\frac{1}{N+4}}\ Pr_C^{\frac{N}{3N+2}} \quad (4.37)$$

where

$$C_2(N) = \frac{(3N+2)^{\frac{2(N+1)}{3N+2}}}{2(N+1)\ \phi(0)}$$

b). $\overline{Nu}$ based on an average temperature difference: The average temperature difference on a surface over which the flow is laminar for a length L is obtained by averaging Equation (4.24)

$$\overline{t_w - t_\infty} = \frac{1}{L}\int_0^L (t_w - t_\infty)\,dx = \frac{3N+2}{2(2N+1)}\,(t_w - t_\infty)_L$$

By defining a mean heat transfer coefficient $\bar{h}$ as

$$\bar{h} = \frac{q}{\overline{t_w - t_\infty}}$$

the mean Nusselt number is obtained by evaluating $(t_w - t_\infty)_L$ from Equation (4.24) to give

$$\overline{Nu} = \frac{\bar{h}L}{k} = C_3(N)\ Gr_C^{\frac{1}{N+4}}\ Pr_C^{\frac{N}{3N+2}} \quad (4.38)$$

where

$$C_3(N) = \frac{2(2N+1)}{(3N+2)^{\frac{2(2N+1)}{3N+2}}\ \phi(0)}$$

c). $\overline{Nu}$ based on temperature difference at L/2: The difference between the plate and ambient temperature at L/2 is

$$(t_w - t_\infty)_{L/2} = (\tfrac{1}{2})^{\frac{N}{3N+2}} (t_w - t_\infty)_L$$

Defining a mean heat transfer coefficient $\overline{h}$ as

$$\overline{h} = \frac{q}{(t_w - t_\infty)_{L/2}}$$

the mean Nusselt number is then

$$\overline{Nu} = C_4(N)\ Gr_C^{\frac{1}{N+4}}\ Pr_C^{\frac{N}{3N+2}} \qquad (4.39)$$

where

$$C_4(N) = \left(\frac{2}{3N+2}\right)^{\frac{N}{3N+2}} \frac{1}{\phi(0)}$$

Values of $C_1(N)$, $C_2(N)$, $C_3(N)$, and $C_4(N)$ will be discussed in more detail in subsequent sections.

4.2.5 Flow parameter: The shear stress at the plate surface is obtained from its power law relationship with the shear strain

$$\tau_w(x) = m \left(\frac{\partial u}{\partial y}\right)^N \Big|_{y=0}$$

$$= \left\{\frac{P}{L}\frac{m^{\frac{1}{N}}}{\left[(3N+2)\frac{x}{L}\right]^{\frac{N}{3N+2}}} f''(0)\right\}^N Gr_C^{\frac{N}{N+4}}\ Pr_C^{\frac{N^2}{3N+2}} \qquad (4.40)$$

where

$$P = \left[\frac{m}{\rho} L^{N+2} \left(\frac{g\beta q}{k}\right)^{N+1}\right]^{\frac{1}{N+4}} \left[\frac{(3N+2)\frac{x}{L}}{Pr_c}\right]^{\frac{N+2}{3N+2}}$$

Note that P has the dimensions of velocity, and the velocity gradient near the wall is always positive.

The local drag coefficient $C_d(x)$ has been defined by Gebhart and Mollendorf (36) by introducing a 'convection velocity', u_c, such that $u_c = u_{max} = P \cdot f'_{max}(\eta)$. The drag coefficient becomes

$$C_d(x) = \frac{\tau_w(x)}{\rho\, u_c^2} \tag{4.41}$$

The local flow parameter can be written

$$C_d(x) \frac{Gr_c^{\frac{1}{N+4}}}{Pr_c^{\frac{4}{3N+2}}} = C_f(N) \left(\frac{x}{L}\right)^{\frac{-4}{3N+2}} \tag{4.42}$$

where

$$C_f(N) = \frac{1}{(3N+2)^{\frac{4}{3N+2}}} \frac{[f''(0)]^N}{[f'_{max}(\eta)]^2}$$

The values of $C_f(N)$ versus N have been plotted in Fig. 4.8 for the region-free solution. It shows that C_f increases rapidly when $N<1$.

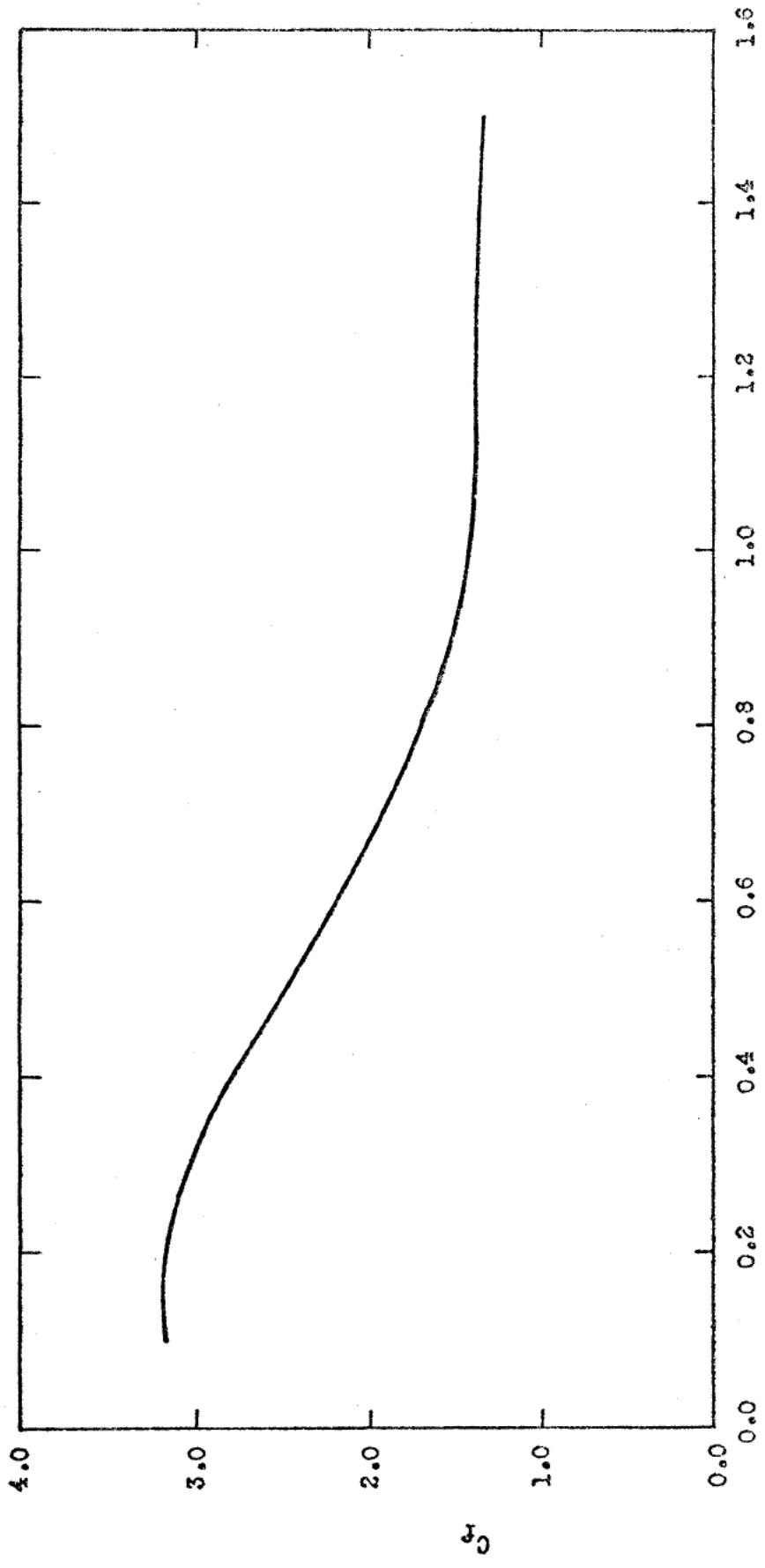

Fig. 4.8 Local flow parameter $C_f(N)$ versus N for the region-free solution.

4.3 Experimental Verification

4.3.1 The experimental data:

Experimental results have been reported by Dale (44). Two vertical flat stainless steel plates of similar construction but different in size were used in his investigation; one has a dimension 18 ½ in. by 24 in. by 1 in. thick and the other 6½ in. by 12 in. by 3/4 in. thick. The temperatures of the plates were measured by using copper-constantan thermocouples spot welded to the back sides of the sheet. The fluid temperatures were measured with a chromel-constantan thermocouple probe. The velocity measurements were made by tracking photographically the macromolecules inherent in the non-Newtonian fluids when possible (the C.M.C. solutions), and he used the neutrally buoyant glass beads when this was not possible (water and carbopol solutions). The physical properties were evaluated at the average fluid temperature taking the arithmetic mean of the fluid temperatures far from the plate and the plate temperatures. Fourier's law is used in his experiments to determine the surface heat flux. The temperature gradients along the plate were reported to have a variation of 7.3% below the average and 4.9% above the average.

All the experimental data reported by Dale (44) has been put in dimensionless form for use in the present analysis. The range of power law fluid index N used in the experiments is from 0.383 to 1.0. All the carbopol

solutions used by Dale were un-neutralized except those 0.06% and 0.065% solutions which were neutralized.

As mentioned earlier, the expression for the variation of wall temperature, Equation (4.27), is an exact solution and may serve as a criterion to justify the accuracy of any temperature measurement along the plate and far from the plate. Fig. 4.9 shows the comparison between the theoretical and experimental wall temperature variations for N=0.888, 0.795, 0.535, and 0.383. The agreement is generally very good. Fig. 4.10 shows the comparisons between the predicted local Nusselt number (with $\frac{hx}{k}$) calculated from the region-free solution and the experimental results calculated from data of Dale for N=0.888, 0.611 and 0.383. The agreement is fair.

The average Nusselt number predicted by Equation (4.35) using the region-free solution was calculated and plotted in Fig. 4.11 with experimental results calculated from data of Dale. The agreement is again fairly good.

In Newtonian flow, heat transfer results sometimes are preferred to be correlated with the Rayleigh number defined as Ra=Gr Pr. Since we have defined a generalized local Rayleigh number Rax_C in Equation (4.29a), it is possible to define a generalized Rayleigh number Ra_C for power law fluid flow as

$$Ra_C = Gr_C^{\frac{3N+2}{N+4}} Pr_C^N \qquad (4.43)$$

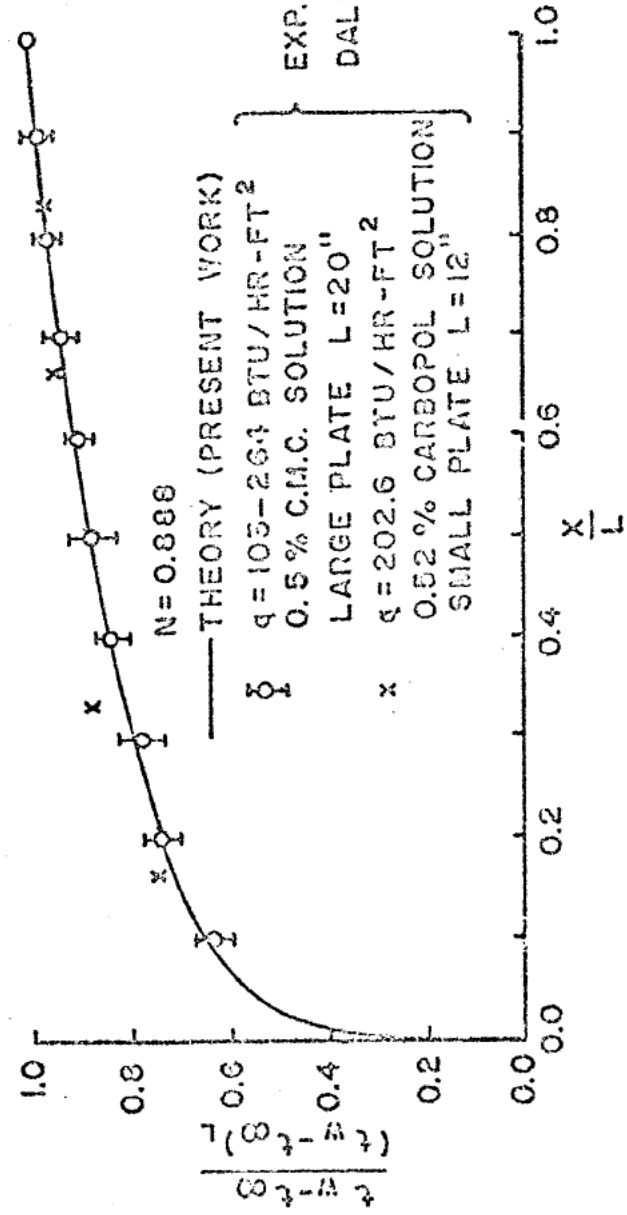

Fig. 4.9a Comparison between predicted wall temperature variation along plate surface and experimental results for N=0.888.

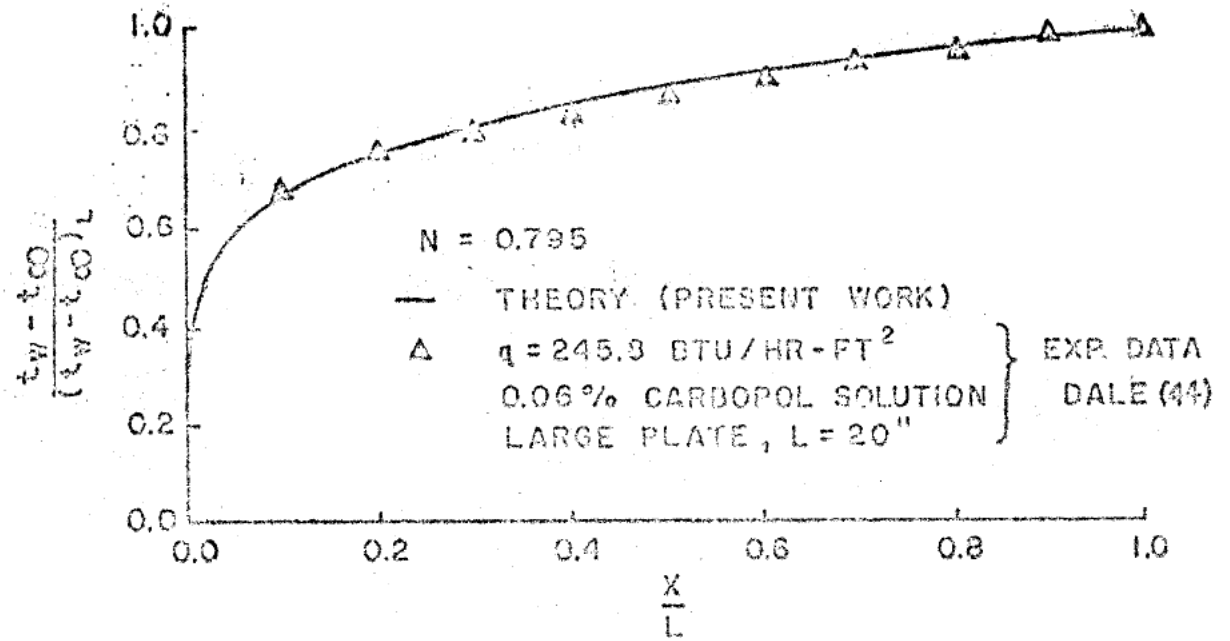

Fig. 4.9b Comparison between predicted wall temperature variation along plate surface and experimental results for N=0.795.

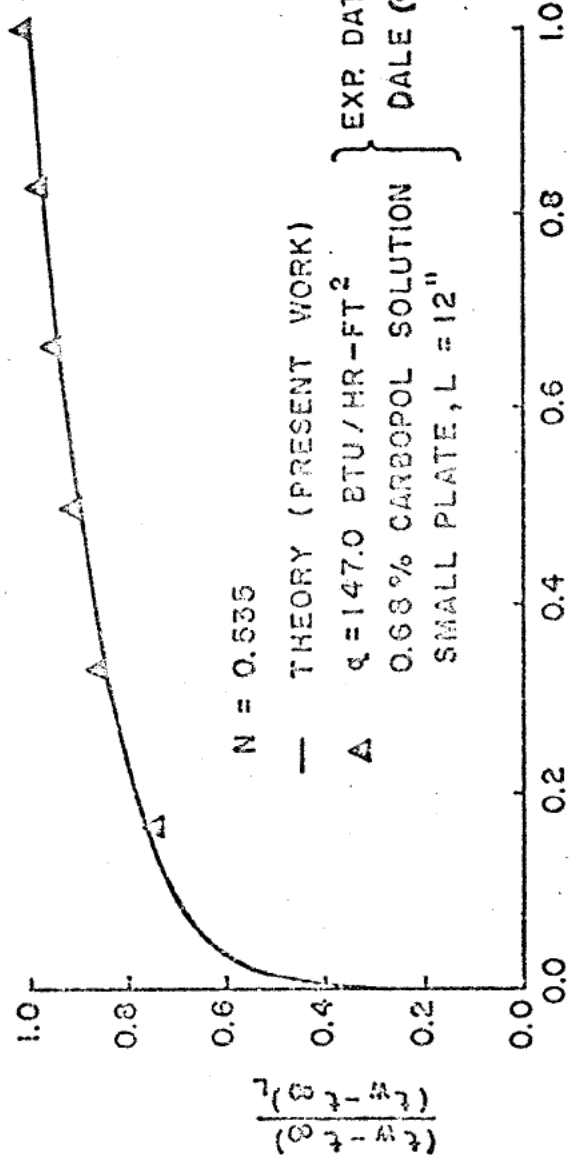

Fig. 4.9c Comparison between predicted wall temperature variation along plate surface and experimental results for N=0.535.

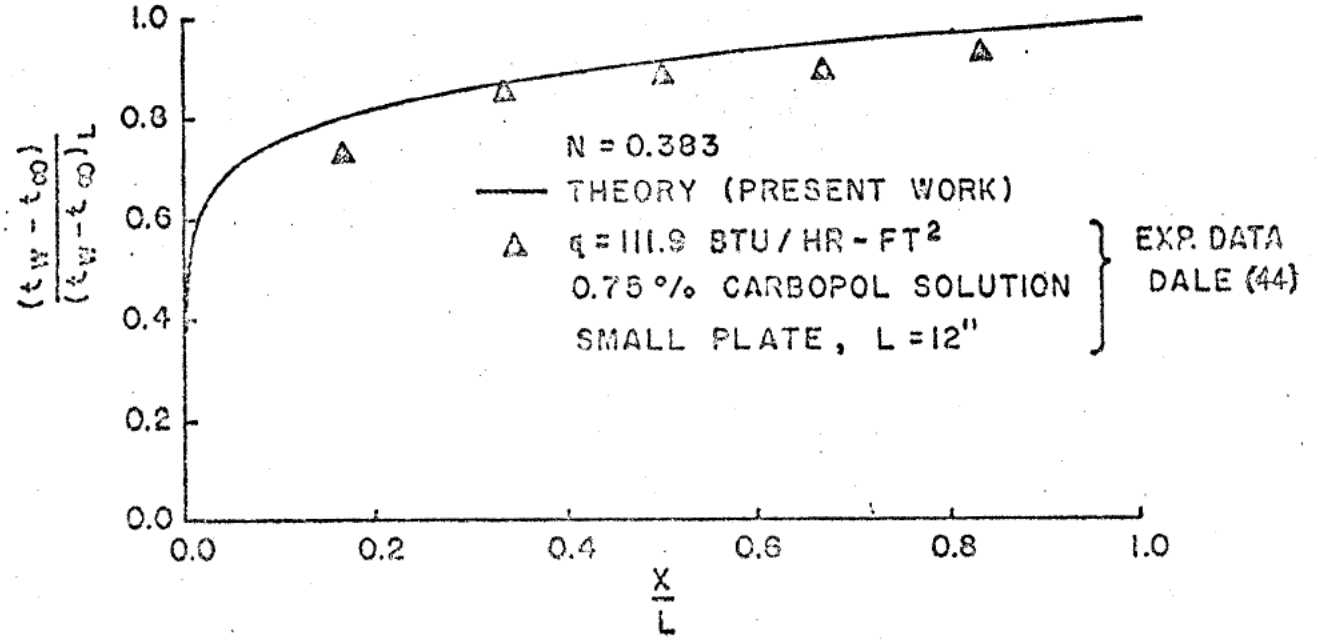

Fig. 4.9d Comparison between predicted wall temperature variation along plate surface and experimental results for N=0.383.

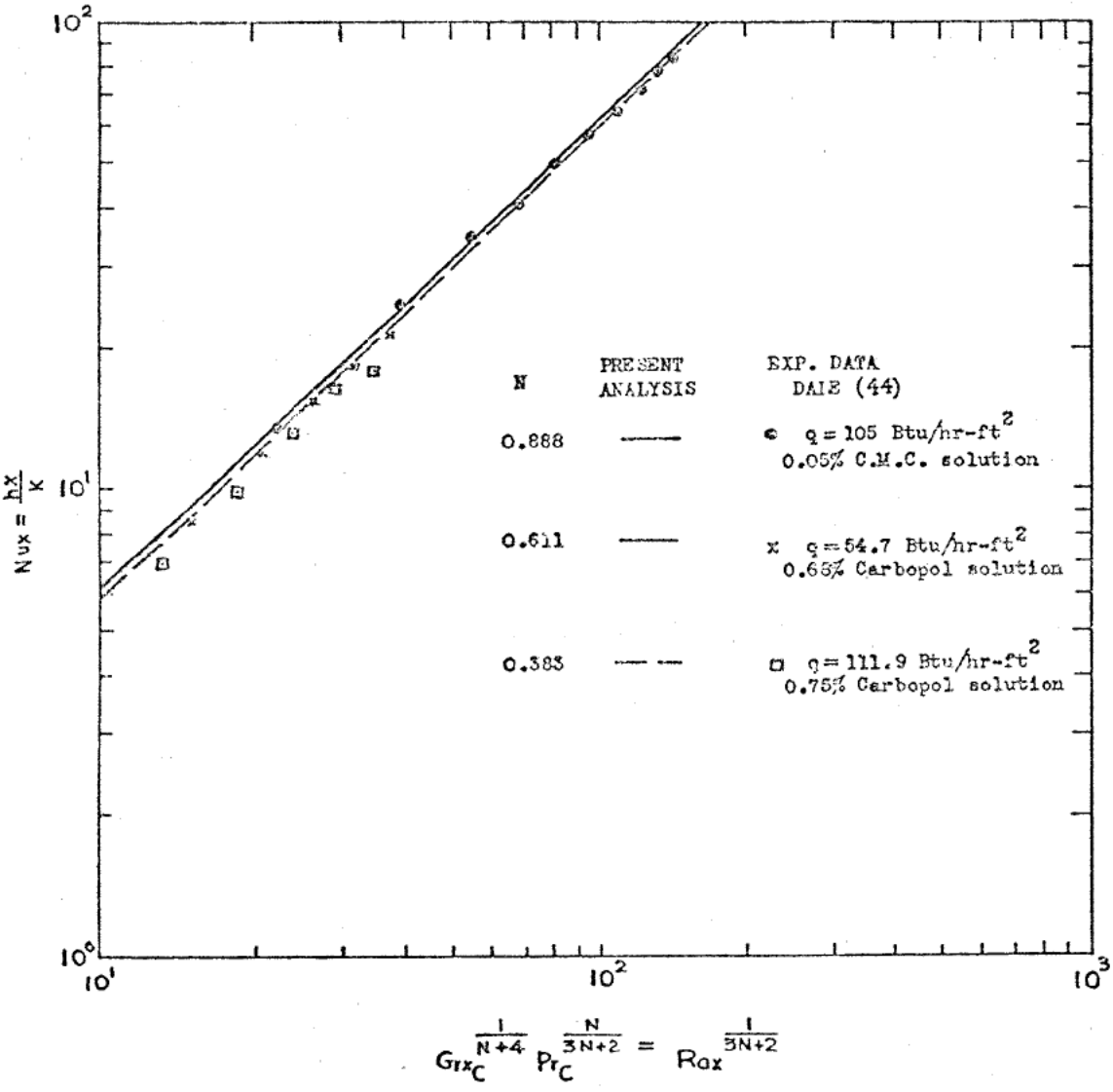

Fig. 4.10 Comparison between the predicted local Nusselt numbers calculated from region-free solution and the experimental results.

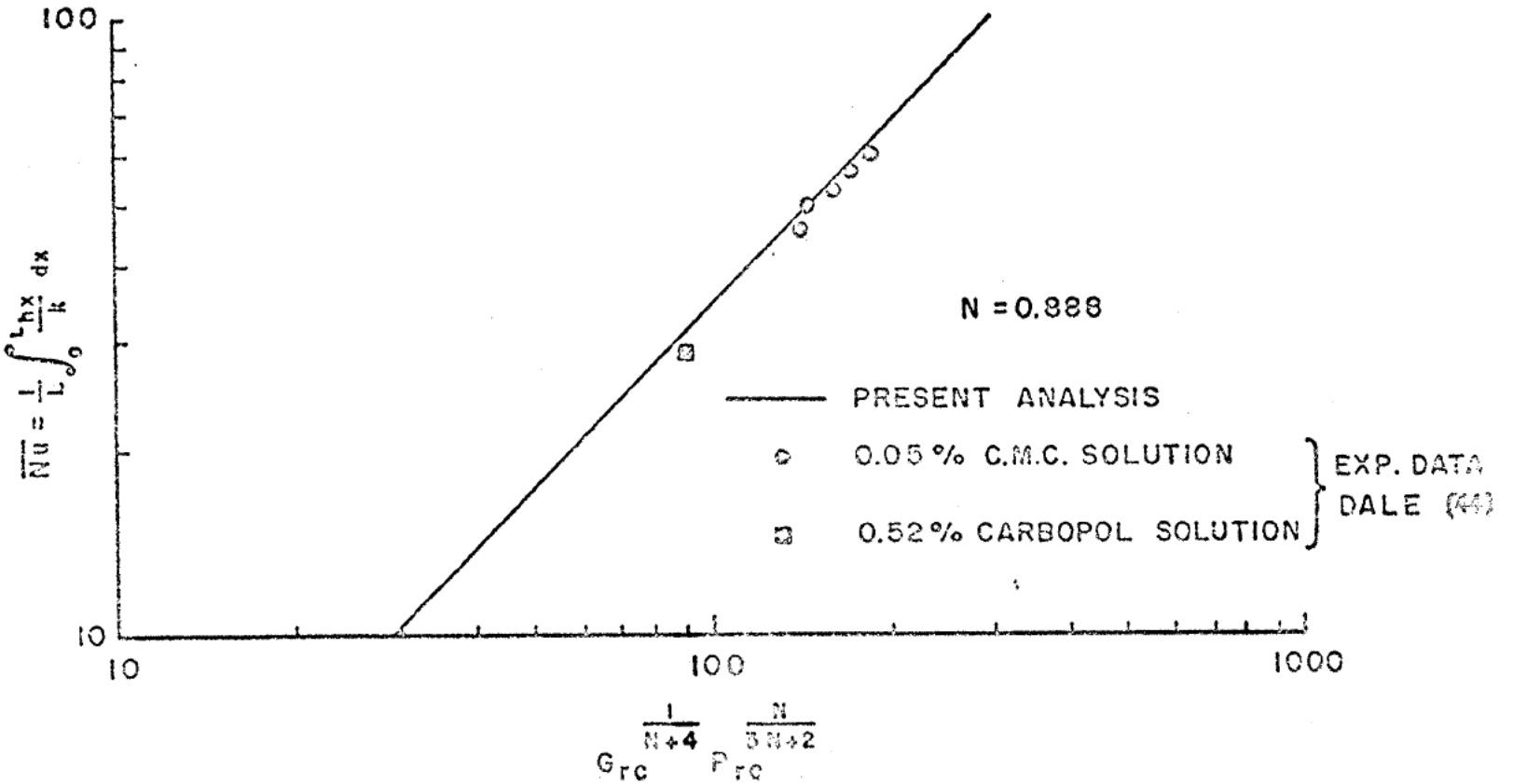

Fig. 4.11 Comparison between the predicted average Nusselt numbers calculated from region-free solution and the experimental results.

Fig. 4.12 shows predicted heat transfer results can be correlated with the generalized Rayleigh number Ra_C and are in good agreement with those experimental results for N=0.888. The predicted average Nusselt number in Fig. 4.12 is calculated from the region-free solution using Equations (4.35) and (4.43) to give

$$\overline{Nu} = C_1(N)\ Ra_C^{\frac{1}{3N+2}} \qquad (4.44)$$

Fig. 4.13 shows a comparison of dimensionless temperature distributions across the boundary layer with those calculated from data of Dale for N=0.888. The agreement is good, though the experimental results are a little higher than those of theory. The disagreement occurred again when a comparison is made on the dimensionless velocity distribution in Fig. 4.14. The velocity far from the plate decreases faster than the theory predicts. A possible reason of such a disagreement may be caused by one or both of the following

1). Experimental error: The flat plate used for testing is too large. It causes a free surface effect on the entire flow field which produces reverse flow, as observed by Dale (44). The free surface effect can be eliminated with a smaller testing plate or a deeper testing container. A significant improvement to the disagreement was observed by Dale when a smaller plate was used; unfortunately the testing fluids were nearly Newtonian. Additional error

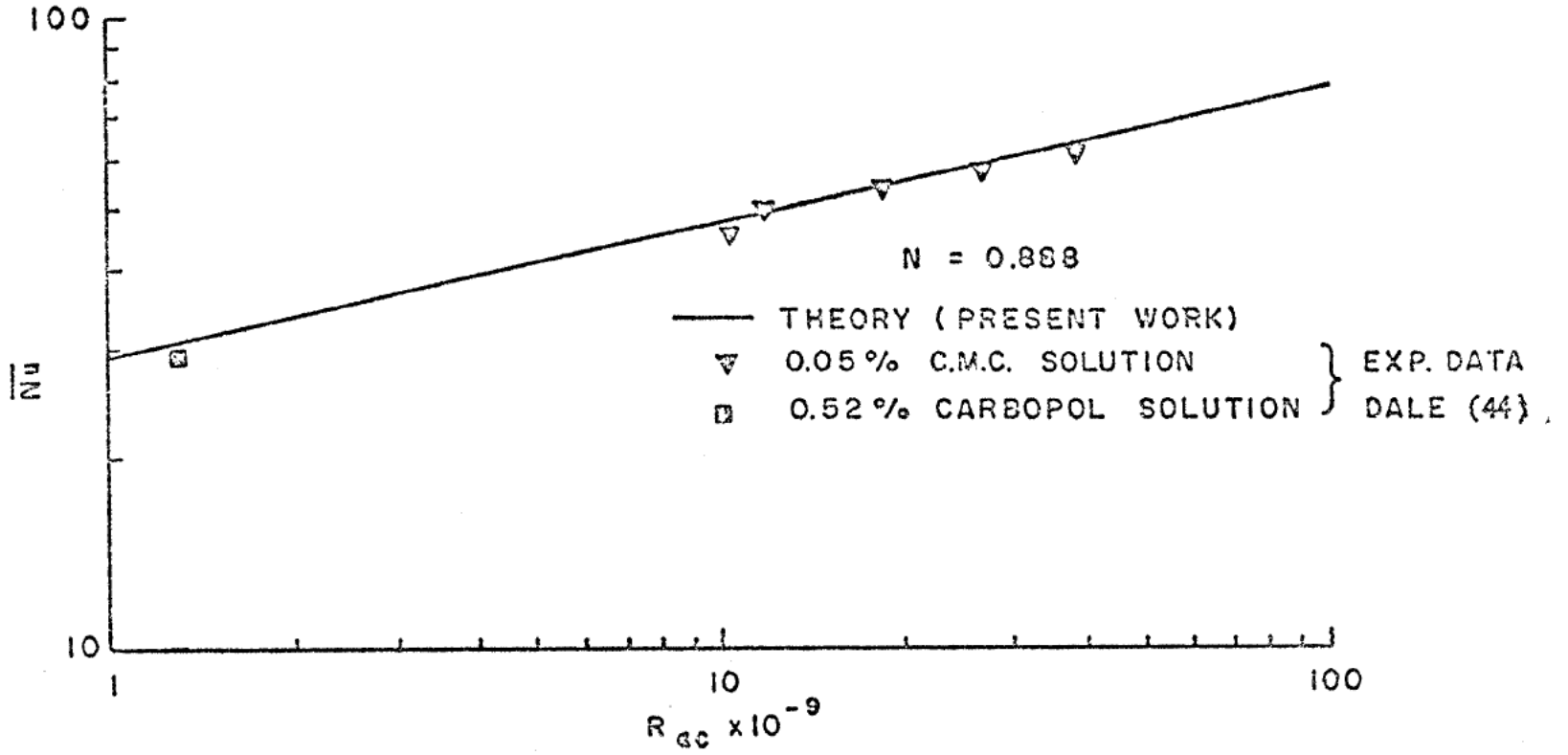

Fig. 4.12 Predicted heat transfer results are correlated with the generalized numbers and compared with experiments.

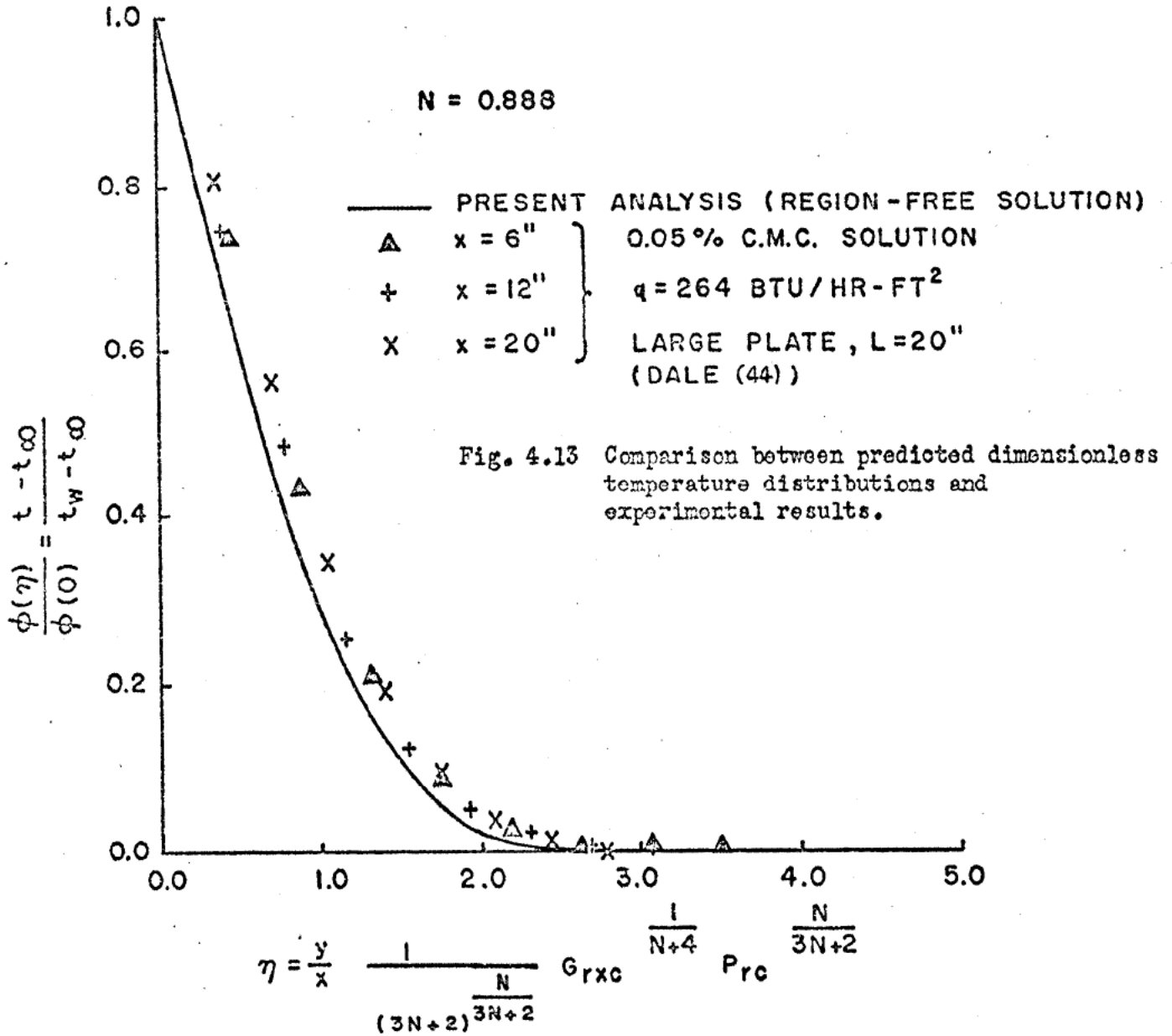

Fig. 4.13 Comparison between predicted dimensionless temperature distributions and experimental results.

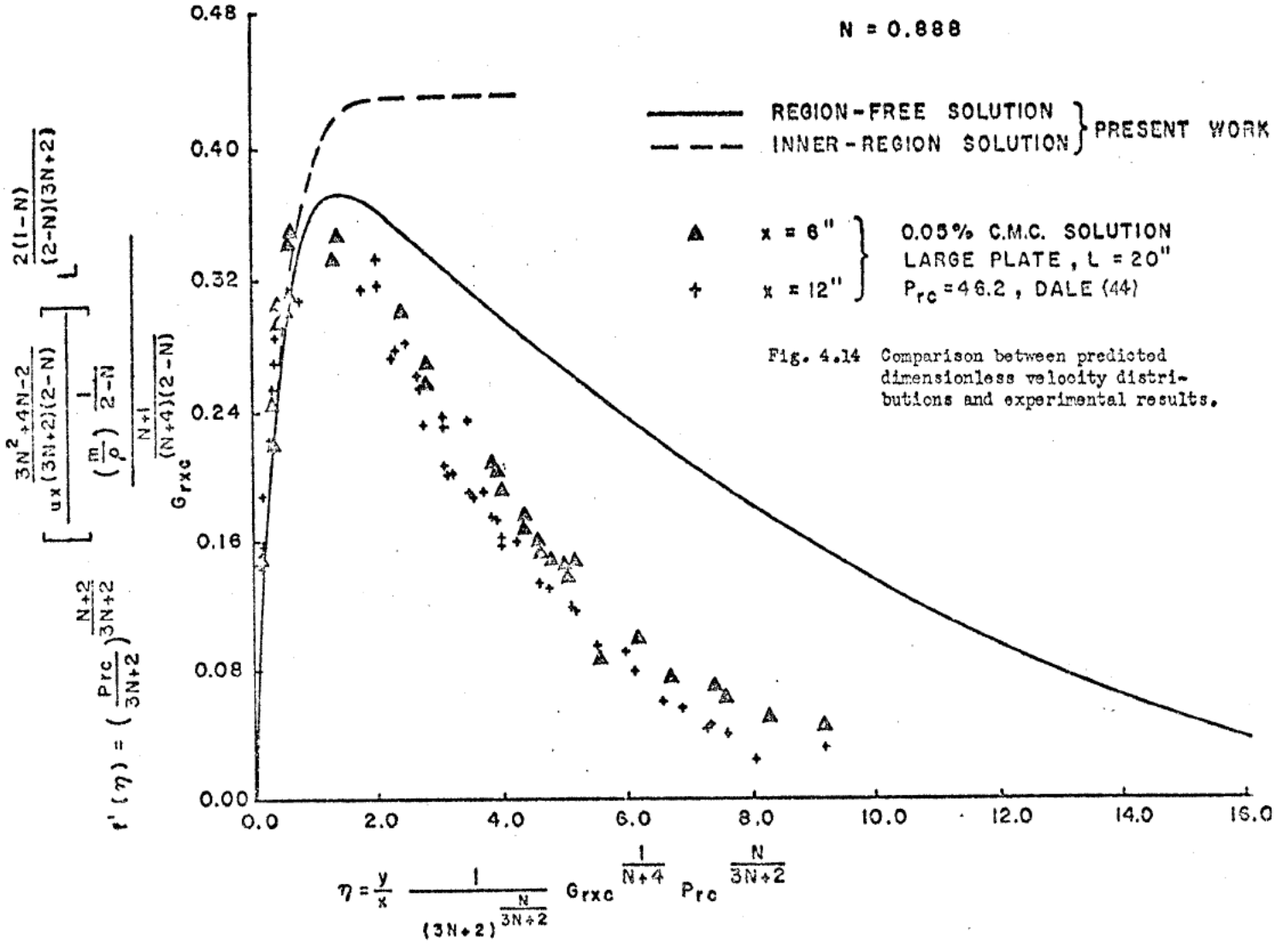

Fig. 4.14 Comparison between predicted dimensionless velocity distributions and experimental results.

might result from the difficulty in keeping the surface heat flux constant.

2). Theoretical error: The main assumption of this research is that the present analysis applies only to those power law fluids of high generalized Prandtl number. It is found that the fluid used in the experimental study shown in Fig. 4.14 has a generalized Prandtl number Pr_C = 46.2. If we use the well-established exact solution for Newtonian flow as a reference, (this is certainly permissible because N=0.888 is actually only slightly non-Newtonian), it can be shown that a fluid with Pr_C =46.2 may suffer a maximum theoretical error in the heat transfer results of less than 2%.

4.3.2 Comparison of heat transfer parameters:

An integral method with assumption of a high generalized Prandtl number has been applied by Tien (42) to the present problem. The local and average heat transfer parameters were derived to give

$$Nux = \frac{hL}{k} = M_1(N)\ (Gr_T\ Pr_T^{\ N})^{\frac{1}{3N+2}}\ (\frac{x}{L})^{\frac{-N}{3N+2}} \qquad (4.45)$$

$$\overline{Nu} = \frac{1}{L}\int_0^L Nux\ dx = M_2(N)\ (Gr_T\ Pr_T^{\ N})^{\frac{1}{3N+2}} \qquad (4.46)$$

where Gr_T and Pr_T were first defined by Tien as

$$Gr_T = \frac{g\beta q\ L^{\frac{4}{2-N}}}{k\ (\frac{m}{\rho})^{2/(2-N)}} \qquad (4.47)$$

$$Pr_T = \frac{\rho C_p}{k} \left(\frac{m}{\rho}\right)^{\frac{1}{2-N}} L^{\frac{2(1-N)}{2-N}} \qquad (4.48)$$

It can easily be verified that

$$Ra_C = Gr_T \, Pr_T^N = Gr_C^{\frac{3N+2}{N+4}} \, Pr_C^N$$

Therefore, the coefficients $M_1(N)$ and $M_2(N)$ of Equations (4.45) and (4.46) are comparable to $C(N)$ and $C_2(N)$ of Equations (4.30) and (4.37).

Figs. 4.15 and 4.16 show the comparisons of the present similarity solutions (region-free and inner-region) with Tien's integral method solution, and also with the experimental results of Dale (44). It appears that the integral method shows fair agreement with the present solution only when the power law fluid index N is greater than one. The fact that the integral method does not work for N<1 can be fully explained by observing Figs. 4.5 and 4.6 for the velocity and temperature distributions of various N across the boundary layers. In fact, the momentum boundary layer is much thicker than the thermal boundary layer for any N<1. This is contrary to the basic assumption of the integral method that the momentum and thermal boundary layers are approximately equal in thickness.

The experimental heat transfer results shown in Fig. 4.16 are below those predicted by all the theories. The best results are found when the experimental data are

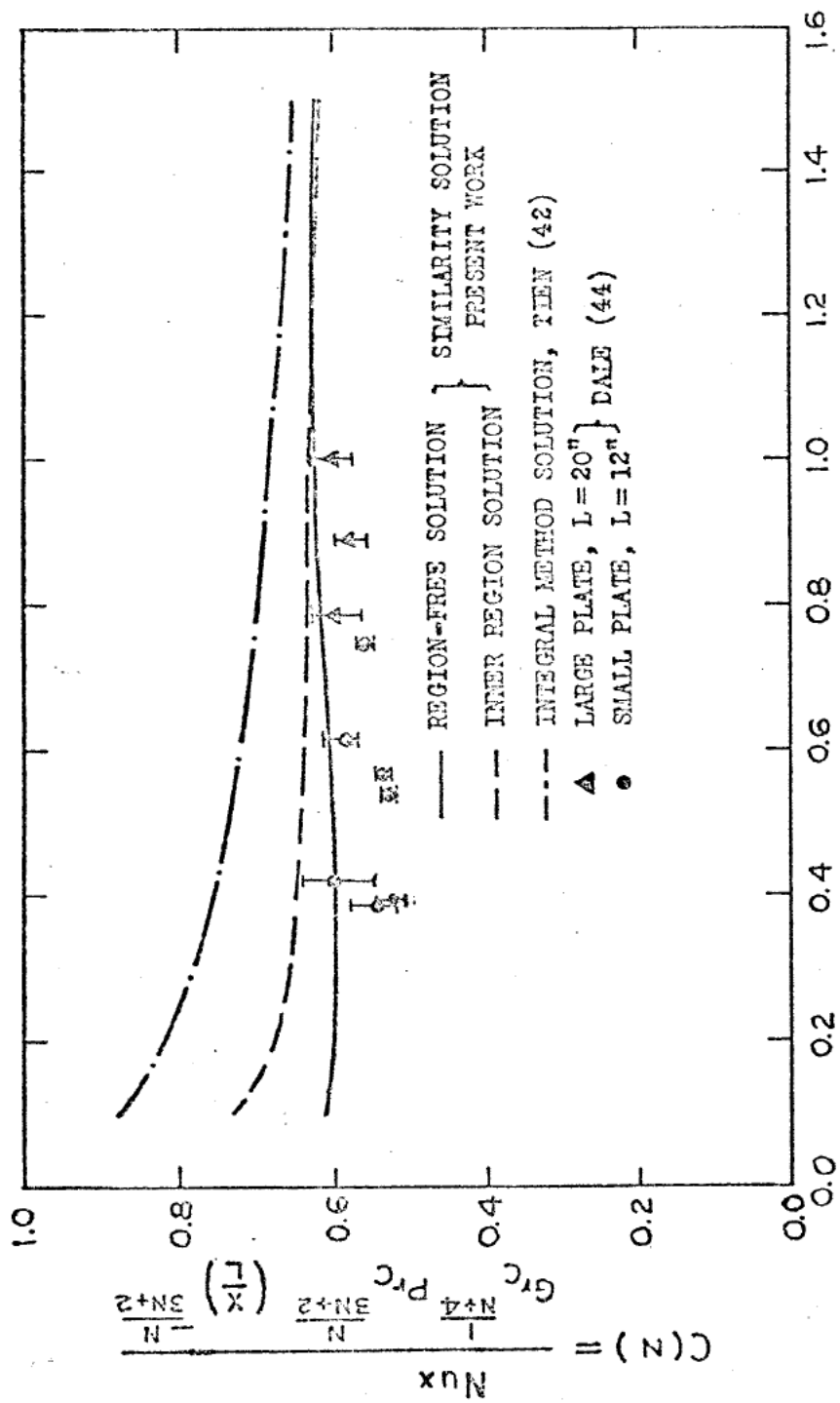

Fig. 4.15 Comparison of local heat transfer parameters using $Nux = \frac{hL}{k}$ and experiments.

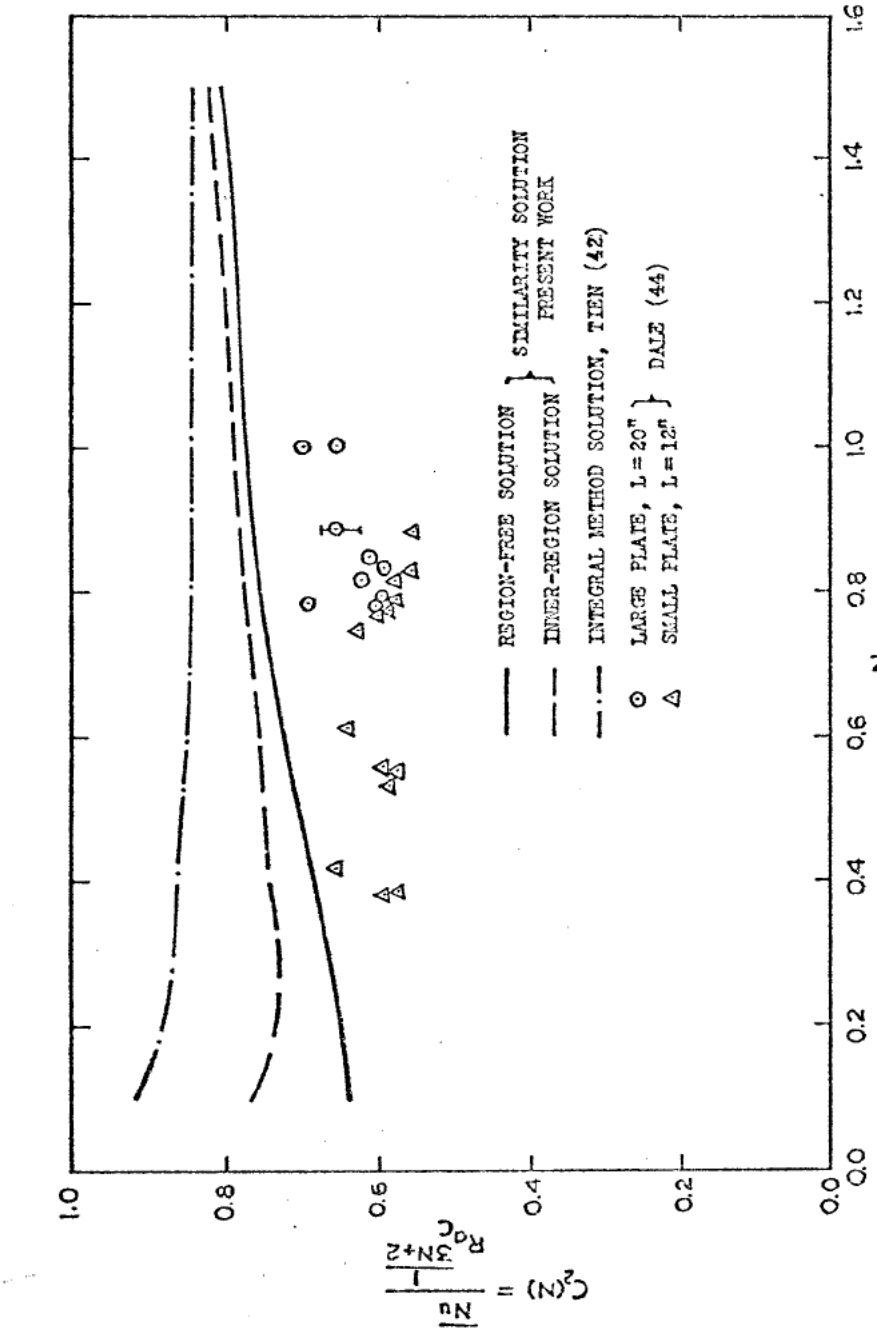

Fig. 4.16 Comparison of average heat transfer parameters using $\overline{Nu} = \frac{1}{L}\int_0^L \frac{hL}{k}\,dx$ and experiments.

correlated using Equation (4.35); This is shown in Fig. 4.17. It appears that differences between the region-free and inner-region solutions are limited except for small values of the power law fluid index.

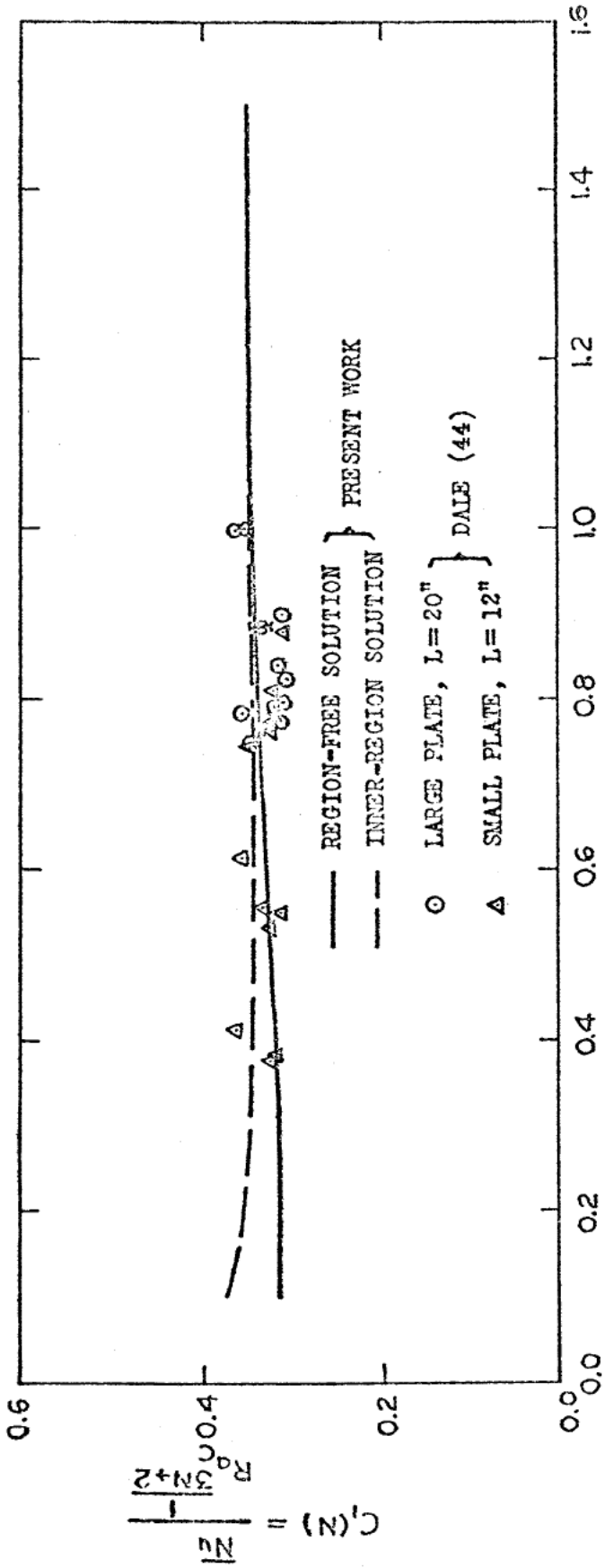

Fig. 4.17 Comparison of average heat transfer parameters using $\overline{Nu} = \frac{1}{L}\int_0^L \frac{hx}{k}\,dx$ and experiments.

CHAPTER V

DISCUSSION

5.1 Generalized Prandtl Number and Non-Newtonian Factor

Using dimensional analysis, it has been shown in Chapters III and IV that the "generalized Prandtl number", Pr_N, differs from the conventional Prandtl number Pr by a "non-Newtonian factor", f_N, such that

$$Pr_N = Pr \cdot f_N \tag{5.1}$$

In all cases, Pr_N=Pr when N=1. For laminar free convection to power law fluids, the non-Newtonian factor is a function of the Grashof number Gr for Newtonian flow, the generalized Grashof number Gr_N for non-Newtonian flow, and the power law fluid index N. That is

$$f_N = f_N(Gr, Gr_N, N) \tag{5.2}$$

or simply

$$f_N = f_N(Gr_N, N) \quad \text{since } Gr_N = Gr \text{ when } N=1.$$

A high Prandtl number fluid flow will show a thin thermal boundary layer and a thick momentum boundary layer, while this is not necessarily true for a high generalized Prandtl number fluid flow. The generalized Prandtl number may be dominated by the non-Newtonian factor which, in turn, may be controlled by the buoyancy force and/or the power law fluid index. Table 5.1 lists a summary of the dimensionless groups for laminar free convection to power law fluids.

Table 5.1 Summary of the dimensionless groups for laminar free convection to power law fluids.

Symbol	Uniform Surface Temperature	Uniform Surface Heat Flux
Pr	$\frac{C_p \mu}{k}$	$\frac{C_p \mu}{k}$
Pr_N	$\frac{\rho C_p}{k} \left(\frac{m}{\rho}\right)^{\frac{2}{1+N}} L^{\frac{1-N}{1+N}} (Lg\beta\Delta t)^{\frac{3(N-1)}{2(N+1)}}$	$\frac{\rho C_p}{k} \left(\frac{m}{\rho}\right)^{\frac{5}{N+4}} L^{\frac{2(N-1)}{N+4}} \left(\frac{g\beta q}{k}\right)^{\frac{3(N-1)}{N+4}}$
Gr	$\left(\frac{\rho}{\mu}\right)^2 L^3 \cdot g\beta (t_w - t_\infty)$	$\left(\frac{\rho}{\mu}\right)^2 L^4 \frac{g\beta q}{k}$
Gr_N	$\left(\frac{\rho}{m}\right)^2 L^{N+2} \cdot (g\beta\Delta t)^{2-N}$	$\left(\frac{\rho}{m}\right)^2 L^4 \left(\frac{g\beta q}{k}\right)^{2-N}$
f_N	$\frac{Gr^{\frac{1}{2}}}{Gr_N^{\frac{1}{1+N}}}$	$\frac{Gr^{\frac{1}{2}}}{Gr_N^{\frac{5}{2(N+4)}}}$

5.2 Relationship between the Uniform Surface Temperature and Uniform Surface Heat Flux Cases

If we define the generalized Prandtl number and the generalized Grashof number for the uniform surface heat flux (USHF) case in the same manner as for uniform surface temperature (UST) case as

$$Gr_A\Big|_{USHF} = Gr_A = \left(\frac{\rho}{m}\right)^2 L^{2+N} \left[g\beta\left(\overline{t_w - t_\infty}\right)\right]^{2-N} \qquad (5.3)$$

$$Pr_A\Big|_{USHF} = Pr_A = \frac{\rho C_p}{K}\left(\frac{m}{\rho}\right)^{\frac{2}{1+N}} \left[L\beta g\left(\overline{t_w - t_\infty}\right)\right]^{\frac{3(N-1)}{2(N+1)}} L^{\frac{1-N}{1+N}} \qquad (5.4)$$

it is possible to rearrange Equation (4.38) to become

$$\frac{\overline{Nu}}{Gr_A^{\frac{1}{2(N+1)}} Pr_A^{\frac{N}{3N+1}}} = \left[C_3(N)\right]^{\frac{3N+2}{3N+1}} \qquad (5.5)$$

and to rearrange Equation (4.39) to give

$$\frac{\overline{Nu}}{Gr_A^{\frac{1}{2(N+1)}} Pr_A^{\frac{N}{3N+1}}} = \left[C_4(N)\right]^{\frac{3N+2}{3N+1}} \qquad (5.6)$$

Equations (5.5) and (5.6) are calculated and compared with the exact solution for Newtonian flow (N=1) in Table 4.1b, and compared with the uniform surface temperature solution from Chapter III and the uniform surface heat flux solution from Chapter IV in Table 5.2 for N=0.1, 0.5, 1.0, and 1.5. It is found that heat transfer rates from a vertical plate with UST are comparable to those with USHF, if

Table 5.2

Numerical values of average heat transfer parameters

$$\frac{\overline{Nu}}{Gr_A^{\frac{1}{2(N+1)}} \, Pr_A^{\frac{N}{3N+1}}}$$

N	Equation	Region-free solution		Inner-region solution		
		USHF*	UST**	UST		USHF
				Acrivos (11)	Present	
0.1	(5.5)	0.4524	0.4338	0.60	0.6246	0.6198
	(5.6)	0.4425				0.6063
0.5	(5.5)	0.5981	0.5690	0.63	0.6212	0.6481
	(5.6)	0.5698				0.6176
1.0	(5.5)	0.6944	0.6574	0.67	0.6703	0.7072
	(5.6)	0.6575				0.6697
1.5	(5.5)	0.7259	0.6823	0.71	0.6998	0.7420
	(5.6)	0.6861				0.7013

* Uniform surface heat flux

** Uniform surface temperature

their dimensionless groups are properly defined. The comparison among the present and exact solutions for Newtonian flow shown in Table 4.1 indicates that the region-free solution will differ from the exact solution well within experimental error (less than 10%) for $Pr > 5$ and is closer to the exact solution than the inner-region solution.

CHAPTER VI

CONCLUDING REMARKS

The region-free solution for laminar free convection to a power law fluid from a body with a uniform surface temperature or a uniform surface heat flux has been shown to be in satisfactory agreement with experimental results and also with the exact solution for Newtonian flow when $Pr > 5$. This solution appears superior to all previously published solutions and is recommended for all calculations.

The flow and heat transfer parameters are derived and plotted for various values of the power law fluid index N. The important physical quantities, such as shear stress and heat transfer rate, can be calculated from these parameters. It is found that these parameters are somewhat dependent on the power law fluid index for the region-free solution. It is also found that, with properly defined dimensionless groups, the laminar free convection heat transfer to a power law fluid about a vertical plate with uniform surface heat flux can be obtained using the heat transfer parameter from the uniform surface temperature case.

The present analysis has concentrated on results for a vertical plate because the experimental data are available. It should be understood that the present solution derived in Chapter III is applicable to other two-

dimensional isothermal bodies, such as a large vertical cylinder, a horizontal cylinder, a vertical cone or a sphere (with the appropriate transformation as demonstrated by Acrivos (11)). However, the work in Chapter IV is limited to the vertical plate having uniform surface heat flux, because a similarity solution apparently does not exist for any other body shapes.

This research program calls for more experimental work in the area of non-Newtonian natural convection for small power law fluid index. More accurate velocity measurements are needed in order to distinguish the region-free solution from the inner-region solution by comparing velocity profiles of fluids with the same power law fluid index.

LITERATURE CITED

1. Fredrickson, A. G., Principles and Applications of Rheology, Prentice-Hall, Inc., Englewood Cliffs, N. J., 1964.

2. Wilkinson, W. K., Non-Newtonian Fluids, Pergamon Press, New York, 1960.

3. Skelland, A. H. P., Non-Newtonian Flow and Heat Transfer, John Wiley and Sons, Inc., 1967.

4. Schlichting, H., Boundary Layer Theory, Chapter 12, 6th Edition, McGraw-Hill, New York, 1968.

5. Goldstein, S., Modern Developments in Fluid Dynamics, Vol. II, Oxford, 1938.

6. Merk, H. J. and J. A. Prins, "Thermal convection in laminar boundary layers I", Appl. Sci. Res., Sect. A, Vol. 4, pp. 11-24, 1954.

7. Bird, R. B., W. E. Stewart, and E. N. Lightfoot, Transport Phenomena, pp. 299, John Wiley and Sons, Inc., New York, Fifth Printing, 1965.

8. Na, T. Y. and A. G. Hansen, "Possible similarity solutions of the laminar natural convection flow of non-Newtonian fluids", Int. J. Heat Mass Transfer 9, pp. 261-262, 1966.

9. Lee, S. Y. and W. F. Ames, "Similarity solutions for non-Newtonian fluids", A.I.Ch. E. Journal, Vol. 12, No. 4, pp. 700-708, July 1966.

10. Sparrow, E. M., R. Eichhorn, and J. L. Gregg, "Combined forced and free convection in a boundary layer flow", Physics Fluids, Vol. 2, No. 3, pp. 319-328, June 1959.

11. Acrivos, A., "A theoretical analysis of laminar natural convection heat transfer to non-Newtonian fluids", A.I.Ch.E. Journal, 6, pp. 584-590, 1960.

12. Morgan, G. W. and W. H. Warner, "On heat transfer in laminar boundary layers at high Prandtl number", J. of Aero. Sci. 23, pp. 937-948, 1956.

13. Stewartson, K. and L. T. Jones, "The heated vertical plate at high Prandtl number", J. of Aero. Sci. 24, pp. 379, 1957.

14. Reilly, I. G., C. Tien, and M. Adelman, "Experimental study of natural convection heat transfer from a vertical plate in a non-Newtonian fluid", Can. J. Chem. Engng. 43, pp. 157-160, 1965.

15. Sharma, K. K. and M. Adelman, "Experimental study of natural convection heat transfer from a vertical plate in a non-Newtonian fluid", Can. J. Chem. Engng. 47, pp. 553-555, 1969.

16. Ostrach, S., "An analysis of laminar free convection flow and heat transfer about a flat plate parallel to the direction of the generating body force", NACA Rept. 1111, 1953.

17. Sparrow, E. M. and J. L. Gregg, "Laminar free convection from a vertical plate with uniform surface heat flux", Trans. ASME 78, pp. 435-440, 1956.

18. Hsu, S. T., Engineering Heat Transfer, Chapter 11, D. Van Nostrand Company, Inc., Princeton, 1963.

19. Grober, H., S. Erk, and U. Grigull, Translated by J. R. Moszynski, Fundamentals of Heat Transfer, Chapter 14, McGraw-Hill Book Co., Inc., New York, 1961.

20. Yang, K. T., "Possible similarity solutions for laminar free convection on vertical plates and cylinders", Trans. ASME, Ser. E., J. Applied Mech., pp. 230-236, June 1960.

21. Schmidt, E. and W. Beckmann, "Das Temperatur-und Geschwindigkeitsfeld von einen Wärme abgebenden senkrechter platte bei natürlicher Konvection", Tech. Mech. and Thermodynamik 1, pp. 341-349 and 391-406, 1930.

22. Nachtsheim, P. R. and P. Swigert, "Satisfaction of asymptotic boundary conditions in the numerical solution of boundary-layer equations", NASA TMX-52118, 1965.

23. Brodowicz, K., "An analysis of laminar free convection around isothermal vertical plate", Int. J. Heat Mass Transfer, Vol. 11, pp. 201-209, 1966.

24. Eckert, E. R. G. and E. Soehngen, "Interferometric studies on the stability and transition to turbulence of a free convection boundary layer", Proc. Gen. Discussion Heat Transfer, Inst. Mech. Engrs., ASME, London, pp. 321, 1951.

25. Kierkus, W. T., "An analysis of laminar free convection flow and heat transfer about an inclined isothermal plate", Int. J. Heat Mass Transfer, Vo. 11, pp. 241-253, 1968.

26. Hansen, K. E. and S. A. Mohamed, "Natural convection from isothermal flat surfaces", Int. J. Heat Mass Transfer, Vol. 13, pp. 1873-1886, December 1970.

27. Chiang, T. and J. Kaye, "On laminar free convection from a horizontal cylinder", Proc. of the fourth U. S. National Congress of Appl. Mech., Vol. 2, pp. 1213-1219, Univ. of California, Berkely, June 1962.

28. Peterka, J. A. and P. D. Richardson, "Natural convection from a horizontal cylinder at moderate Grashof numbers", Int. J. Heat Mass Transfer, Vol. 12, pp. 749-752, 1969.

29. Fendell, F., "Laminar natural convection about an isothermally heated sphere at small Grashof numbers", J. Fluid Mech., 34, Part 1, pp. 163-176, 1968.

30. Ranz, W. E. and W. R. Marshall, Jr., "Evaporation from drops", Chem. Engng. Progress, Vol. 48, No. 3, pp. 141-146, 173-180, March 1952.

31. Meyer, P., "Heat transfer to small particles by natural convection", Trans. Inst. Chem. Engrs. 15, pp. 127-130, 1937.

32. Yuge, T., "Experiments on heat transfer from spheres, including combined natural and forced convection", ASME Trans., Ser. C, 82, pp. 214-220, Aug. 1960.

33. Klyachko, L. S., "Heat transfer between a gas and spherical surface with the combined action of free and forced convection", ASME Trans., Ser. C, 85, pp. 355-357, Nov. 1963.

34. Sparrow, E. M. and J. L. Gregg, "Similar solutions for free convection from a nonisothermal vertical plate", Trans. ASME, 80, pp. 379-386, 1958.

35. Gebhart, B., "Effects of viscous dissipation on natural convection", J. Fluid Mech. 4, pp. 225-232, 1962

36. Gebhart, B. and J. Mollendorf, "Viscous dissipation in external natural convection flows", J. Fluid Mech., 38(1), pp. 97-107, 1969.

37. Dotson, J. P., "Heat transfer from a vertical flat plate by free convection", M.S. thesis, Purdue University, 1954.

38. Goldstein, R. J. and E. R. G. Eckert, "The steady and transient free convection boundary layer on a uniformly heated vertical plate", Int. J. Heat Mass Transfer, 1, pp. 208-218, 1960.

39. Vliet, G. C. and C. K. Liu, "An experimental study of turbulent natural convection boundary layers", J. of Heat Transfer 91, pp. 517-531, Nov. 1969.

40. Rajan, V. S. V. and J. J. C. Picot, "Experimental study of the laminar free convection from a vertical plate", I. & E. C. Fundamentals, Vol. 10, No. 1, pp. 132-134, 1971.

41. Sparrow, E. M., "Laminar free convection on a vertical plate with prescribed non-uniform wall heat flux or prescribed non-uniform wall temperature", NACA TN 3508, 1955.

42. Tien C., "Laminar natural convection heat transfer from vertical plate to power-law fluid", Applied Sci. Res. 17, pp. 233-247, 1967.

43. Kubair, V. G. and D. C. Pei, "Combined laminar free and forced convection heat transfer to non-Newtonian fluids", Int. J. Heat Mass Transfer 11, pp. 855-869, 1968.

44. Dale, J. D., "Laminar free convection of non-Newtonian fluids from a vertical flat plate with uniform surface heat flux", Ph. D. thesis, University of Washington, 1969.

45. Emery, A. F., H. W. Chi, and J. D. Dale, "Free convection through vertical plane layers of non-Newtonian power law fluids", ASME paper No. 70-WA/HT-1-1970; or, J. of Heat Transfer, May 1971, Vol. 93, No. 2, pp. 164-171.

46. Acrivos, A., "On the combined effect of forced and free convection heat transfer in laminar boundary layer flows", Chem. Engng. Sci. 21, pp. 343, 1966.

47. Fox, L., Numerical Solution of Ordinary and Partial Differential Equations, Chapter 5, Pergamon Press, 1962.

APPENDIX A1*

Critique of Lee and Ames' Work on Free Convection

The dimensionless governing differential equations for laminar free convection to power law fluids are given by Equations (60) and (56) of Reference (9)

$$\frac{\partial \psi}{\partial y}\frac{\partial^2 \psi}{\partial y\,\partial x} - \frac{\partial \psi}{\partial x}\frac{\partial^2 \psi}{\partial y^2} = \frac{\partial}{\partial y}\left(\left|\frac{\partial^2 \psi}{\partial y^2}\right|^{n-1}\frac{\partial^2 \psi}{\partial y^2}\right) + \theta \qquad \text{(A1)}$$

$$\frac{\partial \psi}{\partial y}\frac{\partial \theta}{\partial x} - \frac{\partial \psi}{\partial x}\frac{\partial \theta}{\partial y} = \frac{1}{N_{Pr}}\frac{\partial^2 \theta}{\partial y^2} \qquad \text{(A2)}$$

Using the similarity variable and reduced functions given in Equations (57) of Reference (9)

$$\eta = y\,x^{-1/3}\ ,\quad f = \psi x^{-2/3}\ ,\quad g = \theta x^{-t} \qquad \text{(A3)}$$

the following derivatives are obtained

$$\frac{\partial \eta}{\partial y} = x^{-1/3}\ ,\quad \frac{\partial \eta}{\partial x} = -\frac{1}{3}\frac{\eta}{x}$$

$$\frac{\partial \psi}{\partial x} = \frac{1}{3}x^{1/3}(2f - \eta f')\ ,\quad \frac{\partial \psi}{\partial y} = x^{1/3} f'$$

$$\frac{\partial^2 \psi}{\partial y^2} = f''\ ,\quad \frac{\partial^2 \psi}{\partial y\,\partial x} = \frac{1}{3x^{2/3}}(f' - \eta f'')$$

$$\frac{\partial \theta}{\partial x} = x^{t-1}\left(tg - \frac{1}{3}\eta g'\right)$$

$$\frac{\partial \theta}{\partial y} = x^{t-1/3} g'\ ,\qquad \frac{\partial^2 \theta}{\partial y^2} = x^{t-2/3} g''$$

---

* The nomenclature used in Appendix A1 follows (9).

where the primes denote the differentiation with respect to η. Substituting the derivatives into Equations (A1) and (A2), we obtain

$$f'^2 - 2ff'' = 3\frac{d}{d\eta}\left(|f''|^{n-1} f''\right) + 3g\, x^{\frac{1}{3}+t} \qquad (A4)$$

and

$$g'' + \frac{1}{3}\,Pr\,(2fg' - 3tf'g) = 0 \qquad (A5)$$

Equations (A4) and (A5) are ordinary differential equations only if

$$t = -\frac{1}{3} \qquad (A6)$$

Thus from Equation (A3)

$$g \equiv \theta\, x^{1/3} \qquad (A7)$$

instead of $g = \theta\, x^{-1/3}$ as claimed in Equation (61) of Reference (9). The wall temperature variation is now

$$\theta_w = x^{-1/3}$$

which is unrealistic as stated in References (8) and (11).

APPENDIX A2*

Critique of Kubair and Pei's Work on Combined Convection

The combined convection controlling parameter P was defined by Kubair and Pei (43) as

$$P = \frac{N_{Gr'}}{N_{Re'}^{\frac{2}{2-n}}} = \frac{(\frac{\rho}{k})^{\frac{2}{2-n}} x^{\frac{n+2}{2-n}} [\beta g(T_W - T_\infty)]}{(\frac{\rho U_\infty^{2-n} x^n}{K})^{2/(2-n)}}$$

Since $U_\infty = Ax^m$ and $T_W - T_\infty = Bx^{n'}$, P becomes

$$P = \frac{g\beta B}{A^2} x^{1+n'-2m}$$

Therefore, P is constant only when

$$1+n'-2m=0, \quad \text{or,} \quad n' = 2m-1$$

This is exactly the restriction Sparrow et al. (10) found for combined convection to Newtonian flow.

The generalized Prandtl number was defined as (43)

$$N_{Pr'} = \frac{C_p U_\infty \rho x}{k} N_{Re'}^{\frac{-2}{1+n}}$$

or,

$$N_{Pr'} = \frac{\rho C_p}{k} A^{\frac{3(n-1)}{n+1}} (\frac{K}{\rho})^{\frac{2}{1+n}} x^{m+1-\frac{2n}{1+n}-\frac{2m(2-n)}{1+n}}$$

Therefore, $N_{Pr'}$ is a constant only when

$$m+1 - \frac{2n}{1+n} - \frac{2m(2-n)}{1+n} = 0$$

---

*The nomenclature used in Appendix A2 follows (43).

Then $m=\frac{1}{3}$ if $n \neq 1$

Therefore, $n'=2m-1=-1/3$. This is exactly the restriction found by Na and Hansen (8) for the pure free convection to non-Newtonian power law fluids.

Thus, the similarity solution exists only when

$$U_\infty \cong Ax^{1/3} \quad \text{and} \quad T_w-T_\infty \cong Bx^{-1/3}$$

which is unrealistic because of this variation of temperature difference with x.

Upon further investigation of the dimensionless groups of (43), it was found they did not satisfy the continuity equation. This can be demonstrated as follows:

$$\frac{\partial u}{\partial x} = \frac{\partial}{\partial x}\left[\frac{U_\infty}{2} f'(\eta)\right] = \frac{Ax^{m-1}}{2}\left[mf + \frac{2m-mn-2n-1}{n+1}\eta f'\right]$$

$$\frac{\partial v}{\partial y} = \frac{\partial}{\partial y}\left[\frac{2^{n+1}}{A^{2-n}} \frac{K}{\rho} \frac{A}{x} x^{\frac{2mn-m+1}{n+1}} \left(\frac{mn-2m+1}{n+1}\eta f' - \frac{2mn-m+1}{n+1} f\right)\right]$$

$$= 2^n A^{\frac{n^2}{n+1}-\frac{n+1}{n+1}} \left(\frac{K}{\rho}\right)^{\frac{n}{n+1}} x^{\frac{mn+m-3n-1}{n+1}} \left(\frac{mn-2m+1}{n+1}\eta f' - mf\right)$$

where

$$\frac{\partial \eta}{\partial x} = \frac{2m-mn-2n-1}{n+1} \frac{\eta}{x}$$

$$\frac{\partial \eta}{\partial y} = \frac{1}{2x} N_{Re'}^{\frac{1}{n+1}} = \frac{1}{2}\left(\frac{\rho}{K}\right)^{\frac{1}{n+1}} A^{\frac{2-n}{n+1}} x^{\frac{2m-mn-2n-1}{n+1}}$$

Therefore

$$\frac{\partial u}{\partial x} + \frac{\partial v}{\partial y} \neq 0$$

APPENDIX B

Numerical Solution of the Boundary Layer Equations with Asymptotic Boundary Conditions for Non-Newtonian Fluid Flow Problems

B.1 Derivation of the Perturbation Equations

B.1.1 Uniform surface temperature case:

The system of ordinary differential Equations (3.17) and (3.18) can be rewritten to give

$$\frac{d}{d\eta}\left(|f''|^{N-1} f'' \right) = -\phi \qquad \text{(B.1)}$$

$$\phi'' = -f\phi' \qquad \text{(B.2)}$$

B. C. $f(0)=f'(0)=\phi(0)-1=\phi(\infty)=f'(\infty)=0$ (B.3)*

Because f" may be positive (near the wall) or negative (far from the wall), Equation (B.1) can be expanded into parts, namely

$$f''' = \frac{-\phi}{N\,(f'')^{N-1}} \qquad \text{for } f''>0 \qquad \text{(B.4)}$$

$$f''' = \frac{-\phi}{N\,|f''|^{N-1}} \qquad \text{for } f''<0 \qquad \text{(B.5)}$$

and for f"=0: f"' =0 if N<1, f"' =$-\phi$ if N=1, and f"' =∞ if N>1. The divergent characteristics of f"' at N > 1 can be averted by adjusting the increment of η so that the value of f" never equals zero. In fact, this is one of the excellent advantages for solving this type

*The boundary conditions here are for the region-free solution. A slight change can convert this presentation to include the inner-region solution.

of equation by numerical integration. In the following derivations, the work is primarily developed for N<1. However, it may also apply for N≥1 provided specific care be taken to deal with the case when f"=0. Experience tells it is generally all right to use f"' =0 when f"=0 for all values of N because actually the value of f" probably never goes to zero during the numerical process with proper choice of increment.

According to Fox (47), two additional initial conditions (the missing initial boundary values) at the wall can be sought if the following nonlinear equations are satisfied simultaneously

$$f'(\zeta,\xi)\big|_{\eta_{edge}}=0$$

$$\Phi(\zeta,\xi)\big|_{\eta_{edge}}=0$$

where $\zeta=f''(0)$ and $\xi=\phi'(0)$ are the two missing initial boundary values; η_{edge} is the value of η where further extension of η will have little or no effect on the values of f' and ϕ. Thus the necessary corrections to an approximation for ζ and ξ come from a solution of the linear equations (at $\eta=\eta_{edge}$)

$$f' + f'_{\zeta}\Delta\zeta + f'_{\xi}\Delta\xi = 0 \qquad \text{(B.6)}$$

$$\Phi + \Phi_{\zeta}\Delta\zeta + \Phi_{\xi}\Delta\xi = 0 \qquad \text{(B.7)}$$

where the derivatives $f'_{\zeta} = \frac{\partial f'}{\partial \zeta}$, $f'_{\xi} = \frac{\partial f'}{\partial \xi}$ and $\Phi_{\zeta} = \frac{\partial \Phi}{\partial \zeta}$, $\Phi_{\xi} = \frac{\partial \Phi}{\partial \xi}$ come from the perturbation differential equations

for the ζ and ξ derivatives.

For ζ derivatives:

$$\text{at } f''>0, \quad f'''_\zeta = \frac{-(f'')^{1-N}}{N}\left[\phi_\zeta + (1-N)\frac{\phi}{f''} f''_\zeta\right] \tag{B.8}$$

$$\text{at } f''=0, \quad f'''_\zeta = 0 \tag{B.9}$$

$$\text{at } f''<0, \quad f'''_\zeta = \frac{-|f''|^{1-N}}{N}\left[\phi_\zeta - (1-N)\frac{\phi}{|f''|} f''_\zeta\right] \tag{B.10}$$

$$\text{and} \quad \phi''_\zeta = -(f_\zeta \phi' + f\,\phi'_\zeta) \tag{B.11}$$

For ξ derivatives:

$$\text{at } f''>0, \quad f'''_\xi = \frac{-(f'')^{1-N}}{N}\left[\phi_\xi + (1-N)\frac{\phi}{f''} f''_\xi\right] \tag{B.12}$$

$$\text{at } f''=0, \quad f'''_\xi = 0 \tag{B.13}$$

$$\text{at } f''<0, \quad f'''_\xi = \frac{-|f''|^{1-N}}{N}\left[\phi_\xi - (1-N)\frac{\phi}{|f''|} f''_\xi\right] \tag{B.14}$$

$$\text{and} \quad \phi''_\xi = -(f_\xi \phi' + f\,\phi'_\xi) \tag{B.15}$$

Note that $-f''_\zeta$ and $-f''_\xi$ in the bracket of Equations (B.10) and (B.14) are equivalent to $\frac{\partial |f''|}{\partial \zeta}$ and $\frac{\partial |f''|}{\partial \xi}$ respectively.

The initial conditions for the above perturbation equations are

$$\text{at } \eta=0, \quad f_\zeta = f'_\zeta = \phi_\zeta = \phi'_\zeta = f''_\zeta - 1 = 0 \tag{B.16}$$

$$\text{and} \quad f_\xi = f'_\xi = f''_\xi = \phi_\xi = \phi'_\xi - 1 = 0 \tag{B.17}$$

B.1.2 Uniform surface heat flux:

Using the same method as in Section B.1.1 for uniform surface temperature case, the perturbation differential equations, with perturbation variables $\zeta = f''(0)$ and $\xi = \phi(0)$, are derived as follows:

For ζ derivatives:

f'''_ζ same as Equations (B.8-10) for $f'' \lessgtr 0$, and

$$\phi''_\zeta = Nf'_\zeta \phi + Nf'\phi_\zeta - 2(N+1)(f_\zeta \phi' + f\phi'_\zeta) \qquad (B.18)$$

For ξ derivatives:

f'''_ξ same as Equations (B.12-14) for $f'' \lessgtr 0$, and

$$\phi''_\xi = Nf'_\xi \phi + Nf'\phi_\xi - 2(N+1)(f_\xi \phi' + f\phi'_\xi) \qquad (B.19)$$

The initial conditions for the above perturbation equations are (at $\eta=0$)

$$f'_\zeta = f_\zeta = \phi_\zeta = \phi'_\zeta = f''_\zeta - 1 = 0 \qquad (B.20)$$

and

$$f_\xi = f'_\xi = f''_\xi = \phi''_\xi = \phi_\xi - 1 = 0 \qquad (B.21)$$

The necessary corrections to an approximation for ζ and ξ come from the same solution of the linear Equations (B.6) and (B.7), because the boundary conditions far from the wall are the same for both the uniform surface temperature and the uniform surface heat flux cases.

B.2 Convergence Criterion

The convergence criterion for the numerical integration may be obtained from the solution of the linear Equations (B.6) and (B.7) at $\eta = \eta_{edge}$. Then the values of ζ and ξ must be corrected until $\Delta\zeta = \Delta\xi \to 0$. This method is slow and has been modified by Nachtsheim and Swigert (22).

Besides Equations (B.6) and (B.7), two additional equations are supplemented for the convergence criterion such that

$$f'' + f''_\zeta \Delta\zeta + f''_\xi \Delta\xi = 0 \qquad (B.22)$$

and $$\Phi' + \Phi'_\zeta \Delta\zeta + \Phi'_\xi \Delta\xi = 0 \qquad \text{(B.23)}$$

The least-square solution for the system of Equations (B.6), (B.7), (B.22), and (B.23) is given by the solution of the following system of equations:(22)

$$(f'^2_\zeta + \Phi^2_\zeta + f''^2_\zeta + \Phi'^2_\zeta)\Delta\zeta + (f'_\zeta f'_\xi + \Phi_\zeta \Phi_\xi + f''_\zeta f''_\xi + \Phi'_\zeta \Phi'_\xi)\Delta\xi = -(f' f'_\zeta + \Phi \Phi_\zeta + f'' f''_\zeta + \Phi' \Phi'_\zeta) \qquad \text{(B.24)}$$

$$(f'_\zeta f'_\xi + \Phi_\zeta \Phi_\xi + f''_\zeta f''_\xi + \Phi'_\zeta \Phi'_\xi)\Delta\zeta + (f'^2_\xi + \Phi^2_\xi + f''^2_\xi + \Phi'^2_\xi)\Delta\xi = -(f' f'_\xi + \Phi \Phi_\xi + f'' f''_\xi + \Phi' \Phi'_\xi) \qquad \text{(B.25)}$$

If
$$\begin{aligned} d_{11} &= f'^2_\zeta + \Phi^2_\zeta + f''^2_\zeta + \Phi'^2_\zeta \\ d_{21} &= f'_\zeta f'_\xi + \Phi_\zeta \Phi_\xi + f''_\zeta f''_\xi + \Phi'_\zeta \Phi'_\xi \\ d_{12} &= f'_\zeta f'_\xi + \Phi_\zeta \Phi_\xi + f''_\zeta f''_\xi + \Phi'_\zeta \Phi'_\xi \\ d_{22} &= f'^2_\xi + \Phi^2_\xi + f''^2_\xi + \Phi'^2_\xi \\ r_1 &= f' f'_\zeta + \Phi \Phi_\zeta + f'' f''_\zeta + \Phi' \Phi'_\zeta \\ r_2 &= f' f'_\xi + \Phi \Phi_\xi + f'' f''_\xi + \Phi' \Phi'_\xi \end{aligned} \qquad \text{(B.26)}$$

Then
$$\Delta\zeta = \frac{-\begin{bmatrix} r_1 & d_{12} \\ r_2 & d_{22} \end{bmatrix}}{\Delta} \qquad \text{(B.27)}$$

and
$$\Delta\xi = \frac{-\begin{bmatrix} d_{11} & r_1 \\ d_{21} & r_2 \end{bmatrix}}{\Delta} \qquad \text{(B.28)}$$

where
$$\Delta = \begin{bmatrix} d_{11} & d_{12} \\ d_{21} & d_{22} \end{bmatrix} \qquad \text{(B.29)}$$

The convergence criterion is then determined when, after several iteration processes varying η_{edge}, the values of $\Delta\zeta$ and $\Delta\xi$, calculated from Equations (B.27) and (B.28), become very small such that

$$(\zeta + \Delta\zeta)_{n-1} \approx \zeta_n \qquad \text{(B.30)}$$

$$(\xi + \Delta\xi)_{n-1} \approx \xi_n \qquad \text{(B.31)}$$

The condition of $\Delta\zeta, \Delta\xi$ approaching zero proves the stability of the numerical integration; however, it does not show where the true solution, the missing initial boundary values, really are. An additional condition has to be found--that is the value of error E such that (see Equation (3.21))

$$E = [f'(\infty)]^2 + [f''(\infty)]^2 + [\phi(\infty)]^2 + [\phi'(\infty)]^2 \qquad \text{(B.32)}$$

The value of E is specified first and then compared with the calculated value; Iterating cycles continue until the calculated value equals or is less than the specified value and $\Delta\zeta$ and $\Delta\xi$ are also very small.

B.3 Computer Programming

B.3.1 Introduction:

The following information is of importance before computer programming for this specific two-point boundary value problem of non-Newtonian flow.

1. Method of numerical integration--fourth-order Runge-Kutta formula.
2. Accuracy--double precision.

3. Increment--$\Delta\eta \leq 0.06$

4. Execution time--about 20 seconds per iteration cycle; depends on the value of η_{edge}.

5. Error--$E < 10^{-4}$

6. Correction (convergence criterion)--$\Delta\zeta, \Delta\xi < 10^{-4}$

7. Input data--see Table B.1

B.3.2 Flow charts:

A program for integration using the fourth-order Runge-Kutta method is presented in the flow charts of Figs. B.1 and B.2 for $N < 1$. The first flow chart constitutes a general program for reading the necessary parameters, controlling the step size, checking the output, determining the necessity of iteration, and printing the results. It calls a subprogram for the actual integration; in this case the subprogram uses the fourth-order Runge-Kutta method, but any other self-starting method could be used, for example, Adams-Moulton (predictor-corrector) method.

Fig. B.1a Main Program

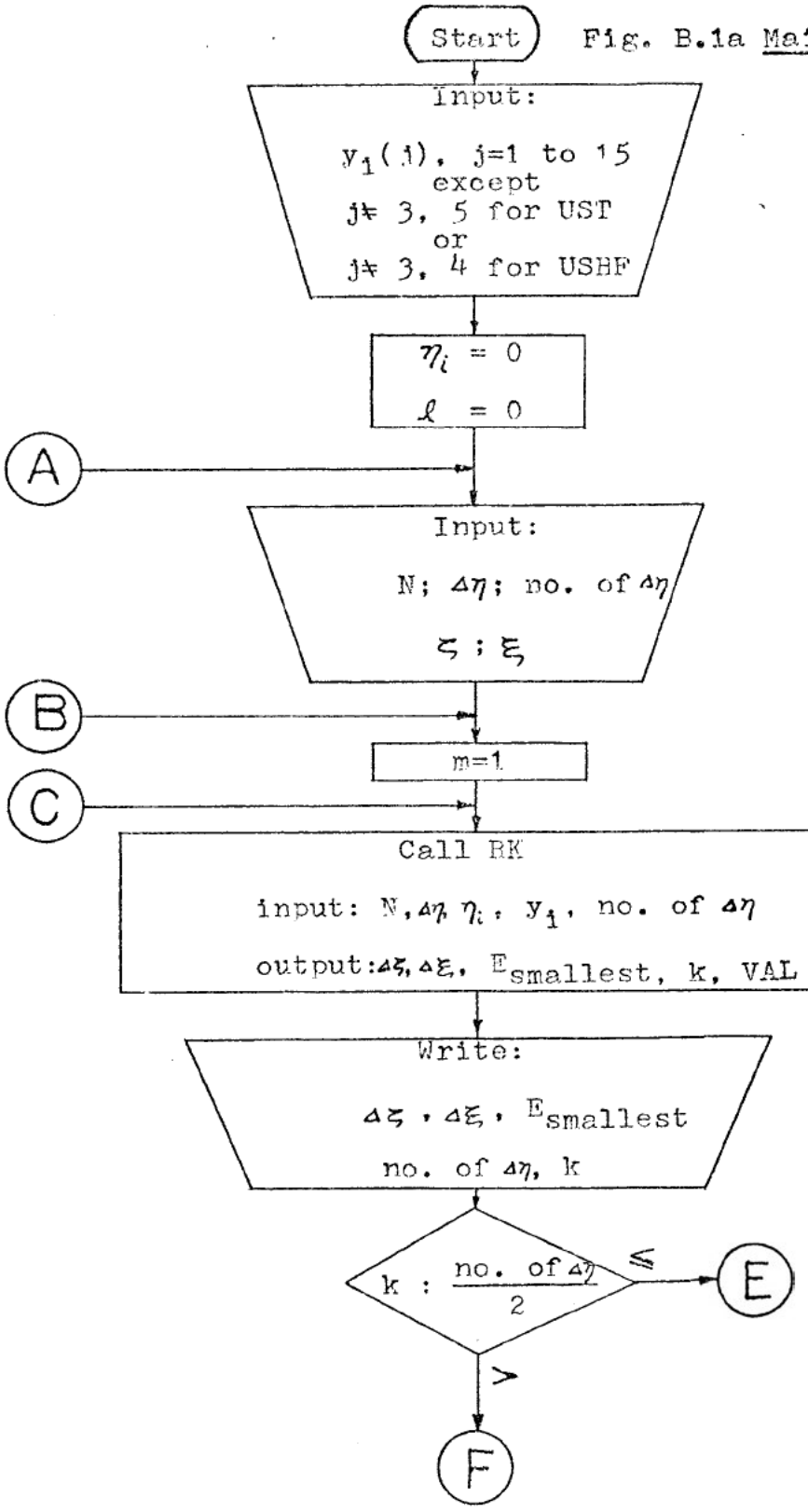

Fig. B. 1b

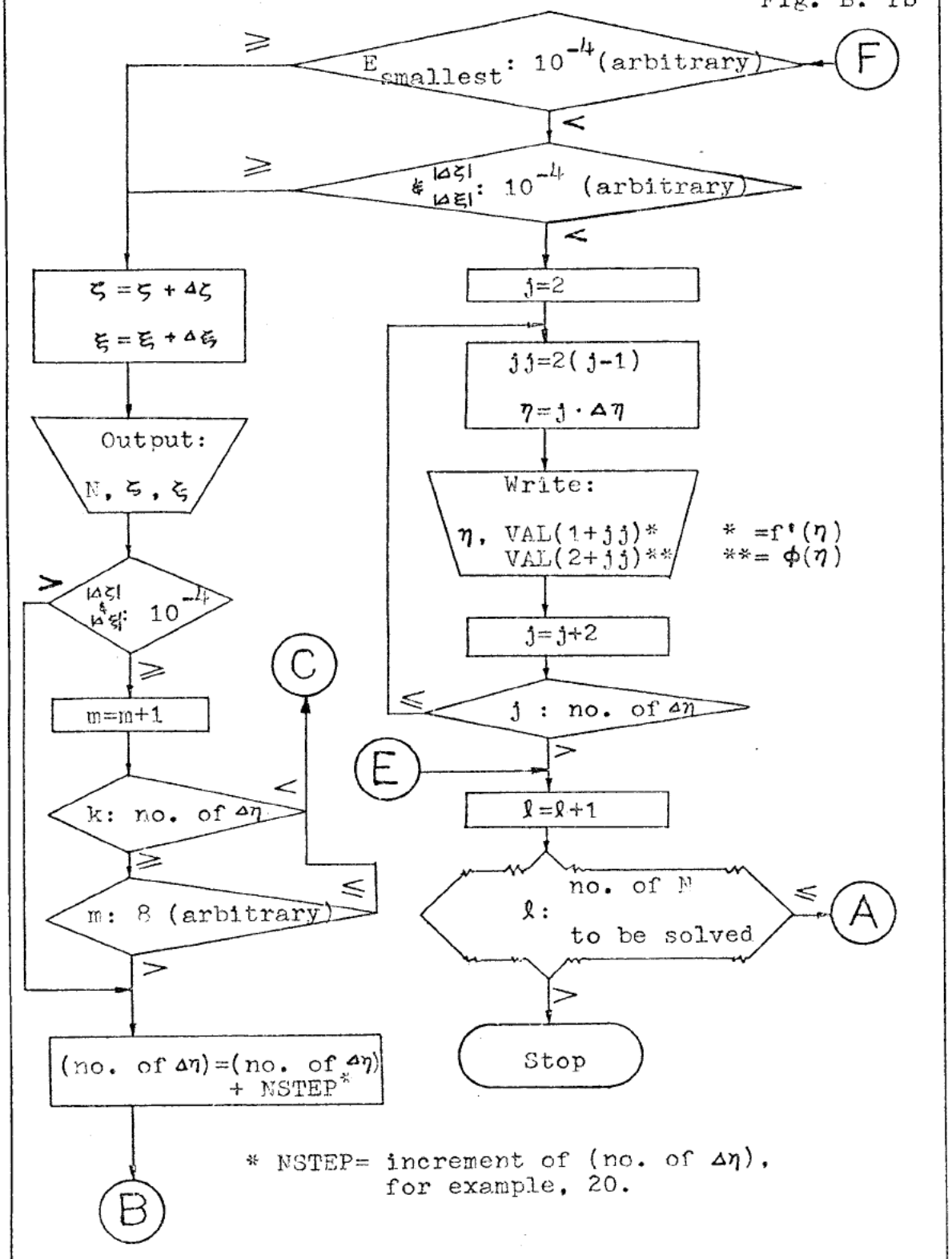

* NSTEP= increment of (no. of $\Delta\eta$), for example, 20.

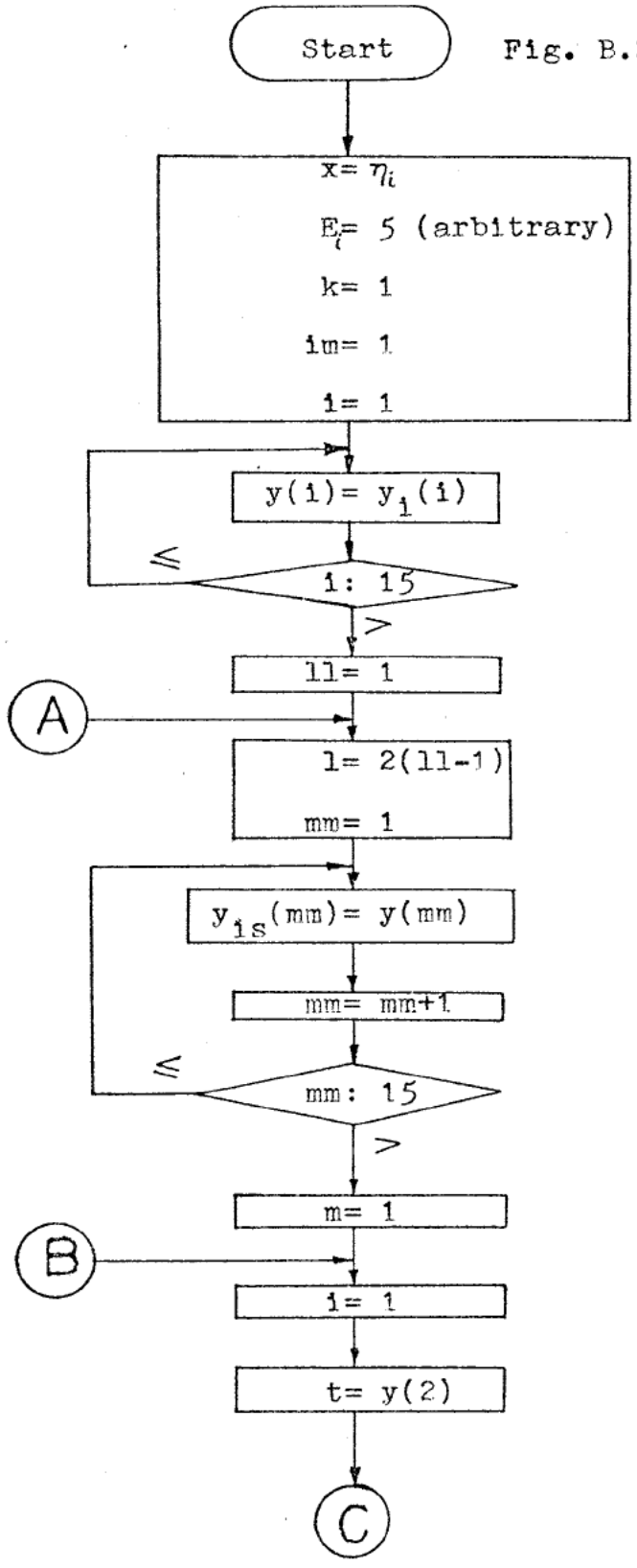

Fig. B.2a Subprogram

Fig. B.2b

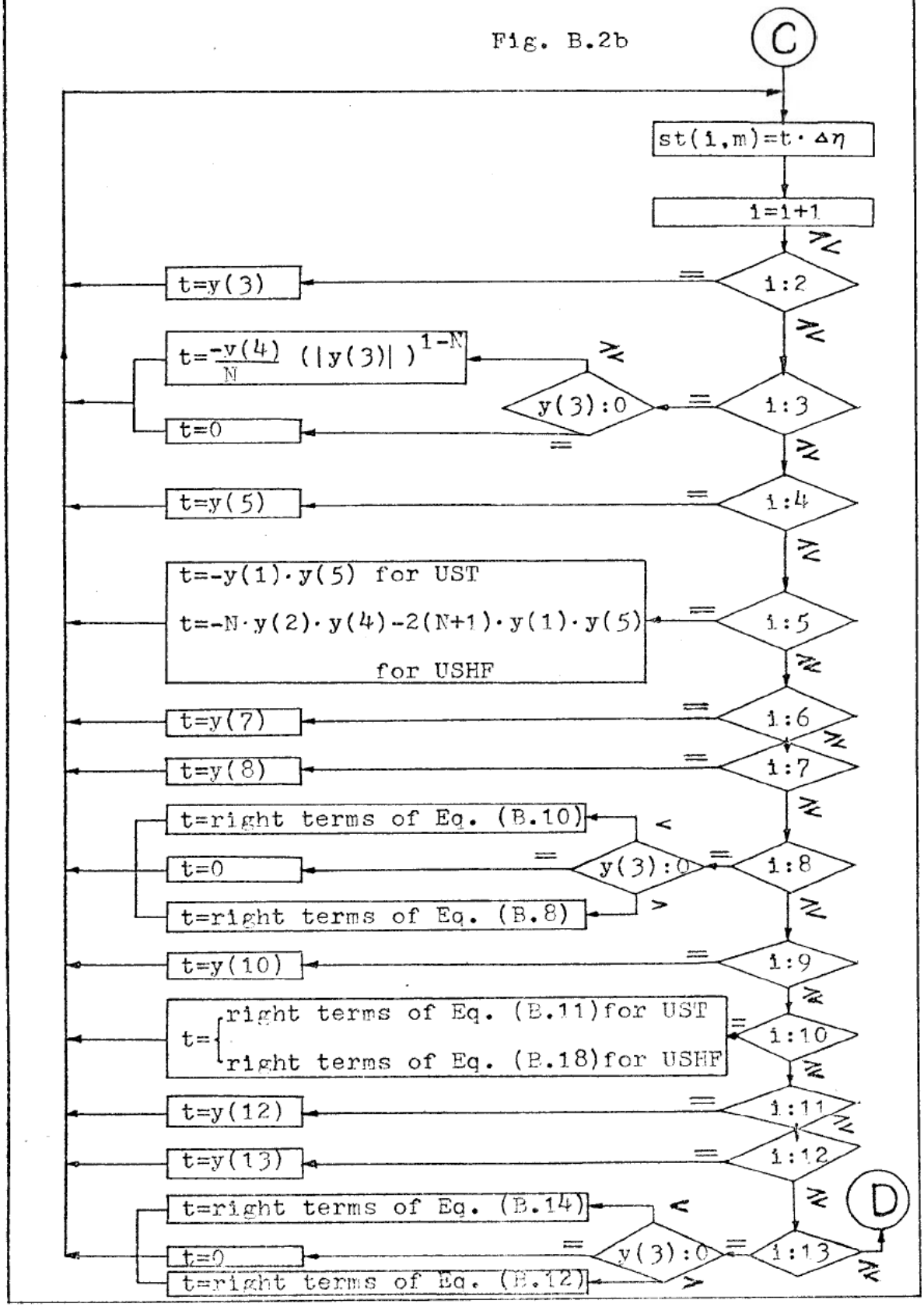
C
st(i,m)=t·Δη
i=i+1
i:2
t=y(3)
t=-y(4)/N (|y(3)|)^(1-N)
y(3):0
t=0
i:3
t=y(5)
i:4
t=-y(1)·y(5) for UST
t=-N·y(2)·y(4)-2(N+1)·y(1)·y(5) for USHF
i:5
t=y(7)
i:6
t=y(8)
i:7
t=right terms of Eq. (B.10)
t=0
y(3):0
t=right terms of Eq. (B.8)
i:8
t=y(10)
i:9
t=right terms of Eq. (B.11)for UST
right terms of Eq. (B.18)for USHF
i:10
t=y(12)
i:11
t=y(13)
i:12
t=right terms of Eq. (B.14)
t=0
y(3):0
t=right terms of Eq. (B.12)
i:13
D

Fig. B.2c

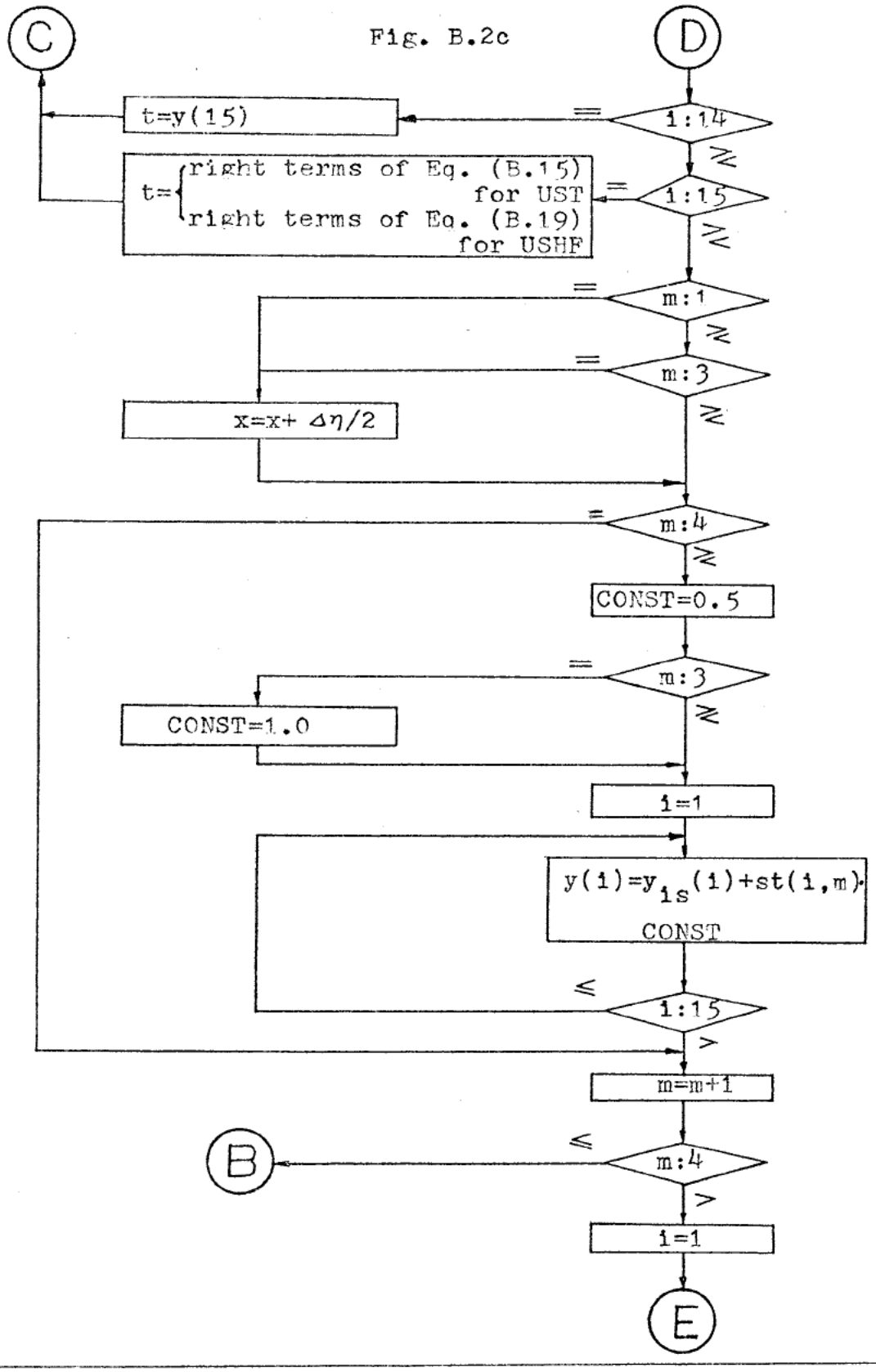
C
D
t=y(15)
i:14
t=right terms of Eq. (B.15) for UST
right terms of Eq. (B.19) for USHF
i:15
m:1
m:3
x=x+ Δη/2
m:4
CONST=0.5
m:3
CONST=1.0
i=1
y(i)=y_is(i)+st(i,m)·CONST
i:15
m=m+1
B
m:4
i=1
E

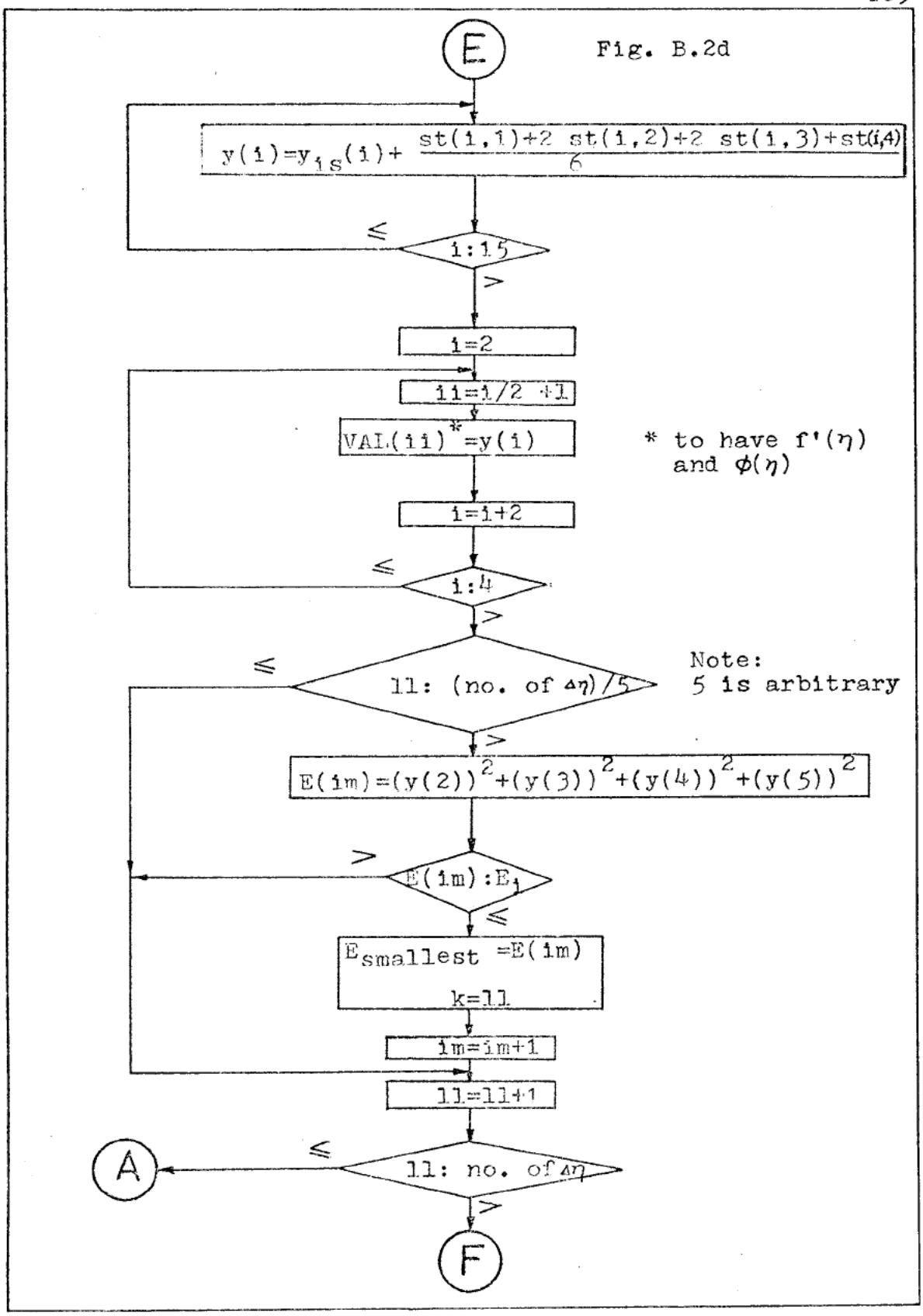
E
y(i)=y_is(i)+ (st(i,1)+2 st(i,2)+2 st(i,3)+st(i,4))/6
≤
i:15
>
i=2
ii=i/2 +1
VAL(ii)*=y(i)
* to have f'(η) and φ(η)
i=i+2
≤
i:4
>
≤
ll: (no. of Δη)/5
Note:
5 is arbitrary
>
E(im)=(y(2))^2+(y(3))^2+(y(4))^2+(y(5))^2
>
E(im):E_1
≤
E_smallest =E(im)
k=ll
im=im+1
ll=ll+1
A
≤
ll: no. of Δη
>
F

Fig. B.2d

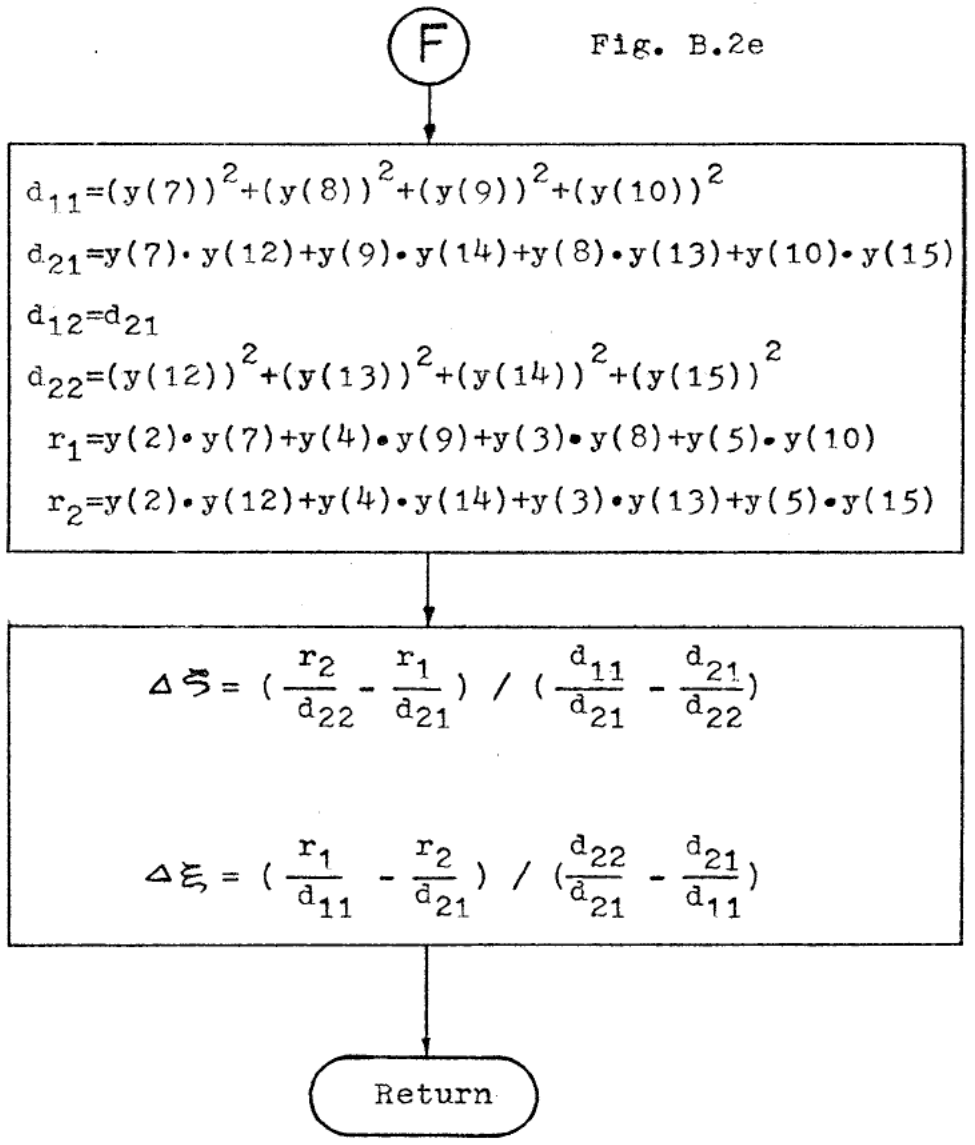
F
$d_{11}=(y(7))^2+(y(8))^2+(y(9))^2+(y(10))^2$
$d_{21}=y(7)\cdot y(12)+y(9)\cdot y(14)+y(8)\cdot y(13)+y(10)\cdot y(15)$
$d_{12}=d_{21}$
$d_{22}=(y(12))^2+(y(13))^2+(y(14))^2+(y(15))^2$
$r_1=y(2)\cdot y(7)+y(4)\cdot y(9)+y(3)\cdot y(8)+y(5)\cdot y(10)$
$r_2=y(2)\cdot y(12)+y(4)\cdot y(14)+y(3)\cdot y(13)+y(5)\cdot y(15)$
$\Delta\eta = \left(\frac{r_2}{d_{22}} - \frac{r_1}{d_{21}}\right) / \left(\frac{d_{11}}{d_{21}} - \frac{d_{21}}{d_{22}}\right)$
$\Delta\xi = \left(\frac{r_1}{d_{11}} - \frac{r_2}{d_{21}}\right) / \left(\frac{d_{22}}{d_{21}} - \frac{d_{21}}{d_{11}}\right)$
Return

Fig. B.2e

Table B.1 Summary of Input Data

j	Variable, y(j)	Initial value, $y_1(j)$	
		UST*	USHF**
1	f=y(1)	0	0
2	f'=y(2)	0	0
3	f"=y(3)	trial value	trial value
4	ϕ=y(4)	1	trial value
5	ϕ'=y(5)	trial value	-1
6	f_ζ=y(6)	0	0
7	f'_ζ=y(7)	0	0
8	f''_ζ=y(8)	1	1
9	ϕ_ζ=y(9)	0	0
10	ϕ'_ζ=y(10)	0	0
11	f_ξ=y(11)	0	0
12	f'_ξ=y(12)	0	0
13	f''_ξ=y(13)	0	0
14	ϕ_ξ=y(14)	0	1
15	ϕ'_ξ=y(15)	1	0

* UST = Uniform Surface Temperature

** USHF = Uniform Surface Heat Flux

APPENDIX C

The Region-Free Solution for the Uniform Surface Temperature Case

The values of $f''(0)$ and $\phi'(0)$ associated with the governing Equations (3.17) and (3.18) and boundary conditions (3.19) (the so-called 'region-free solution') are listed below:

N	$f''(0)$	$\phi'(0)$
0.1	2.6254	-0.4029
0.3	1.3112	-0.4378
0.5	1.1437	-0.4760
0.72	1.0734	-0.5025
0.891	1.0536	-0.5191
1.0	1.0533	-0.5298
1.5	0.9525	-0.5412

Appendix D

Average Heat Transfer Parameters Calculated from the Data of Sharma and Adelman (Table 3 of (15))

Run*	Δt ^{o}F	Average temperature ^{o}F	N	h $\frac{Btu}{hr\text{-}ft^2\text{-}^{o}F}$	$\overline{Nu}$	Pr_A x_{10}^{-2}	Gr_A x_{10}^{-3}	$\frac{\overline{Nu}}{Gr_A^{\frac{1}{2(N+1)}} Pr_A^{\frac{N}{3N+1}}}$
1	19.1	81.0	0.388	6.4	14.28	21.54	0.275	0.4767
2	38.1	90.5	0.355	7.8	17.23	15.05	0.683	0.4405
3	50.1	98.4	0.333	7.9	17.39	12.86	1.022	0.3923
4	64.3	107.2	0.311	8.5	18.46	10.31	1.574	0.3650
5	70.3	110.5	0.310	9.3	20.13	10.35	1.727	0.3837
6	88.5	120.0	0.290	9.4	20.09	7.91	2.769	0.3305
7	116.	144.2	0.265	10.1	21.30	6.00	5.169	0.2822

*Test conditions:

1.5% carbopol solution, vertical small plate, L=0.656'

Note: All the numerical values of the respective physical properties were taken from (15) for the calculation of the non-dimensional groups.

APPENDIX E

Method of Similarity Solution

The dimensionless boundary layer equations for laminar free convection to an arbitrary two-dimensional body having uniform surface heat flux have been derived in Chapter IV (see Equations (4.8), (4.9a) and (4.10)). A dimensionless stream function can be defined as

$$U = \frac{\partial \psi}{\partial Y} \qquad \text{and} \qquad V = -\frac{\partial \psi}{\partial X} \tag{E.1}$$

Equations (4.8), (4.9a) and (4.10) can then be written as

$$\frac{\partial}{\partial Y}\left(\left|\frac{\partial^2 \psi}{\partial Y^2}\right|^{N-1} \frac{\partial^2 \psi}{\partial Y^2}\right) + T \sin\alpha = 0 \tag{E.2}$$

$$\frac{\partial \psi}{\partial Y}\frac{\partial T}{\partial X} - \frac{\partial \psi}{\partial X}\frac{\partial T}{\partial Y} = \frac{\partial^2 T}{\partial Y^2} \tag{E.3}$$

with the boundary conditions*

$$\begin{aligned} &\text{at} \quad Y=0: \quad \frac{\partial \psi}{\partial Y} = \frac{\partial \psi}{\partial X} = 0, \quad \frac{\partial T}{\partial Y} = -1 \\ &\text{at} \quad Y=\infty \text{ and } X=0, \quad \frac{\partial \psi}{\partial Y} = T = 0 \end{aligned} \tag{E.4}$$

Let

$$\eta = b(X) \cdot Y \tag{E.5}$$

$$\psi = c(X) \cdot f(\eta) \tag{E.6}$$

$$T = d(X) \cdot \phi(\eta) \tag{E.7}$$

where $f(\eta)$ and ϕ are the reduced functions and $b(X)$, $c(X)$ and $d(X)$ are the arbitrary functions of X to be determined.

---

* Only the region-free solution will be discussed here.

Equations (E.5-7) are substituted into Equations (E.2) and (E.3) and rearranged to give

$$\phi + \frac{c^N b^{2N+1}}{d \sin\alpha} \frac{\partial}{\partial\eta}\left(|f''|^{N-1} f'' \right) = 0 \qquad \text{(E.8)}$$

$$\phi'' + \frac{c_X}{b} f \phi' - \frac{c\, d_X}{b\, d} f' \phi = 0 \qquad \text{(E.9)}$$

Equations (E.8) and (E.9) are ordinary differential equations only if

$$\frac{c^N b^{2N+1}}{d \sin\alpha} = \ell = \text{constant} \qquad \text{(E.10)}$$

$$\frac{c_X}{b} = s = \text{constant} \qquad \text{(E.11)}$$

$$\frac{c\, d_X}{b\, d} = r = \text{constant} \qquad \text{(E.12)}$$

Solving the system of Equations (E.10-12) for b, c and d, we obtain

$$b(X) = \frac{(\ell \sin\alpha)^{\frac{1}{2N+1}}}{\left[\frac{s\,(3N+1-r/s)}{2N+1} \int_0^X (\ell \sin\alpha)^{\frac{1}{2N+1}} dX\right]^{\frac{N-r/s}{3N+1-r/s}}} \qquad \text{(E.13)}$$

$$c(X) = \left[s \left(\frac{3N+1-r/s}{2N+1}\right) \int_0^X (\ell \sin\alpha)^{\frac{1}{2N+1}} dX\right]^{\frac{2N+1}{3N+1-r/s}} \qquad \text{(E.14)}$$

$$d(X) = \left[\frac{s(3N+1-r/s)}{2N+1} \int_0^X (\ell \sin\alpha)^{\frac{1}{2N+1}} dX\right]^{\frac{r}{s}\frac{2N+1}{3N+1-r/s}} \qquad \text{(E.15)}$$

Using Sparrow and Gregg's derivation (17) for Newtonian fluids as a reference, we can make the best choice for each constant ℓ, r and s. Thus, let $\ell=1$, r=N and s=2(N+1). Equations (E.13-15) become

$$b(X) = \frac{(\sin\alpha)^{\frac{1}{2N+1}}}{\left[(3N+2)\int_0^X \sin\alpha)^{\frac{1}{2N+1}}dX\right]^{\frac{N}{3N+2}}} \qquad (E.16)$$

$$c(X) = \left[(3N+ \;)_0 \; (\sin\alpha)^{\frac{1}{2N+1}}dX\right]^{\frac{2(N+1)}{3N+2}} \qquad (E.17)$$

$$d(X) = \left[(3 \quad \int^X \quad \right]^{\frac{N}{2}} \qquad (E.18)$$

In order to satisfy the boundary conditions (E.4), it is necessary to find the product of b and d such that

$$b(X)\cdot d(X) = \text{constant}$$

or

$$(\sin\alpha)^{\frac{1}{2N+1}} = \text{constant}$$

Thus $\sin\alpha=1$ (for a vertical plate)

is the restriction to this similarity transformation. Equations (E.16-18) become

$$b(X) = [(3N+2)\cdot X]^{-N/(3N+2)} \qquad (E.19)$$

$$c(X) = [(3N+2)\cdot X]^{2(N+1)/(3N+2)} \qquad (E.20)$$

$$d(X) = [(3N+2)\cdot X]^{N/(3N+2)} \qquad (E.21)$$

Substituting Equations (E.19-21) into (E.5-9), we obtain Equations (4.15-17) and Equations (4.20) and (4.21).

APPENDIX F

The Region-Free Solution for the Uniform Surface Heat Flux Case

The values of $f''(0)$ and $\phi(0)$ associated with Equations (4.20) and (4.21) and boundary conditions (4.22) (the so-called 'region-free solution') are listed below:

N	$f''(0)$	$\phi(0)$
0.1	4.2038	1.5757
0.3	1.4674	1.5066
0.383	1.2348	1.4470
0.5	1.0480	1.3795
0.611	0.9465	1.3217
0.888	0.8259	1.2010
1.0	0.7986	1.1644
1.5	0.7260	1.0478

VITA

Tommy Yih-Wen Chen was born in Shanhua, Tainan, Taiwan, on [redacted]

In September 1955, he entered the Mechanical Engineering Department of the Provincial Tainan Industrial Vocational High School, Tainan, Taiwan. After graduation in July 1958, he spent two years as a supervisor in a feed refinery factory. He then resumed his study in mechanical engineering at the Tatung Institute of Technology, Taipei, Taiwan. After three years of study, he enlisted in the Chinese Air Force for one year as a second-lieutenant at Pington Air Base under the ROTC program and returned to TIT in 1964 to finish his undergraduate study.

In 1965 he entered the University of Cincinnati, from which he was granted a M.S.M.E. in 1966. He then spent two years as a mechanical engineer in mechanical related industries in the States. In September 1968, he left York Division of Borg-Warner Corporation and entered the doctoral program in the Mechanical and Aerospace Engineering Department, University of Missouri, Columbia. During his graduate study, he held the title of Research Assistant. He is member of ASME and AIAA.

Tommy married Shu-Mei Hsu in September, 1970.

University Libraries
University of Missouri

Digitization Information Page

Local identifier Chen1971

Source information

Format	Book
Content type	Text
Source ID	Gift copy from department; not added to MU collection.
Notes	

Capture information

Date captured	February 2024
Scanner manufacturer	Fujitsu
Scanner model	fi-7460
Scanning system software	ScandAll Pro v. 2.1.5 Premium
Optical resolution	600 dpi
Color settings	8 bit grayscale
File types	tiff
Notes	

Derivatives - Access copy

Compression	Tiff: LZW compression
Editing software	Adobe Photoshop
Resolution	600 dpi
Color	grayscale
File types	pdf created from tiffs
Notes	Images cropped, straightened, brightened